Title: Reference Model for MERIS Level 2 Processing

Doc. no: PO-TN-MEL-GS-0026

Issue: 4

Revision: 1

Date: 13 July 2001

	Function	Name	Company	Signature	Date
Prepared:	Ocean Colour Task Force	F. Montagner	ACRI		
Approved:	Project Manager	L. Bourg	ACRI		
Released:			ESA		

Distribution

S. DELWART (ESTEC)
J-P. GUIGNARD (ESRIN)

J. AIKEN (PML)
C. BROCKMANN (SCICON)
F. FELL (INFORMUS)
J. FISCHER (FUB)
R. DOERFFER (GKSS)
A. MOREL (LPCM)
M. BABIN (LPCM)
D. ANTOINE (LPCM)
R. SANTER (LISE)

Change Record

Issue	Revision	Date	Description	Change pages
Draft	0	13/03/98	Initial Draft	-
1	0	30/04/98	Reviewed and completed	
1	1	06/11/98	Update of water reflectance model, additional aerosol properties tables, band settings	2, 3, 7, 8 (additional page), 10, 16, 23, 24, 25, 29, 30, 31, 34 -46 (new pages)
1	2	08/01/99	Aerosol models presentation, spectral dependencies, minor corrections /clarifications	1, 4, 5, 6, 7, 10, 12, 15 to 19, 34 to 45
2	Draft	25/06/99	Revision of water reflectance model	
2	0	30/08/99	with comments from Task Force	
2	1	07/09/99	Clarification following inputs from Task Force Correction of a bug in table 14	6, 7, 10, 13, 14, 18, 22 (pagin. change) 37 to 48
2	2	17/12/99	Correction of errors in §6.6, 10, 11 following Task Force inputs	18, 26-31
3	Draft	26/01/00	Revision of Sections 4, 5 to take Task Force results into account New section 2.3, 5.3, 16	all (pagin. change)
3	0	21/07/00	with Task Force comments (change bars refer to Iss.2.2)	
3	1	30/08/00	with tables 10.1, 11-1, 14-1 & 15-1 updated for bands 9 & 12 shifts: 705 → 708.75 & 775 → 778.75 (change bars refer to Iss.2.2)	
4	Draft	31/12/00	Section 4 is deeply revised, by separating more clearly a model for Case 1 waters IOPs and a model for Case 2 waters IOPs.	
4	0	05/06/01	Complete model, full revision	
4	1	13/07/01	Various errata in sections 2, 3, 4.4, 4.5	

Table of Contents

List Of Figures

List Of Tables

1. - Purpose and Scope

The specifications provided here define the parameters to be used to generate inherent optical properties for the ocean and atmosphere as a function of geophysical properties and wavelengths, which can be the basis upon which to generate test data and auxiliary parameters needed for operation and end-to-end tests of the MERIS ground segment processor (*i.e.*, mostly to generate water-leaving reflectances or total reflectances at the top of the atmosphere level). Parameters have been selected from various measurements and models in water, surface and atmosphere. The underlying geo-physical models are the same as those of the MERIS geo-physical algorithms, as described in the "MERIS Algorithms Theoretical Basis Document" (ATBD), PO-TN-MEL-GS-0005, Iss. 4.1.

Parts of the model might be subject to evolution in the future, thanks to more field and research work. In its current state, this model has severe limitations when used as a predictive tool. The inherent and/or apparent optical properties computed with this model for given geo-physical properties may deviate from locally measured properties. This is due in general to deviation between parameter values or parameterisations adopted in the model and those that may be derived locally in any given water body.

This model is intended to apply to the generation of operational auxiliary parameters for the MERIS processing.

2. - References, Abbreviations, Definitions

2.1 - Reference Documents

[RD1] Table Generation Requirements Document, PO-TN-MEL-GS-0012, Iss. 2.1
[RD2] Algorithm Theoretical Basis Document, PO-TN-MEL-GS-0005, Iss. 4.1
[RD3] MERIS Level 2 Detailed Processing Model, PO-TN-MEL-GS-0006, Iss .4.6

2.2 References (open literature)

AHN, Y.-H. 1990 Propriétés optiques de particules biologiques et minérales présentes dans l'océan; Application: inversion de la réflectance. Thèse de Doctorat, Université Pierre et Marie Curie, Paris, 214 pp.

AUSTIN, R.W., 1974, The remote sensing of spectral radiance from below the ocean surface, in « Optical aspects of Oceanography », Ed. N.G. Jerlov and E. Steemann Nielsen, Academic, London, 317-344 .

BRICAUD, A., A. MOREL, M. BABIN, K. ALLALI and H. CLAUSTRE, 1998, Variations of light absorption by suspended particles with Chlorophyll-a concentration in oceanic (case 1) waters: Analysis and implications for bio-optical models, *J. Geo. Res* **103**: 31033-31044

BROGNIEZ G., J-C. BURIEZ, V. GIRAUD, F. PAROL, C. VANBAUCE, 1995, *Monthly Weather Review*, **123**, 1025.

CARDER K.L., S.K. HAWES, K.A. BAKER, R.C. SMITH, R.G. STEWARD and B.G. MITCHELL. 1991. Reflectance model for quantifying chlorophyll *a* in the presence of productivity degradation products. *Journal of Geophysical Research*, **96**: 20 599-20 611.

CARDER K.L., R.G. STEWARD, J.H. PAUL and G. A. VARGO; 1986. Relationships between chlorophyll and ocean color constituents as they affect remote-sensing reflectance models. *Limnology and Oceanography*, **31**: 403-413.

COX, C. and W. MUNK. 1954. Statistics of the sea surface derived from sun glitter. *J. Mar. Res.*, **13**: 198-227.

COX, C. and W. MUNK. 1954. Some problems in optical oceanography. *J. Mar. Res.*, **14**: 63-78.

ELTERMAN L. 1968. UV, visible, and IR attenuation for altitudes to 50 km, Air Force Cambridge Research Laboratories, Environmental Research papers, N° 285, AFCRL-68-0153, 49pp.

GORDON, H.R., 1979, Diffuse reflectance of the ocean : the theory of its augmentation by Chl-a fluorescence, Applied Optics **18**, 1161-1166.

GORDON, H. R. and W. R. McLUNEY. 1975. Estimation of the depth of sunlight penetration in the sea for remote sensing. *Appl. Opt.*, **14**:413-416.

GORDON, H. R. and A. MOREL. 1983. Remote assessment of ocean color for interpretation of satellite visible imagery. A review. Lecture Notes on Coastal and Estuarine Study, Vol. 4, Springer Verlag.

HALE, G.M. and M.R. QUERRY 1973: Optical constants of water in the 200nm to 200 μm wavelength region, *Appl. Opt.*, **12**: 555-563.

KATTAWAR G.W. and J.C. VALERIO, 1982, Exact 1-D solution to the problem of the Chl-a fluorescence from the ocean, Applied Optics **21**, 2489-2492.

KISHINO, M., S. SUGIHARA, and N. OKAMI, 1984, Influence of fluorescence of Chl-a on underwater upward irradiance spectrum, La Mer **22**, 224-232.

KRONFELD, U., 1988. Die optischen Eigenschaften der ozeanischen Schwebstoffe und ihre Bedeutung für die Fernerkundung von Phytoplankton, GKSS Report 88/E/40, pp.1-153

LOISEL, H. and A. MOREL,. 1998. Light scattering and chlorophyll concentration in Case 1 waters: A re-examination. *Limnol Oceanogr.* **43**(5): 847-858.

MALONE, 1982

MARITORENA S., A. MOREL and B. GENTILI, 2000, determination of the fluorescence quantum yield by oceanic phytoplankton in their natural habitat, *Applied Optics* **39**, in press.

MOBLEY, C.D., B. GENTILI, H.R. GORDON, Z. JIN, G.W. KATTAWAR, A. MOREL, P. REINERSMANN, K. STAMNES, and R.H. STAVN 1993. Comparison of numerical models for computing underwater light fields. *Appl. Opt.*, **32**, No. 36, pp. 7484-7504

MOBLEY, C.D 1994 Light and water: Radiative transfer in natural waters, Academic Press

MOREL, A. 1966. Etude expérimentale de la diffusion de la lumière par l'eau, les solutions de chlorure de sodium et l'eau de mer optiquement pure. *J. Chim. Phys.*, 10: 1359-1366.

MOREL, A. 1974. Optical properties of pure water and sea water. In : Optical aspects of Oceanography, N. G. Jerlov and E. Steemann-Nielsen, N. G. Jerlov and E. Steemann-Nielsen, Academic, pp. 1-24.

MOREL, A. 1987. Chlorophyll-specific scattering coefficient of phytoplankton. A simplified theoretical approach. *Deep-Sea Res.*, **34**: 1093-1105.

MOREL A. 1988. Optical modelling of the upper ocean in relation to its biogenous matter content (case 1 waters). *Journal of Geophysical Research*, **93**: 10 749-10 768.

MOREL A. and D. ANTOINE. 1994. Heating rate within the upper ocean in relation to its bio-optical state. *J. Phys. Oceanogr.*, **24**: 1652-1665.

MOREL, A. and S. MARITORENA, 2001, Bio-optical properties of oceanic waters : a reappraisal, *J. Geophys. Res*. In press.

NECKEL H. and D. LABS, 1984. The solar radiation between 300 and 12500 Angström. *Sol. Phys.* **90**, 205-258.

PETZOLD, T. L. 1972. Volume scattering functions for selected ocean waters. San Diego: Scripps Inst. Oceanogr., Ref. 72-78, 79 pp.

POPE R. M. and E. S. FRY. 1997. Absorption spectrum (380-700 nm) of pure water. II. integrating cavity measurements. *Appl. Opt.* **36**: 8710-8723.

ROTHMAN, L.S *et al.*, 1983: AFGL atmospheric absorption lines compilation, *Appl. Opt.* **22**, 2247-2256.

SATHYENDRANATH, S. and T. PLATT. 1998. An ocean color model incorporating trans-spectral processes, Applied Optics **27**, 2216-2227.

SATHYENDRANATH, S., L. PRIEUR and A. MOREL. 1989. A three-component model of ocean colour and its application to remote sensing of phytoplankton pigments in coastal waters. *Int. J. Remote Sensing*, **10**: 1373-1394.

SCHÜTZ, L., 1980. Long-range transport of desert dust with special emphasis on the Sahara, *Ann. N.Y. Acad. Sci.* **338**, 515-532

SHETTLE E.P. and R.W. FENN. 1979. Models for the aerosols of the lower atmosphere and the effects of humidity variations on their optical properties. Environmental Research Papers, AFGL-TR-79-0214, 20 September 1979, AFGL, Hanscom, MA.

SPITZY A. and V. ITTEKOTT. 1986. Gelbstoff : An uncharacterized fraction of dissolved organic carbon. *In* the influence of yellow substances on remote sensing of sea-water consitutents from space (GKSS Geesthacht Research Center, Geesthacht, FRG), VOl. II, pp 31.

THUILLIER G., M. HERSÉ, P. C. SIMON, D. LABS, H. MANDEL, D. GILLOTAY and T. FOUJOLS, 1998a "Observation of the visible solar spectral irradiance between 350 and 850 nm during the ATLAS I mission by the SOLSPEC spectrometer", *Solar Phys.* **177**, 41-61

THUILLIER G., M. HERSÉ, P. C. SIMON, D. LABS, H. MANDEL and D. GILLOTAY, 1998b "Observation of the solar spectral irradiance from 200 to 870 nm during the ATLAS 1 and 2 missions by the SOLSPEC Spectrometer", *Metrologia*, in press

WHITLOCK, C. H., L. R. POOLE, J. W. USRY, W. M. HOUGHTON, W. G. WITTE, W. D. MORRIS and E. A. GURGANUS. 1981. Comparison of reflectance with backscatter and absorption parameters for turbid waters. *Appl. Opt.*, **20**: 517-522.

WALRAFEN G.E., 1967, Raman studies of the effect of temperature on water structure, J. Chem. Phys. **47**, 114-126.

WORLD CLIMATE RESEARCH PROGRAM. 1986. A preliminary cloudless standard atmosphere for radiation computation. Int. Ass. for Meteor. and Atm. Phys., Radiation Commission, March 1986, WCP-112, WMO/TD-N° 24.

2.3 - Abbreviations and definitions

AOP: Apparent Optical Property
ATBD: Algorithm Theoretical Basis Document
CDOM: Coloured Dissolved Organic Matter
IOP: Inherent Optical Property
RH: Relative Humidity
SPM: Suspended Particulate Matter
TBD: To Be Defined
TGRD: Table Generation Requirements Document
TSM: Total Suspended Matter
VSF: Volume Scattering Function
WCRP: World Climate Research Programme

Case 2(S) water :case 2 water dominated by suspended matter (see RD2)
Case 2(Y) water :case 2 water dominated by yellow substance (see RD2)

2.4 – Notations and conventions

The Geometry notations and conventions in this document are those of RD3. They are recalled here. In a Cartesian frame linked to the Earth ellipsoid at a given point, the directions of the Sun and of the observer are represented in figure 2-1 below.

Equations in this document are numbered. The number sequence does *not* reflect a model or algorithm logic.

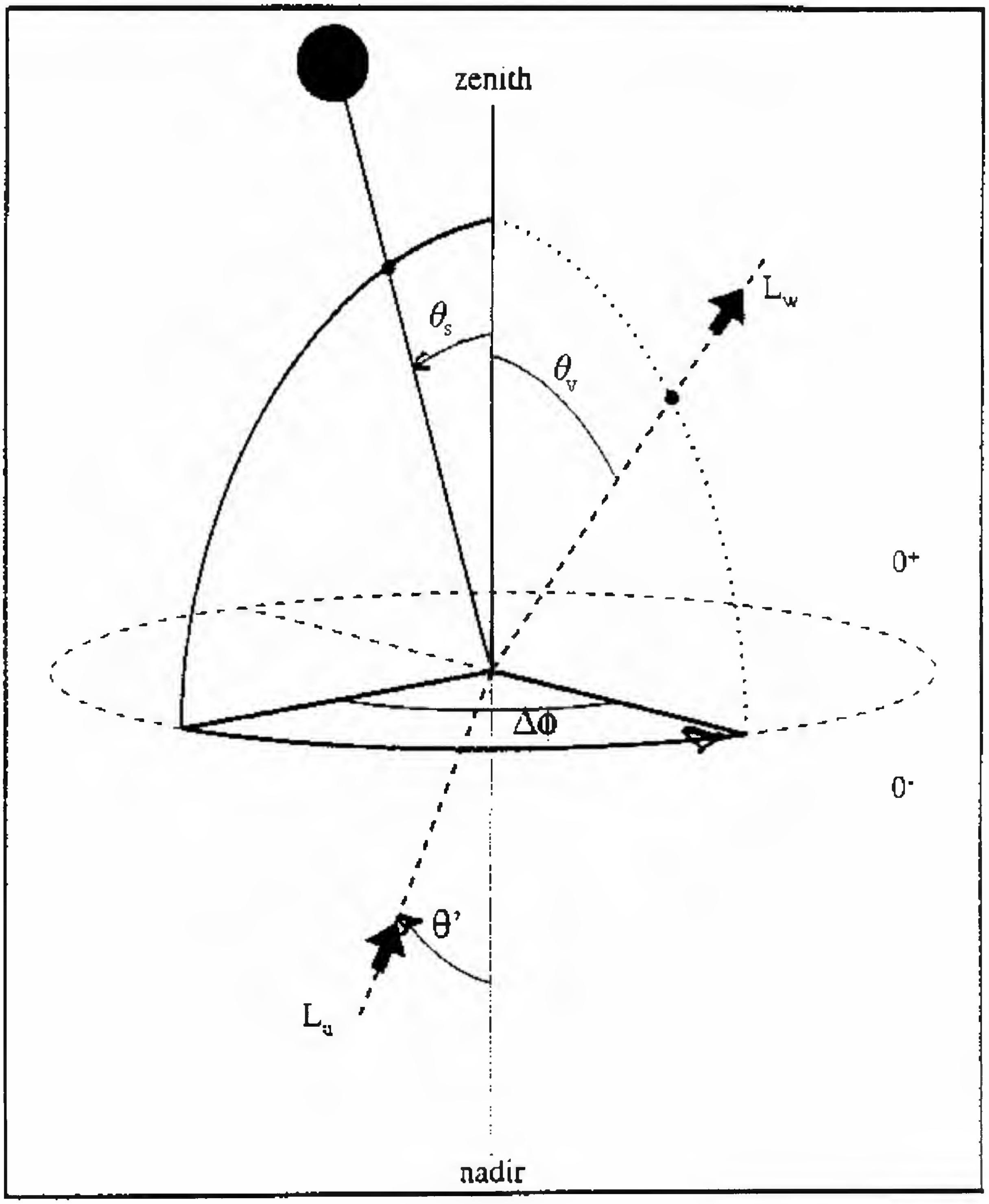

Figure 2-1: Geometry notations (see table of symbols)

2.5 TABLE OF SYMBOLS

Symbol	definition	Dimension / units
Geometry (see fig. 2.1)		
λ	Wavelength	nm
θ_s	Sun zenith angle ($\mu_s = \cos(\theta_s)$)	degrees
θ_v, θ	Satellite viewing angle ($\mu_v = \cos(\theta_v)$)	degrees
θ'	Refracted viewing angle ($\theta' = \sin^{-1}(n.\sin(\theta_v))$)	degrees
$\Delta\phi$	Azimuth difference between the sun-pixel and pixel-sensor half vertical planes	degrees
ψ	Scattering angle (not represented)	degrees
Radiometric quantities		
$L(\lambda,\theta_s,\theta_v,\Delta\phi)$	Radiance	$W\ m^{-2}\ nm^{-1}\ sr^{-1}$
Inherent Optical Properties ("IOPs")		
$\beta(\theta,\lambda)$	volume scattering function (VSF)	sr^{-1}
$\tilde{\beta}(\theta,\lambda)$	normalised volume scattering function $\tilde{\beta}(\theta,\lambda) = \frac{\beta(\theta,\lambda)}{b(\lambda)}$ where $\beta(\theta,\lambda) = \frac{d\Phi(\theta,\lambda)}{\Phi_o(\lambda)} \frac{1}{d\omega dr}$, $\Phi_o(\lambda)$ is the radiant flux onto a volume element of thickness dr, and $d\Phi(\theta,\lambda)/d\omega$ is the radiant intensity scattered from this volume in the direction θ with respect to the direction of the incident flux.	$sr^{-1}m^{-1}$
$a(\lambda)$	Absorption coefficient	m^{-1}
$b(\lambda)$	Scattering coefficient	m^{-1}
$c(\lambda)$	Attenuation coefficient for wavelength λ	m^{-1}
$b_b(\lambda)$	Backscattering coefficient	m^{-1}
Apparent Optical Properties ("AOPs") and derived quantities		
$\rho(\lambda,\theta_s,\theta_v,\Delta\phi)$	Reflectance ($\pi L / E_d(0^+)$)[1] where the product $\pi.L$ is the TOA upwelling irradiance if upwelling radiances are equal to $L(\lambda,\theta_s,\theta_v,\Delta\phi)$, for any values of θ_v within 0-π/2 and any $\Delta\phi$ within 0-2π.	dimensionless

[1] This definition actually corresponds to the transformation of the normalised water-leaving radiance *sensu* Gordon and Clark (1981) (*i.e.*, $L / (\varepsilon_c\ t_{\theta s}\ \mu_s)$) into reflectance through the usual equation $\rho = \pi L / F_0\ \mu_s$ (with μ_s = 1 in this last case).

	Subscripts t : total reflectance w : water-leaving reflectance u : reflectance just below the sea surface	
$[\rho_w]_N(\lambda)$	Normalised water-leaving reflectance (*i.e.*, the reflectance if there were no atmosphere, and for $\theta_s = \theta_v = 0$)	dimensionless
E_u	Upwelling irradiance	dimensionless
E_d	downwelling irradiance	dimensionless
$R(\lambda, 0^-)$	Diffuse reflectance at null depth, or irradiance reflectance (E_u / E_d)	dimensionless
$F_0(\lambda)$	Mean extraterrestrial spectral irradiance	W m^{-2} nm^{-1}
f	Ratio of $R(0^-)$ to (b_b/a); subscript 0 when $\theta_s = 0$	dimensionless
f'	Ratio of $R(0^-)$ to $(b_b/(a + b_b))$; subscript 0 when $\theta_s = 0$	dimensionless
$Q(\lambda,\theta_s,\theta_v,\Delta\phi)$	Factor describing the bidirectional character of $R(\lambda, 0^-)$ subscript 0 when $\theta_s = \theta_v = 0$; $Q = E_u/L_u$	sr

Other atmosphere and aerosol properties

$F_a(\lambda)$	Aerosol forward scattering probability (section 15)	dimensionless
$\tau_a(\lambda)$	Optical thickness due to aerosol scattering	dimensionless
$\tau_r(\lambda)$	Optical thickness due to Rayleigh scattering	dimensionless
$\varpi_a(\lambda)$	Aerosol single scattering albedo	dimensionless
$\varpi_r(\lambda)$	Rayleigh single scattering albedo	dimensionless
ν	Exponent of the Junge law for the distribution of aerosol particles (sensitivity studies)	dimensionless
RH	Relative humidity	percents
$t_{\theta_s}(\lambda,\theta_s)$	Irradiance transmittance for a sun zenith angle θ_s $t_{\theta_s}(\lambda,\theta_s) = E_d(0^+) / (\mu_s\, \varepsilon_c\, F_0)$, where $E_d(0^+)$ is the downwelling irradiance just above the sea surface	dimensionless

Geophysical properties

Chl	Chlorophyll concentration	mg m^{-3}
TSM	Total Suspended Matter concentration	mg m^{-3}
YS	yellow substance absorption	m^{-1}

Air-water interface

$\Re(\theta')$	Geometrical factor, accounting for all refraction and reflection effects at the air-sea interface (Morel and Gentili, 1996)	dimensionless

$$\Re(\theta') = \left[\frac{(1-\bar{\rho})}{(1-\bar{r}R)}\,\frac{(1-\rho_F(\theta'))}{n^2}\right] \text{ (subscript 0 when } \theta' = 0)$$

where

	n is the refractive index of water	dimensionless
	$\rho_F(\theta)$ is the Fresnel reflection coefficient for incident angle θ	dimensionless
	$\bar{\rho}$ is the mean reflection coefficient for the downwelling irradiance at the sea surface	dimensionless
	$\bar{r}$ is the average reflection for upwelling irradiance at the water-air interface	dimensionless
σ	Root-mean square of wave facet slopes	dimensionless
β	Angle between the local normal and the normal to a wave facet	
p	Probability density of surface slopes for the direction $(\theta_s, \theta_v, \Delta\phi)$	dimensionless

Miscellaneous

W	Wind speed	dimensionless
ε_c	Correction factor applied to $F_0(\lambda)$, and accounting for the changes in the Earth-sun distance. It is computed from the eccentricity of the Earth orbit, e = 0.0167, and from the day number D, as $\varepsilon_c = \left(1 + e\cos\left(\frac{2\pi(D-3)}{365}\right)\right)^2$	dimensionless
ln	natural (or Neperian) logarithm	
log₁₀	decimal logarithm	

3. - MERIS Spectral bands

The following MERIS spectral bands are considered in this document:

Channel number	Wavelength (nm)	Width (nm)
1	412.5	10
2	442.5	10
3	490.0	10
4	510.0	10
5	560.0	10
6	620.0	10
7	665.0	10
8	681.25	7.5
9	708.75	10
10	753.75	7.5
11	760.625	3.75
12	778.75	15
13	865.0	20
14	885.0	10
15	900.0	10

Table 3-1: MERIS spectral bands

NOTE: due to the programmable nature of the MERIS and optimisation of the processing, this list of bands may evolve in the future.

The refractive index of sea water relative to air shall be taken from table 3-2 below. Values are interpolated from Mobley (1994) at the MERIS wavelengths, for a pressure 1013 hPa, salinity 35 psu, and temperature 15°C.

λ (nm)	n
412.5	1.349
442.5	1.347
490.0	1.344
510.0	1.343
560.0	1.341
620.0	1.339
665.0	1.338
681.25	1.338
708.75	1.337
778.75	1.336
865.0	1.334

Table 3-2: Refractive index of sea water

4. - Water Optical Properties

At a given λ, the optical properties described below apply to Case 1 and Case 2 ocean waters (tentatively to inland waters). Water optical properties shall be computed at least for the following MERIS bands:

1, 2, 3, 4, 5, 6, 7, 9, 12, 13 for algorithms which include atmosphere correction;

1, 2, 3, 4, 5, 6, 7, 9 for algorithms based on water-leaving radiance (or reflectance)

4.1 - Remotely sensed layer

The geometrical thickness of the vertical water layer from which 90% of the remotely sensed ocean colour signal emerges [denoted $Z_{90}(\lambda)$; m] can be approximated by (Gordon and McCluney 1975):

$$Z_{90}(\lambda) = 1/K_d(\lambda) \qquad (1a)$$

where $K_d(\lambda)$ (m^{-1}) is the vertical attenuation coefficient for downward irradiance. Here, we assume that (whatever λ)

$$z >> Z_{90}(\lambda) \qquad (1b)$$

where z (m) is the geometrical thickness of the water column. In other words, bottom effect is not accounted for in the present model.

4.2 - Water constituents

4.2.1 – Overview

This section presents the concepts and terminology used through the discussion and specification of the water optical properties models.

The apparent optical properties of sea waters can be determined according to the inherent optical properties (absorption and scattering) of 5 groups of substances (*cf.* Fig. 4-1):

1. pure sea water, denoted "*w*"
2. phytoplankton and other associated particles (detritus, bacteria, …), denoted "p1"
3. endogenous coloured dissolved organic matter (associated with biological activity), denoted "y1"
4. terrestrial (exogenous) particles (sediment resuspended from the bottom, brought by rivers, …), denoted "p2"
5. exogenous coloured dissolved organic matter from land drainage (present in Case 2 waters only), denoted "y2".

While only groups 1, 2 and 3 are present in Case 1 waters, all of them (1 to 5 above) co-exist in Case 2 waters. In this case, however, the individual components y1 and y2 cannot be practically separated (a measure of CDOM absorption provides the sum y1 + y2).

IOPs of groups 2, 3, 4 and 5 are related to the following "concentrations":

1. p1 and y1 IOPs will be a function of the concentration of chlorophyll *a* (including the divinyl form and pheopigments) denoted "*[chl]*" and with units as mg m^{-3}
2. p2 IOPs will be ideally related to the sea water particles dry weight (denoted "*TSM*" and with units as g m^{-3}) from which the contribution of p1 has been subtracted; practically it is related to the corresponding scattering coefficient (units m^{-1}).

3. y2 IOPs will be a function of the CDOM concentration as determined by its absorption coefficient at 443 nm, denoted indifferently "$a_{y2}(443)$" or *CDOM* and with units as m^{-1} (*i.e.* the total measured CDOM absorption from which a_{y1} has been subtracted)

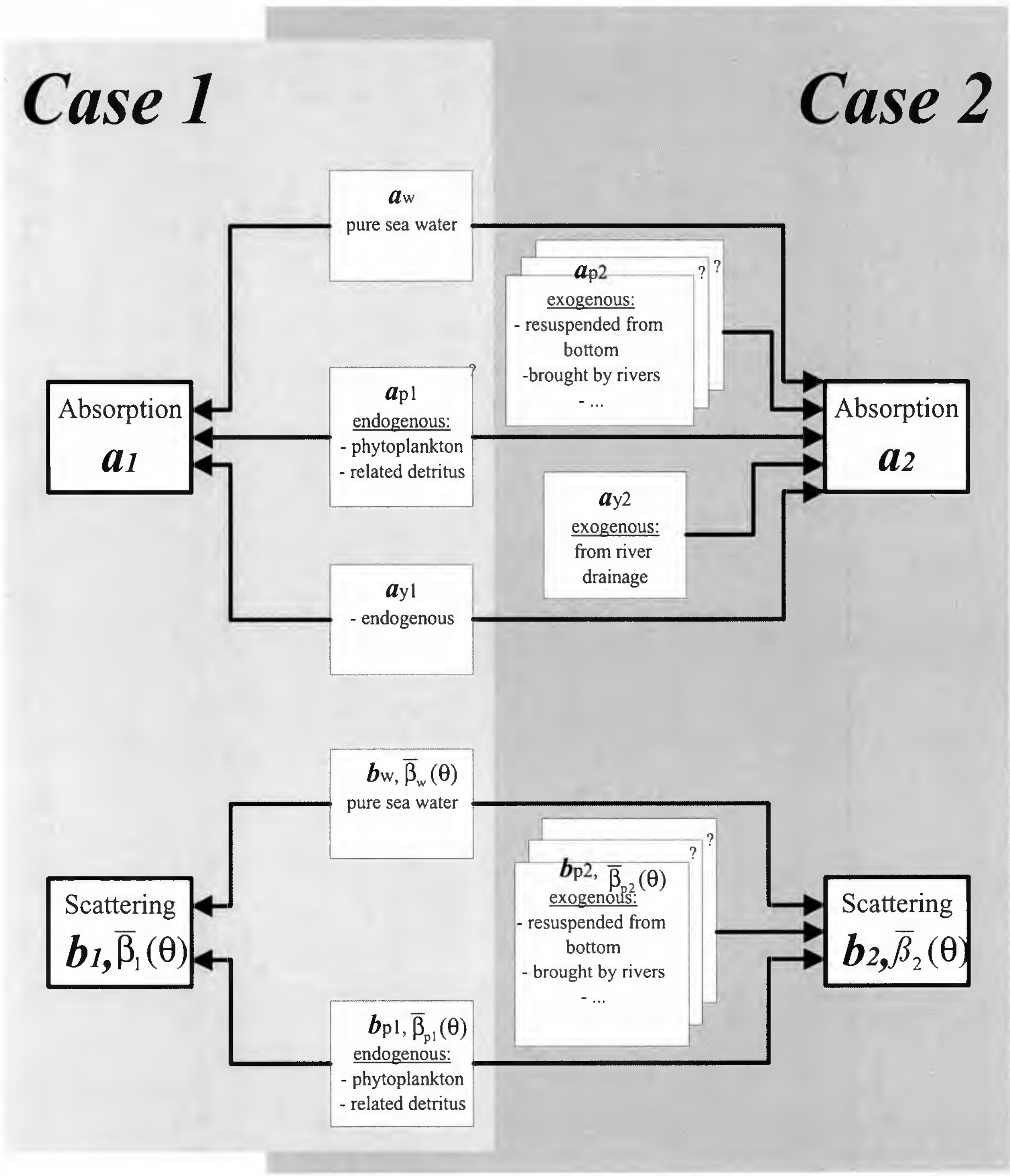

Figure 4-1: Schematic representation of IOP compartments.

Comments on Figure 4-1

Case 2 waters are seen as Case 1 waters to which other optically active substances are added. In other words, Case 1 waters can be seen as particular Case 2 waters when these additional substances are lacking.

Case 1 waters include 3 components:

- *pure sea water for which 2 spectral IOPs must be specified:* $a_w(\lambda)$ *and* $\beta_w(\lambda,\theta)$*; this last term can be split into* $\overline{\beta}_w(\theta)$ *(independent from* λ*) and* $b_w(\lambda)$
- *all particulate matter found in open ocean, such as living algal cells, heterotrophic bacteria and organisms, various debris, ... Again, this compartment is described by its absorption and scattering properties:* $a_{p1}(\lambda)$, $b_{p1}(\lambda)$ *and* $\overline{\beta}_{p1}(\theta)$
- *coloured dissolved organic material presumably generated in open ocean (through processes like excretion, organism decay, ...), and likely related to the particulate matter abundance. This compartment comes into play through its absorption coefficient* $a_{y1}(\lambda)$

In summary, there are 3 components in forming the absorption coefficient of Case 1 waters and 2 components in forming the scattering properties.

Case 2 waters include the three above components and in addition:

- *exogenous particles, mainly sediment, either transported by rivers, or re-suspended from the bottom in shallow waters. The proportions between organic and mineral particles is varying according to the location and origin; the mineral particles are also geographically differing (clay, calcareous, ...). Therefore, several types of particles may be simultaneously present, and to each type corresponds a couple of properties like* $a_{p2}(\lambda)$ *and* $\beta_{p2}(\lambda,\theta)$
- *exogenous CDOM resulting from land drainage which acts only as absorber:* $a_{y2}(\lambda)$*. As for particles, it is likely that several types may be distinguished depending on the location.*

4.2.2 – RELATIONSHIP WITH MERIS LEVEL 2 PRODUCTS

The way the IOPs presented above will be practically related to the MERIS Level 2 products is explained separately for Case 1 and Case 2 waters in sections 4.5 and 4.6 below, respectively.

To summarise:

- The Algal Pigment Index 1 product corresponds to p_1 (and take y_1 into account), *in Case 1 waters.*
- The Algal Pigment Index 2 product corresponds to the absorption of p_1.
- The Total Suspended Matter product corresponds to the aggregate scattering of p1 and p_2.
- The Yellow Substance product corresponds to the aggregate absorption of p_2, y_1 and y_2.

4.3 - VERTICAL DISTRIBUTION

It is assumed that all substances are homogeneously distributed in the upper part of the water column. For many coastal waters, this is a realistic assumption, especially when considering the $Z_{90}(\lambda)$ layer; this may be false for river plumes, where very strong vertical gradients associated with fresh water spreading may be observed.

4.4 INHERENT OPTICAL PROPERTIES (IOPS) OF PURE SEA WATER

These Inherent Optical Properties are involved in both Case 1 and Case 2 waters and include absorption, scattering, and emission (Raman) properties.

4.4.1 ABSORPTION COEFFICIENT

The absorption coefficients of pure sea water, $a_w(\lambda)$, are taken from Pope and Fry (1997) for wavelengths up to 709 nm, *i.e.* up to and including MERIS band 9, and from Hale and Querry (1973) for wavelengths above 709nm (see Table 4.4.1-1 below).

λ (nm)	a_w (m^{-1})	σ (m^{-1})	Percent
380.0	0.01137	0.0016	14
382.5	0.01044	0.0015	15
385.0	0.00941	0.0011	13
387.5	0.00917	0.0014	16
390.0	0.00851	0.0012	15
392.5	0.00829	0.0011	14
395.0	0.00813	0.0010	13
397.5	0.00775	0.0011	15
400.0	0.00663	0.0007	11
402.5	0.00579	0.0007	12
405.0	0.00530	0.0007	14
407.5	0.00503	0.0006	13
410.0	0.00473	0.0006	13
412.5	0.00452	0.0005	13
415.0	0.00444	0.0006	13
417.5	0.00442	0.0006	14
420.0	0.00454	0.0006	14
422.5	0.00474	0.0006	13
425.0	0.00478	0.0006	14
427.5	0.00482	0.0006	13
430.0	0.00495	0.0006	12
432.5	0.00504	0.0005	11
435.0	0.00530	0.0005	11
437.5	0.00580	0.0005	10
440.0	0.00635	0.0005	9
442.5	0.00696	0.0005	9
445.0	0.00751	0.0006	8
447.5	0.00830	0.0005	7
450.0	0.00922	0.0005	6
452.5	0.00969	0.0004	6
455.0	0.00962	0.0004	5
457.5	0.00957	0.0004	5
460.0	0.00979	0.0005	6
462.5	0.01005	0.0005	6
465.0	0.01011	0.0006	7
467.5	0.0102	0.0006	6
470.0	0.0106	0.0006	6
472.5	0.0109	0.0008	8
475.0	0.0114	0.0007	7
477.5	0.0121	0.0008	8
480.0	0.0127	0.0008	7
482.5	0.0131	0.0008	7
485.0	0.0136	0.0007	6
487.5	0.0144	0.0007	6
490.0	0.0150	0.0007	5
492.5	0.0162	0.0014	9
495.0	0.0173	0.0010	6
497.5	0.0191	0.0014	8
500.0	0.0204	0.0011	6
502.5	0.0228	0.0012	6
505.0	0.0256	0.0013	6
507.5	0.0280	0.0010	5
510.0	0.0325	0.0011	4
512.5	0.0372	0.0012	4
515.0	0.0396	0.0012	4
517.5	0.0399	0.0015	5
520.0	0.0409	0.0009	3
522.5	0.0416	0.0014	4
525.0	0.0417	0.0010	4
527.5	0.0428	0.0017	5
530.0	0.0434	0.0011	4
532.5	0.0447	0.0017	5
535.0	0.0452	0.0012	4
537.5	0.0466	0.0015	4
540.0	0.0474	0.0010	3
542.5	0.0489	0.0016	4
545.0	0.0511	0.0011	3
547.5	0.0537	0.0016	4
550.0	0.0565	0.0011	3
552.5	0.0593	0.0012	3
555.0	0.0596	0.0012	3
557.5	0.0606	0.0014	4
560.0	0.0619	0.0010	3
562.5	0.0640	0.0015	4
565.0	0.0642	0.0009	3
567.5	0.0672	0.0014	3
570.0	0.0695	0.0011	3
572.5	0.0733	0.0017	4
575.0	0.0772	0.0011	3
577.5	0.0836	0.0016	3
580.0	0.0896	0.0012	3
582.5	0.0989	0.0016	3
585.0	0.1100	0.0012	3
587.5	0.1220	0.0018	3
590.0	0.1351	0.0012	3
592.5	0.1516	0.0017	3
595.0	0.1672	0.0014	3
597.5	0.1925	0.0019	3
600.0	0.2224	0.0017	3
602.5	0.2470	0.0023	3
605.0	0.2577	0.0019	3
607.5	0.2629	0.0028	3
610.0	0.2644	0.0019	3
612.5	0.2665	0.0023	3
615.0	0.2678	0.0019	3
617.5	0.2707	0.0026	3
620.0	0.2755	0.0025	3
622.5	0.2810	0.0039	3
625.0	0.2834	0.0028	3
627.5	0.2904	0.0039	3
630.0	0.2916	0.0027	3
632.5	0.2995	0.0038	3
635.0	0.3012	0.0028	3
637.5	0.3077	0.0049	3
640.0	0.3108	0.0028	3
642.5	0.322	0.005	3
645.0	0.325	0.003	3
647.5	0.335	0.004	3
650.0	0.340	0.003	3
652.5	0.358	0.006	3
655.0	0.371	0.003	3
657.5	0.393	0.006	3
660.0	0.410	0.004	3
662.5	0.424	0.005	3
665.0	0.429	0.004	3
667.5	0.436	0.005	3
670.0	0.439	0.004	3
672.5	0.448	0.007	3
675.0	0.448	0.004	3
677.5	0.461	0.006	3
680.0	0.465	0.004	3
682.5	0.478	0.006	3
685.0	0.486	0.004	3
687.5	0.502	0.006	3
690.0	0.516	0.004	3
692.5	0.538	0.007	3

Table 4.4.1-1: Absorption coefficient of pure water, $a_w(\lambda)$, from Pope and Fry (1997)

λ (nm)	a_w (m^{-1})	σ (m^{-1})	Percent
695.0	0.559	0.005	3
697.5	0.592	0.008	3
700.0	0.624	0.006	3
702.5	0.663	0.008	3
705.0	0.704	0.006	3
707.5	0.756	0.009	3
710.0	0.827	0.007	3
712.5	0.914	0.011	3
715.0	1.007	0.009	3
717.5	1.119	0.014	3
720.0	1.231	0.011	3
722.5	1.356	0.008	3
725.0	1.489	0.006	3
727.5	1.678	0.007	3

Table 4.4.1-1: Continued

λ (nm)	k(λ)	a(λ)
700	3.35 10^{-8}	0.6014
725	9.15 10^{-8}	1.5859
750	1.56 10^{-7}	2.6138
775	1.48 10^{-7}	2.4000
800	1.25 10^{-7}	1.9635
825	1.82 10^{-7}	2.7722
850	2.93 10^{-7}	4.3317
875	3.91 10^{-7}	5.6153
900	4.86 10^{-7}	6.7858

Table 4.4.1-2 : Imaginary part of the complex refractive index of water from Hale & Querry (1973), and for the 700-900 nm domain. The absorption coefficient of pure water, $a_w(\lambda)$, is computed as $4\pi k(\lambda)/\lambda$, with λ in meters.

4.4.2 NORMALISED VSF, TOTAL SCATTERING AND BACKSCATTERING COEFFICIENTS

The normalised volume scattering function of pure sea water is that published by Morel (1966, 1974), which can be expressed as:

$$\tilde{\beta}_w(\theta) = \frac{3}{4\pi(3+p)}(1 + p\cos^2\theta) \tag{2}$$

where the parameter p (polarisation factor at 90°) equals 0.84.

The backscattering probability corresponding to this normalised VSF is

$$\tilde{b}_{bw} = \frac{1}{2} \tag{2'}$$

The total scattering coefficient for seawater (in the salinity range 35-38 psu), $b_w(\lambda)$, is determined from Morel (1974):

$$b_w(\lambda) = 0.00288\left(\frac{\lambda}{500}\right)^{-4.32} \qquad (3)$$

Note that for freshwater it is

$$b_w(\lambda) = 0.00222\left(\frac{\lambda}{500}\right)^{-4.32} \qquad (3')$$

Note that the variation of b_w with salinity is roughly a linear function of salinity.

4.4.3 EMISSION

See section 4.5.4.1

4.5 CASE 1 WATERS IOPS

4.5.1 TOTAL ABSORPTION COEFFICIENT (PURE SEA WATER AND PHYTOPLANKTON2)

Here, the analytical approach suggested by Fig. 4.1, and which consists of explicitly modelling a_1 as the sum $[a_w + a_{p1} + a_{y1}]$ is not used, by lack of knowledge of a stable relationship (if any) between [Chl] and the associated endogenous yellow substance. The indirect approach used here rests on the consideration of $K_d(\lambda)$. Indeed, this coefficient merges the influences of all absorbing substances, without discriminating their separate contributions. Therefore a_1 is globally determined as a function of [Chl] as described in Morel and Maritorena (2000)

$$a_1(\lambda) = K_d(\lambda) u(\lambda) \qquad (8)$$

where $K_d(\lambda)$ is given as a function of $[chl]$ (see table 4.5.1-1 below) :

$$K_d(\lambda) = K_w(\lambda) + \chi(\lambda)[\mathrm{Chl}]^{e(\lambda)} \qquad (9)$$

The factor u is determined by iterations as described in Morel (1988) and Morel and Maritorena (2000). This scheme consists of introducing $b_b(\lambda)$ in the following equation

$$R(\lambda) = f(\lambda)\frac{b_b(\lambda)}{a_1(\lambda)} \qquad (10)$$

where R is the irradiance reflectance (E_u / E_d), and $b_b = b_{bw} + b_{bp1}$. The coefficient b_{bw} is calculated according to Eqs. (2') and (3) above, and b_{bp1} according to Eq. (18) below (§4.5.2.2). Then $a_1(\lambda)$ is replaced by u_1 $K_d(\lambda)$, with u_1 = 0.75, whatever the wavelength and f is set to 0.33. A first set of $R(\lambda)$ values is thus derived. Then, an exact relationship (derived from the Gershun's equation), namely

$$a_1 = K_d\, \mu_d\, [1 + R\, (\mu_d/\mu_u)]^{-1}\, [\, 1 - R + (K_d)^{-1}\, dR/dZ\,] \qquad (11)$$

---

[2] Here, "phytoplankton" means the living algal cells as well as all other particulate or dissolved matter found in open ocean, such as heterotrophic bacteria and organisms, various debris, yellow substances etc.... (see comments on Fig. 4.1).

is operated by letting μ_u equal to 0.42, by interpolating μ_d from the values given in table 4.5.1-2 below as a function of the chlorophyll concentration and wavelength, and by neglecting dR/dZ, which results in

$$a_1(\lambda) = K_d(\lambda)\mu_d [1 + (\mu_d /0.42)\, R(\lambda)]^{-1} [1 - R(\lambda)] \quad (11')$$

or

$$a_1(\lambda) = K_d(\lambda)\, u_2(\lambda) \quad (11'')$$

The first set of $R(\lambda)$ values is used to produce the spectrally varying $u_2(\lambda)$ values through Eq .11' and a new set of $a_1(\lambda)$ values through Eq. 11''. The value of a_1 shall be constrained to be higher than or equal to $a_w(\lambda)$ (from §4.4.1 above). With these adjusted $a_1(\lambda)$ values, through a second loop using Eq. (10), a more accurate set of $R(\lambda)$ values is derived, and so forth. Stable $R(\lambda)$ values (then stable $a_1(\lambda)$ values) are obtained within three loops in this iterative process. The final $a_1(\lambda)$ values are given in Table 4.5.1-3.

λ	K_w	e	χ	λ	K_w	e	χ	λ(nm)	a(λ) (m^{-1})
350	0.02710	0.77800	0.15300	530	0.04454	0.67224	0.04829	775	2.400
355	0.02380	0.76700	0.14900	535	0.04630	0.66739	0.04611	800	1.963
360	0.02160	0.75600	0.14400	540	0.04846	0.66195	0.04419	825	2.772
365	0.01880	0.73700	0.14000	545	0.05212	0.65591	0.04253	850	4.331
370	0.01770	0.72000	0.13600	550	0.05746	0.64927	0.04111	875	5.615
375	0.01595	0.70000	0.13100	555	0.06053	0.64204	0.03996	900	6.786
380	0.01510	0.68500	0.12700	560	0.06280	0.64000	0.03900		
385	0.01376	0.67300	0.12300	565	0.06507	0.63000	0.03750		
390	0.01271	0.67000	0.11900	570	0.07034	0.62300	0.03600		
395	0.01208	0.66000	0.11800	575	0.07801	0.61500	0.03400		
400	0.01042	0.64358	0.11748	580	0.09038	0.61000	0.03300		
405	0.00890	0.64776	0.12066	585	0.11076	0.61400	0.03280		
410	0.00812	0.65175	0.12259	590	0.13584	0.61800	0.03250		
415	0.00765	0.65555	0.12326	595	0.16792	0.62200	0.03300		
420	0.00758	0.65917	0.12269	600	0.22310	0.62600	0.03400		
425	0.00768	0.66259	0.12086	605	0.25838	0.63000	0.03500		
430	0.00770	0.66583	0.11779	610	0.26506	0.63400	0.03600		
435	0.00792	0.66889	0.11372	615	0.26843	0.63800	0.03750		
440	0.00885	0.67175	0.10963	620	0.27612	0.64200	0.03850		
445	0.00990	0.67443	0.10560	625	0.28400	0.64700	0.04000		
450	0.01148	0.67692	0.10165	630	0.29218	0.65300	0.04200		
455	0.01182	0.67923	0.09776	635	0.30176	0.65800	0.04300		
460	0.01188	0.68134	0.09393	640	0.31134	0.66300	0.04400		
465	0.01211	0.68327	0.09018	645	0.32553	0.66700	0.04450		
470	0.01251	0.68501	0.08649	650	0.34052	0.67200	0.04500		
475	0.01320	0.68657	0.08287	655	0.37150	0.67700	0.04600		
480	0.01444	0.68794	0.07932	660	0.41048	0.68200	0.04750		
485	0.01526	0.68903	0.07584	665	0.42947	0.68700	0.04900		
490	0.01660	0.68955	0.07242	670	0.43946	0.69500	0.05150		
495	0.01885	0.68947	0.06907	675	0.44844	0.69700	0.05200		
500	0.02188	0.68880	0.06579	680	0.46543	0.69300	0.05050		
505	0.02701	0.68753	0.06257	685	0.48642	0.66500	0.04400		
510	0.03385	0.68567	0.05943	690	0.51640	0.64000	0.03900		
515	0.04090	0.68320	0.05635	695	0.55939	0.62000	0.03400		
520	0.04214	0.68015	0.05341	700	0.62438	0.60000	0.03000		
525	0.04287	0.67649	0.05072	705	0.74200	0.60000	0.02500		
				710	0.83400	0.60000	0.02000		
				715	1.00200	0.60000	0.01500		
				720	1.17000	0.60000	0.01000		
				725	1.48500	0.60000	0.00700		
				730	1.80000	0.60000	0.00500		
				735	2.09000	0.60000	0.00200		
				740	2.38000	0.60000	0.00000		
				745	2.42000	0.60000	0.00000		
				750	2.47000	0.60000	0.00000		

Table 4.5.1-1: K_w, x and e values. Values are reproduced from Morel and Maritorena (2000), and from Morel and Antoine (1994). Above 775nm, only a*(λ) is specified (see also Table 4.4.1-1)*

Note that the K_w values in table 4.5.1-1 have been obtained by using the absorption and scattering coefficients of pure sea water as described in sections 4.4.1 and 4.4.2 ($K_w = a_w + 0.5 b_w$).

	0.03	0.1	0.3	1.	3.	10.
350.	0.770	0.769	0.766	0.767	0.767	0.767
400.	0.770	0.769	0.766	0.767	0.767	0.767
412.	0.765	0.770	0.774	0.779	0.782	0.782
443.	0.800	0.797	0.796	0.797	0.799	0.799
490.	0.841	0.824	0.808	0.797	0.791	0.791
510.	0.872	0.855	0.834	0.811	0.796	0.796
555.	0.892	0.879	0.858	0.827	0.795	0.795
620.	0.911	0.908	0.902	0.890	0.871	0.871
670.	0.914	0.912	0.909	0.901	0.890	0.890
700.	0.914	0.912	0.909	0.901	0.890	0.890
710.	0.914	0.912	0.909	0.901	0.890	0.890

Table 4.5.1-2: mean cosines of the downwelling irradiance (μ_d) as a function of wavelength (lines) and chlorophyll concentration (columns), sun zenith angle: 30°, no Raman emission.

	0.03	0.1	0.3	1	3	10
412.5	0.0115643	0.0228673	0.0445606	0.095627	0.194528	0.425296
442.5	0.0126095	0.0223262	0.0415189	0.0877143	0.179471	0.399036
490.0	0.0173563	0.0234732	0.0358357	0.0663681	0.128137	0.280947
510.0	0.0325	0.0372764	0.0470969	0.0713008	0.120455	0.244057
560.0	0.0619	0.0619	0.0672771	0.0807731	0.106826	0.174669
620.0	0.2755	0.2755	0.2755	0.276348	0.301871	0.375383
665.0	0.429	0.429	0.429	0.429	0.467546	0.58095
681.25	0.4715	0.4715	0.4715	0.4715	0.504934	0.617897
708.5	0.7915	0.7915	0.7915	0.7915	0.7915	0.7915

Table 4.5.1-3:total absorption coefficients a_1 (m^{-1}), computed as function of Chl and λ through eq. (8) to (11"), with μ_d from table 4.5.1-2 above.

4.5.2 NORMALISED VSF, TOTAL SCATTERING, AND BACKSCATTERING COEFFICIENTS

4.5.2.1 Pure Sea Water

See section 4.4 above.

4.5.2.2 Case 1 Waters Particles (phytoplankton and its retinue)

The normalised VSF for Case 1 waters particles is obtained as a mixture of two separately computed VSFs (Fig. 4.2). The first one (Table 4.5.2-1) corresponds to a population of "small" non-absorbing particles of spheroidal shape, with a relative index of refraction equal to 1.06, and assumed to obey a Junge law with the exponent set equal to –4.2. The second population corresponding to "large" particles (Table 4.5.2-2) is identical except that the Junge exponent is equal to –3. The weighted sum of these two VSFs provides

$$\tilde{\beta}_{pl}(\theta, \mathrm{Chl}) = w_s(\mathrm{Chl})\ \tilde{\beta}_{pl,s}(\theta) + w_l(\mathrm{Chl})\ \tilde{\beta}_{pl,l}(\theta) \qquad (12)$$

where the subscripts s and l stand for small and large particles, respectively, and where the weights w_s and w_l are such that :

$$w_s(\mathrm{Chl}) + w_l(\mathrm{Chl}) = 1 \qquad (13)$$

$$w_s(\mathrm{Chl}) = 0.855\ (0.5 - 0.25\ \log_{10}(\mathrm{Chl})) \qquad (14)$$

The normalised VSF computed through Eq. (12) are assumed to be wavelength independent (no change in shape).

The backscattering efficiency for Case 1 water particles that derives from the use of the above chlorophyll-varying normalised VSF exactly matches the following expression (from Morel and Maritorena, 2000) :

$$\tilde{b}_{bpl}(\lambda) = 0.002 + [0.01\ [0.5 - 0.25\log_{10}(\mathrm{chl})]] \qquad (15)$$

At 550 nm, the particle scattering coefficient, $b_{pl}(550)$, is taken from Loisel and Morel (1998):

$$b_{pl}(550) = A_{bpl}.[\mathrm{chl}]^{B_{pl}} \qquad (16)$$

where A_{bpl} and B_{bpl} equal 0.416 and 0.766, respectively. The factor of variation in A_{bpl} equals 1.3.

θ	$\tilde{\beta}(\theta)$	θ	$\tilde{\beta}(\theta)$	θ	$\tilde{\beta}(\theta)$	θ	$\tilde{\beta}(\theta)$
0.	42.282829537580	47.0	2.2451516277360D-02	94.0	2.7766892922530D-03	141.0	2.0547500762672D-03
1.0	34.958732391211	48.0	2.1023504641344D-02	95.0	2.7211555064079D-03	142.0	2.0626834742451D-03
2.0	23.065450213275	49.0	1.9706560577018D-02	96.0	2.6576883225850D-03	143.0	2.0626834742451D-03
3.0	15.406801674179	50.0	1.8492750686405D-02	97.0	2.6021545367400D-03	144.0	2.0706168722230D-03
4.0	10.720368953898	51.0	1.7382074969504D-02	98.0	2.5545541488728D-03	145.0	2.0706168722230D-03
5.0	7.6237177877997	52.0	1.6358666630359D-02	99.0	2.5069537610056D-03	146.0	2.0785502702008D-03
6.0	5.5174720252582	53.0	1.5406658873015D-02	100.0	2.4593533731384D-03	147.0	2.0785502702008D-03
7.0	4.0755214089952	54.0	1.4533985095450D-02	101.0	2.4196863832490D-03	148.0	2.0864836681787D-03
8.0	3.0647033724414	55.0	1.3716845103730D-02	102.0	2.3800193933597D-03	149.0	2.0944170661566D-03
9.0	2.3450331082773	56.0	1.2971105693810D-02	103.0	2.3482858014483D-03	150.0	2.0944170661566D-03
10.0	1.8249354036444	57.0	1.2272966671758D-02	104.0	2.3165522095368D-03	151.0	2.1023504641344D-03
11.0	1.4415460129661	58.0	1.1622428037573D-02	105.0	2.2848186176253D-03	152.0	2.1023504641344D-03
12.0	1.1551186123732	59.0	1.1019489791255D-02	106.0	2.2530850257139D-03	153.0	2.1102838621123D-03
13.0	0.93748963904439	60.0	1.0464151932805D-02	107.0	2.2292848317803D-03	154.0	2.1102838621123D-03
14.0	0.76994420714985	61.0	9.9405476662657D-03	108.0	2.2054846378467D-03	155.0	2.1182172600901D-03
15.0	0.63911454109686	62.0	9.4566103896159D-03	109.0	2.1896178418909D-03	156.0	2.1182172600901D-03
16.0	0.53574236544527	63.0	9.0044067048776D-03	110.0	2.1658176479573D-03	157.0	2.1261506580680D-03
17.0	0.45312395890378	64.0	8.5760032140728D-03	111.0	2.1499508520016D-03	158.0	2.1340840560459D-03
18.0	0.38633268132813	65.0	8.1793333151796D-03	112.0	2.1340840560459D-03	159.0	2.1340840560459D-03
19.0	0.33187783760806	66.0	7.7985302122420D-03	113.0	2.1182172600901D-03	160.0	2.1420174540237D-03
20.0	0.28700653864525	67.0	7.4494607012159D-03	114.0	2.1023504641344D-03	161.0	2.1420174540237D-03
21.0	0.24977510193512	68.0	7.1162579861456D-03	115.0	2.0944170661566D-03	162.0	2.1499508520016D-03
22.0	0.21861271467807	69.0	6.7989220670309D-03	116.0	2.0785502702008D-03	163.0	2.1499508520016D-03
23.0	0.19234523397335	70.0	6.5053863418499D-03	117.0	2.0706168722230D-03	164.0	2.1499508520016D-03
24.0	0.17006031905353	71.0	6.2277174126246D-03	118.0	2.0626834742451D-03	165.0	2.1578842499795D-03
25.0	0.15102809730463	72.0	5.9579818813772D-03	119.0	2.0547500762672D-03	166.0	2.1578842499795D-03
26.0	0.13469323086820	73.0	5.7041131460855D-03	120.0	2.0468166782894D-03	167.0	2.1658176479573D-03
27.0	0.12058764926356	74.0	5.4661112067495D-03	121.0	2.0468166782894D-03	168.0	2.1658176479573D-03
28.0	0.10834641618371	75.0	5.2360426653914D-03	122.0	2.0388832803115D-03	169.0	2.1658176479573D-03
29.0	9.7675995903483D-02	76.0	5.0218409199890D-03	123.0	2.0388832803115D-03	170.0	2.1737510459352D-03
30.0	8.8330453085557D-02	77.0	4.8235059705424D-03	124.0	2.0309498823336D-03	171.0	2.1737510459352D-03
31.0	8.0119386178466D-02	78.0	4.6331044190736D-03	125.0	2.0309498823336D-03	172.0	2.1737510459352D-03
32.0	7.2868260426697D-02	79.0	4.4506362655827D-03	126.0	2.0309498823336D-03	173.0	2.1816844439131D-03
33.0	6.6442208064625D-02	80.0	4.2840349080475D-03	127.0	2.0230164843558D-03	174.0	2.1816844439131D-03
34.0	6.0730161520562D-02	81.0	4.1253669484902D-03	128.0	2.0230164843558D-03	175.0	2.1816844439131D-03
35.0	5.5636920018772D-02	82.0	3.9746323869107D-03	129.0	2.0230164843558D-03	176.0	2.1816844439131D-03
36.0	5.1091082977455D-02	83.0	3.8397646212870D-03	130.0	2.0230164843558D-03	177.0	2.1816844439131D-03
37.0	4.7005383018854D-02	84.0	3.7048968556633D-03	131.0	2.0309498823336D-03	178.0	2.1896178418909D-03
38.0	4.3332219755103D-02	85.0	3.5858958859953D-03	132.0	2.0309498823336D-03	179.0	2.1896178418909D-03
39.0	4.0016059400355D-02	86.0	3.4748283143052D-03	133.0	2.0309498823336D-03	180.0	2.1975512398688D-03
40.0	3.7025168362699D-02	87.0	3.3637607426151D-03	134.0	2.0309498823336D-03		
41.0	3.4311946254269D-02	88.0	3.2606265689028D-03	135.0	2.0388832803115D-03		
42.0	3.1852592881131D-02	89.0	3.1654257931684D-03	136.0	2.0388832803115D-03		
43.0	2.9615374651373D-02	90.0	3.0781584154119D-03	137.0	2.0388832803115D-03		
44.0	2.7576491371061D-02	91.0	2.9988244356332D-03	138.0	2.0468166782894D-03		
45.0	2.5712142846263D-02	92.0	2.9194904558546D-03	139.0	2.0468166782894D-03		
46.0	2.4014395679000D-02	93.0	2.8480898740538D-03	140.0	2.0547500762672D-03		

Table 4.5.2-1: normalised VSF for small particles (see text)

θ	$\tilde{\beta}(\theta)$	θ	$\tilde{\beta}(\theta)$	θ	$\tilde{\beta}(\theta)$	θ	$\tilde{\beta}(\theta)$
0.	99.652707830456	47.0	5.4847330202340D-03	94.0	4.9069761508587D-04	141.0	1.8994746390421D-04
1.0	73.481769997167	48.0	5.1127525700883D-03	95.0	4.6695418209784D-04	142.0	1.8994746390421D-04
2.0	36.927670628662	49.0	4.7803445082559D-03	96.0	4.5112522677249D-04	143.0	1.8203298624153D-04
3.0	20.353147764054	50.0	4.4795943570742D-03	97.0	4.2738179378447D-04	144.0	1.8203298624153D-04
4.0	12.851924552535	51.0	4.2184165942059D-03	98.0	4.1155283845912D-04	145.0	1.8203298624153D-04
5.0	8.5125509962107	52.0	3.9809822643257D-03	99.0	3.9572388313377D-04	146.0	1.8203298624153D-04
6.0	5.7523452534420	53.0	3.7752058450961D-03	100.0	3.7989492780842D-04	147.0	1.8203298624153D-04
7.0	4.0082080674853	54.0	3.5852583811919D-03	101.0	3.7198045014574D-04	148.0	1.8203298624153D-04
8.0	2.8410204741822	55.0	3.4269688279384D-03	102.0	3.5615149482039D-04	149.0	1.8203298624153D-04
9.0	2.0484251086536	56.0	3.2765937523476D-03	103.0	3.4823701715771D-04	150.0	1.8203298624153D-04
10.0	1.5064337638360	57.0	3.1499621097448D-03	104.0	3.3240806183236D-04	151.0	1.8203298624153D-04
11.0	1.1225736827185	58.0	3.0312449448046D-03	105.0	3.2449358416969D-04	152.0	1.8203298624153D-04
12.0	0.85049768410875	59.0	2.9283567351899D-03	106.0	3.1657910650701D-04	153.0	1.8203298624153D-04
13.0	0.65265948597486	60.0	2.8333830032378D-03	107.0	3.0866462884434D-04	154.0	1.8203298624153D-04
14.0	0.50766625519465	61.0	2.7463237489483D-03	108.0	3.0075015118166D-04	155.0	1.8203298624153D-04
15.0	0.39944368763522	62.0	2.6671789723216D-03	109.0	2.9283567351899D-04	156.0	1.8203298624153D-04
16.0	0.31787708084369	63.0	2.5880341956948D-03	110.0	2.8492119585631D-04	157.0	1.8203298624153D-04
17.0	0.25567720089273	64.0	2.5168038967308D-03	111.0	2.8492119585631D-04	158.0	1.8203298624153D-04
18.0	0.20747803192703	65.0	2.4455735977667D-03	112.0	2.7700671819364D-04	159.0	1.8203298624153D-04
19.0	0.17005838153790	66.0	2.3664288211399D-03	113.0	2.6909224053096D-04	160.0	1.8203298624153D-04
20.0	0.14039491925820	67.0	2.2872840445132D-03	114.0	2.6909224053096D-04	161.0	1.8203298624153D-04
21.0	0.11692057851070	68.0	2.2081392678864D-03	115.0	2.6117776286829D-04	162.0	1.8203298624153D-04
22.0	9.8052463762885D-02	69.0	2.1210800135970D-03	116.0	2.5326328520561D-04	163.0	1.8203298624153D-04
23.0	8.2753778440933D-02	70.0	2.0340207593076D-03	117.0	2.5326328520561D-04	164.0	1.8203298624153D-04
24.0	7.0351791943521D-02	71.0	1.9390470273555D-03	118.0	2.4534880754293D-04	165.0	1.8203298624153D-04
25.0	6.0102543370356D-02	72.0	1.8361588177407D-03	119.0	2.4534880754293D-04	166.0	1.8203298624153D-04
26.0	5.1681539137270D-02	73.0	1.7332706081259D-03	120.0	2.3743432988026D-04	167.0	1.8203298624153D-04
27.0	4.4661397450477D-02	74.0	1.6303823985111D-03	121.0	2.3743432988026D-04	168.0	1.8203298624153D-04
28.0	3.8780940547109D-02	75.0	1.5274941888963D-03	122.0	2.3743432988026D-04	169.0	1.8203298624153D-04
29.0	3.3858135440925D-02	76.0	1.4246059792816D-03	123.0	2.2951985221758D-04	170.0	1.8203298624153D-04
30.0	2.9663462279707D-02	77.0	1.3296322473295D-03	124.0	2.2951985221758D-04	171.0	1.8203298624153D-04
31.0	2.6125690764491D-02	78.0	1.2425729930400D-03	125.0	2.2160537455491D-04	172.0	1.8203298624153D-04
32.0	2.3094445819687D-02	79.0	1.1555137387506D-03	126.0	2.2160537455491D-04	173.0	1.8203298624153D-04
33.0	2.0490582668666D-02	80.0	1.0842834397865D-03	127.0	2.2160537455491D-04	174.0	1.8203298624153D-04
34.0	1.8258699967792D-02	81.0	1.0130531408224D-03	128.0	2.1369089689223D-04	175.0	1.8203298624153D-04
35.0	1.6319652940437D-02	82.0	9.4973731952104D-04	129.0	2.1369089689223D-04	176.0	1.8994746390421D-04
36.0	1.4641783675949D-02	83.0	8.9433597588231D-04	130.0	2.1369089689223D-04	177.0	1.8994746390421D-04
37.0	1.3185519786017D-02	84.0	8.3893463224358D-04	131.0	2.0577641922956D-04	178.0	1.8994746390421D-04
38.0	1.1903374404664D-02	85.0	7.9144776626753D-04	132.0	2.0577641922956D-04	179.0	1.8994746390421D-04
39.0	1.0787433054226D-02	86.0	7.5187537795416D-04	133.0	2.0577641922956D-04	180.0	2.1369089689223D-04
40.0	9.8060378240547D-03	87.0	7.0438851197810D-04	134.0	1.9786194156688D-04		
41.0	8.9433597588231D-03	88.0	6.6481612366473D-04	135.0	1.9786194156688D-04		
42.0	8.1756554255436D-03	89.0	6.2524373535135D-04	136.0	1.9786194156688D-04		
43.0	7.5029248242162D-03	90.0	5.9358582470065D-04	137.0	1.8994746390421D-04		
44.0	6.9093389995156D-03	91.0	5.6192791404995D-04	138.0	1.8994746390421D-04		
45.0	6.3790689961163D-03	92.0	5.3818448106192D-04	139.0	1.8994746390421D-04		
46.0	5.9042003363558D-03	93.0	5.1444104807390D-04	140.0	1.8994746390421D-04		

Table 4.5.2-2: normalised VSF for large particles (see text)

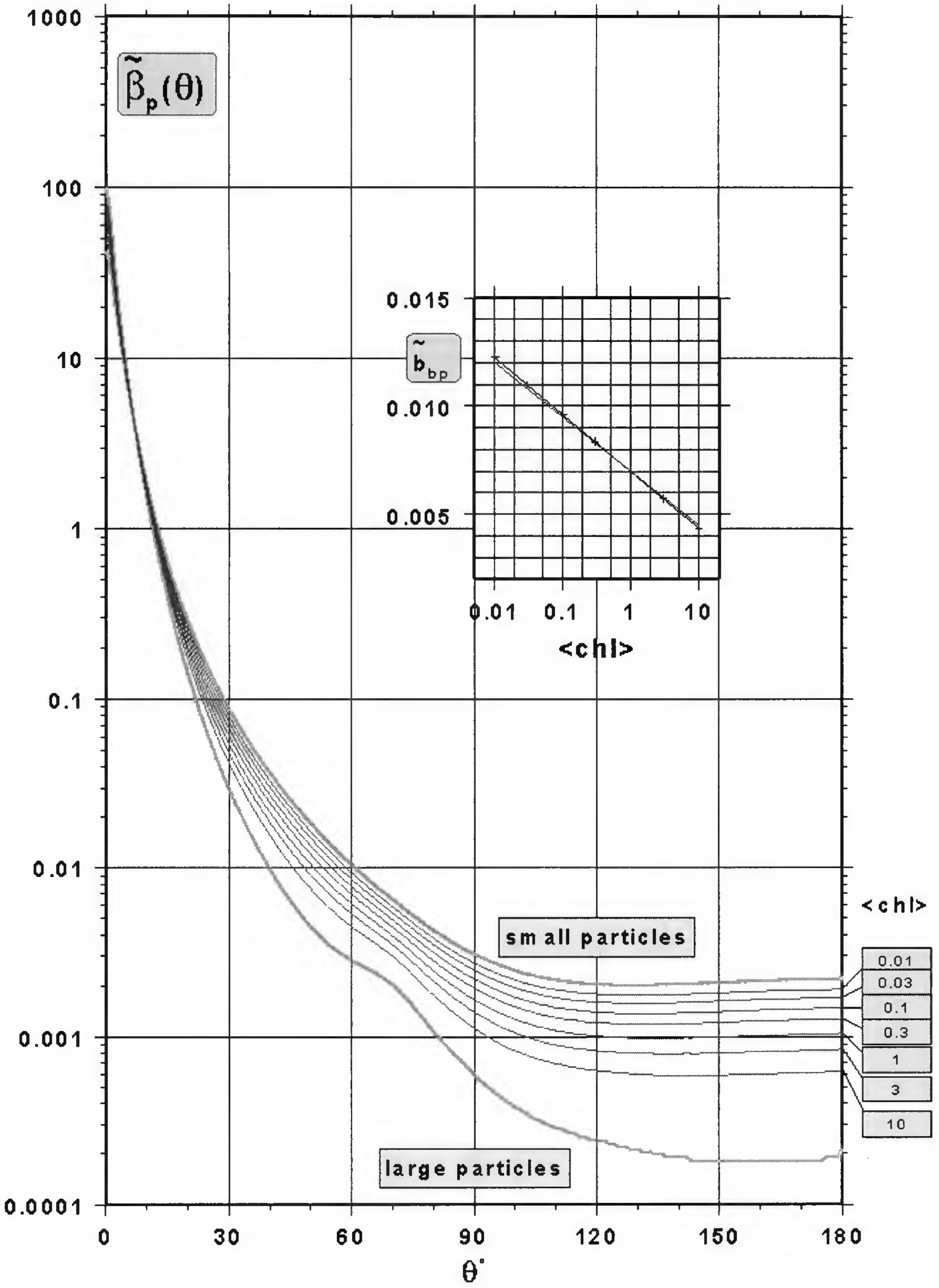

Figure 4.2. : normalised VSFs of large, small particles (blue curves; tables 4.5.2-1 & 4.5.2-2), and of mixed populations following a mixing rule depending on Chl (Eqs. (12) & (13)). These "mixed VSFs" are shown as red curves, and the corresponding Chl concentration is indicated in the green box on the side of the figure. In insert is shown the resulting backscattering probability, as a function of the Chl concentration (Eq. 15)

At any other wavelength, the particle scattering coefficient, $b_{p1}(\lambda)$, is expressed from its value at 550 nm according to :

$$b_{p1}(\lambda) = b_{p1}(550)\left(\frac{\lambda}{550}\right)^{-\nu} \tag{17}$$

where $\nu = 0.5\left[0.3 - \log_{10}(chl)\right]$ when $[chl] < 2$ mg m^{-3}

and $\nu = 0$ when $[chl] \geq 2$ mg m^{-3}

From the above equations, it results that the backscattering coefficient for Case 1 water particles is expressed as :

$$b_{bp1}(\lambda) = \left\{0.002 + \left[0.01\ \left[0.5 - 0.25\log_{10}(chl)\right]\ \right]\right\}\left\{b_{p1}(550)\left(\frac{\lambda}{550}\right)^{-\nu}\right\} \tag{18}$$

4.5.3 TOTAL IOPS IN CASE 1 WATERS

Case 1 waters absorption and backscattering coefficients denoted $a_1(\lambda)$ and $b_{b1}(\lambda)$, respectively, as well as the normalised VSF for these waters, denoted $\tilde{\beta}(\theta,\lambda)$, can be expressed as:

$a_1(\lambda)$ as per section 4.5.1

$$b_{b1}(\lambda) = 0.5 b_w(\lambda) + \tilde{b}_{bp1}(\lambda) b_{p1}(\lambda) \tag{19}$$

$$\tilde{\beta}_1(\theta,\lambda) = \eta(\lambda)\tilde{\beta}_w(\theta) + (1-\eta(\lambda))\tilde{\beta}_{p1}(\theta) \tag{20}$$

where

$$\eta(\lambda) = b_w(\lambda) / \left(b_w(\lambda) + b_{p1}(\lambda)\right) \tag{21}$$

4.5.4 WARNING CONCERNING THE USE OF THE MODEL FOR CASE 1 WATERS IOPS: STATE-OF-THE-ART AND UNCERTAINTIES

4.5.4.1 Raman Emission

The Raman emission by water molecules is a trans-spectral (or inelastic) scattering process by which absorbed energy at a given wavelength λ' is re-emitted as radiation at longer wavelengths around λ. The Raman VSF $\beta^R(\theta)$ is symmetrical with respect to $\theta = \pi/2$ and expresses as :

$$\beta^R(\theta) = 0.067\ (1 + 0.55\cos^2(\theta)) \qquad (4)$$

The Raman emission undergoes a frequency shift that is independent of the incident frequency and thus occurs within the whole (visible) spectrum. According to Walrafen (1967), the shape of the redistribution function $f^R(\kappa_R)$ is the sum of 4 Gaussian functions (i = 1 to 4) :

$$f^R(\kappa_R) = \left[\left(\frac{\pi}{4\ln(2)}\right)^{1/2} \sum_1^4 A_i\right]^{-1} \sum_1^4 A_i \frac{1}{\Delta\kappa_i} \exp\left(-\frac{(\kappa_R - \kappa_i)^2}{\Delta\kappa_i^2}\right) \qquad (5)$$

where κ_R is the wavenumber shift of the Raman emission, κ_i is the centre of the ith Gaussian function, $\Delta\kappa_i$ the width at half maximum of this function and the A_i's are the weights of each function (see table 4.5.4-1).

i	A_i	κ_i (cm^{-1})	$\Delta\kappa_i$ (cm^{-1})
1	0.41	3250	210
2	0.39	3425	175
3	0.10	3530	140
4	0.10	3625	140

Table 4.5.4-1 : Data from Walrafen (1967)

To an incident (exciting) radiation with a wavelength λ' and a wavenumber κ' will correspond a Raman emission within a spectral band described by Eq. (5) such as $\kappa = \kappa' - \kappa^R$, leading to redistribution functions expressed in terms of wavelengths $f^R(\lambda' \rightarrow \lambda)$ as shown in Fig. 4.3 below.

The magnitude of the phenomenon is expressed through the Raman coefficient $a^R(\lambda')$ through

$$a^R(\lambda') = \int_{\lambda'}^{\infty} b^R(\lambda' \rightarrow \lambda)\, d\lambda \qquad (6)$$

where b^R is the Raman scattering coefficient for an exciting wavelength λ' and an emission at wavelength λ ($\lambda > \lambda'$). This coefficient, according to recent determinations at 488 nm, is :

$$a^R(488) = 2.6\ 10^{-4}\ m^{-1} \quad (7)$$

it varies according to a λ^{-5} law.

This phenomenon is important in clear Case 1 waters (low Chl) to the extent that the elastic scattering is low, in the red part of the spectrum in particular. With an almost isotropic function (Eq. (4)), it strongly modifies the upward radiance distribution and thus affects the Q (and f/Q) behaviour.

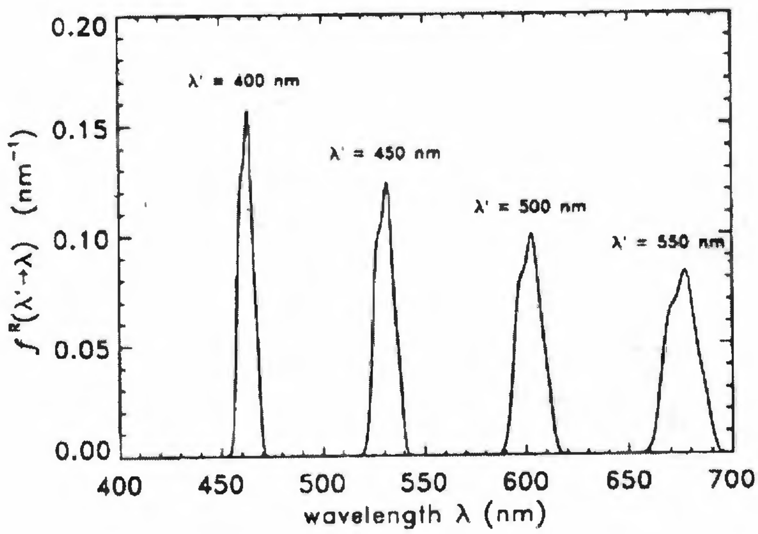

Figure 4.3. : the Raman wavelength redistribution function $f^R(\lambda' \rightarrow \lambda)$, for selected incident wavelengths λ'. Figure reproduced from Mobley (1994).

Conversely the Raman emission at a fixed wavelength λ is excited by a spectral band centred on λ', the shape of which is approximately the reverse image of those shown in this figure.

4.5.4.2 Fluorescence by Phytoplankton

The emission of fluorescence by phytoplankton is isotropic ($\tilde{\beta}^F(\theta)$ = constant). Its intensity depends on the chlorophyll-a concentration and on the quantum yield for fluorescence, ϕ_f. This yield ϕ_f is defined as the number of photons emitted divided by the number of photons absorbed by the algal cells. It is known as being varying within a factor of 10, approximately with the lower values observed near the surface (Maritorena *et al.* 2000). If ϕ_f is fixed, this emission can be (but has not been) incorporated into the IOP model for Case 1 waters. Any radiation within the 380-680 nm domain, after being weighted by the algal absorption spectrum, is able to excite the Chl-a fluorescence around 683 nm. In contrast, the emission spectrum is independent from the excitation spectrum and is currently modelled (*e.g.*, see Gordon, 1979; Kattawar and Valerio, 1982; Kishino et al., 1984; Sathyendranath and Platt, 1998) as a Gaussian spectral distribution, peaked around 683 nm, and with a standard deviation σ = 10.64 nm, corresponding to a width of about 25 nm at half maximum (see Fig. 4.4). This curve, modelled through $\exp(-(\lambda - 683) / 2\sigma^2)$ accounts very well for observations for natural populations as well as for algae grown in culture, except beyond 710 nm where a weak shoulder (around 730 nm) often appears.

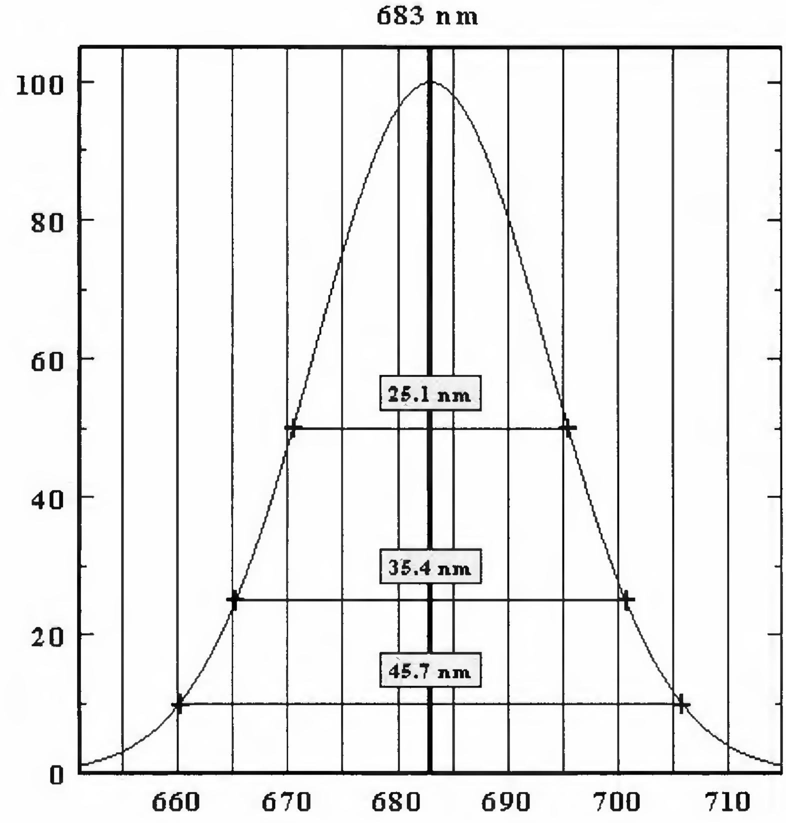

Figure 4.4. : Typical Gaussian spectral distribution for the Chl-a fluorescence, peaked around 683 nm, and with a standard deviation σ = 10.64 nm, corresponding to a width of about 25 nm at half maximum

4.5.4.3 Fluorescence by Endogenous Yellow Substance

This term which may be important in presence of high amount of yellow substance is less documented than the chlorophyll-a fluorescence, and depends on the chemical composition of the organic matter collectively forming the "yellow substance". This emission is believed to be negligible in Case 1 waters, and has not been incorporated within the IOP model for Case 1 waters.

4.5.4.4 Other Warnings and Limitations

The Case 1 waters IOP model include some uncertainties in its parameterisation or even some assumptions. These properties with their corresponding uncertainties are listed in table 4.5.4-2 below. The column "Expectation" indicates which scientific evolutions are foreseen.

IOP	Equation number or table	Comment	Expectation
$a_w(\lambda)$	Table 4.4.1-1	Known with sufficient accuracy	Will not evolve
$a^R(\lambda)$	Eqs. (6) and (7), Table 4.5.4-1	Known with sufficient accuracy	Will not evolve
$a_I\ (\lambda)$	Eqs. (8) to (11''), Table 4.5.1-1 and 4.5.1-2	Well documented for World Ocean (but see the large variation factor). Seasonal variability under investigation.	Will not evolve significantly
$b_w(\lambda)$	Eqs. (3) and (3')	Known with sufficient accuracy	Will not evolve
$b_{pI}(\lambda)$	Eqs. (16) and (17)	Well documented for World Ocean (but see the large variation factor)	Will not evolve significantly
$b_{bpI}(\lambda)$	Eqs. (15) and (18)	Best guess	Could evolve
$\tilde{\beta}_w(\theta,\lambda)$	Eqs. (2) and (2')	Slight uncertainty on *p*; very weak influence on the result	Will not evolve
$\beta^R(\theta)$	Eqs. (4) and (5)	Known with sufficient accuracy	Will not evolve
$\tilde{\beta}_p(\theta)$	Eqs. (12) to (14), Table 4.5.2-1 and Table 4.5.2-2		Could evolve

Table 4.5.4-2: Comments on model parameterisation

As a general warning, the present model is based on statistical relationships (between K_d or b_p and Chl) that represent "average" situations. Therefore, its use as a predictive tool leads to various results when the large standard errors associated with each input parameters are taken into account; it may fail when compared case by case to actual data (as reflectance for instance).

4.6 Case 2 waters IOPs

4.6.1 Introduction

Water constituents comprise a large number of different substances, which include mineralic dissolved and particulate compounds, a large variety of organic macromolecules, living organisms such as phytoplankton, zooplankton, bacteria etc. and their debris and excrements. All of these constituents of water exhibit different optically properties concerning scattering and absorption.

For the purpose of optical remote sensing this diversity of substances has to be grouped into a small number of classes each of which includes constituents with similar optical properties and / or correlated concentrations. For the majority of the world ocean areas it is sufficient to comprise all substances into one group using phytoplankton chlorophyll *a* as a proxy. This type of water is called case I water. The concentration of this class of substances - in terms of chlorophyll *a* - can be derived from the blue to green shift of the water colour. In many coastal waters one needs more than one class of substances to describe the variability of water colour. By tradition and experience three classes are defined: (1) phytoplankton pigment with chlorophyll *a* as a proxy, (2) the dry weight of all particles (total suspended matter, TSM) and (3) the absorption caused by the dissolved fraction of all water constituents (gelbstoff). Dissolved and particulate is defined by the pore size of the filter used for separation, which traditionally was 0.45 μm and nowadays is 0.2 μm.

However, each of the three groups of substances is variable with respect to their composition and thus their chemical, physical and in particular optical properties. Any remote sensing system and retrieval algorithm has to take this variability into account.

For the MERIS case 2 water algorithm two approaches have been prepared. One approach, endorsed in the previous issue of this document, is to base the algorithm directly on optical and concentration measurements and harmonize the case 2 with the case 1 algorithm. The other approach, which is described here, uses optical components, which do not directly reflect a water constituent, but which describe the dominant optical property of a group of substances. The quantitative relationship between the concentration of a bio-geochemical component and its optical proxy is described by a conversion factor or equation, which can be adapted by the user based on his experience to local conditions.

This alternative model is based on the experience with the first MERIS reference model (Version of 1996) as well as on measurements of water constituents (concentrations, scattering and absorption) during the marine optics projects COASTlOOC, COLORS and MAPP.

Due to the restrictions of the MERIS processor, only three components can be defined. For this model these are:

(1) phytoplankton pigment absorption a_{pig},

(2) absorption of all other substances a_{yp}(dissolved gelbstoff a_y and bleached particulate matter a_p) and

(3) scattering of all particles b_p with the assumption that the scattering component is not absorbing, *i.e.* that the absorption, which modifies the volume scattering of absorbing particles, is covered by the absorption a_p.

All three optical components are defined for the wavelength of MERIS band 2 (442 nm).

Phytoplankton pigment absorption $a_{pig}(442)$ is related to chlorophyll a concentration (in µg/l), the scattering of non absorbing particles b_p is related to the dry weight of total suspended matter (TSM, in mg/l) and the sum of the absorption of gelbstoff a_y and of the bleached particulate matter, a_p, is related to the gelbstoff absorption $a_y(442)$. The mean conversion factors and equations based on the results of COASTIOOC, COLORS, MAPP are submitted with the product as well as the reverse function so that the user can replace them by his own to convert the digital numbers of the data product into concentration units of his choice.

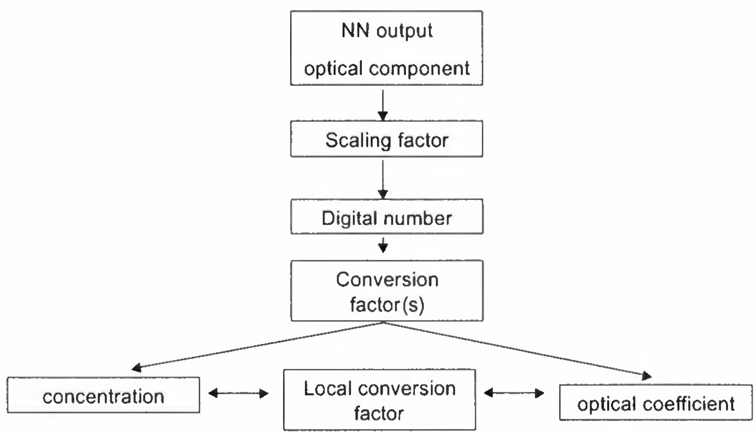

Figure 4.5: Processing to provide different case 2 water products

4.6.2 COMPONENTS

4.6.2.1 Scattering particles

In order to include also particles with a flat scattering spectrum (as found in many COASTIOOC and COLORS samples), an exponent of s_{bp}=0.4 is used with a standard deviation of 0.2. The scattering spectrum is computed using

$$s_{bp}=0.4+randn*0.2 \quad (22)$$

$$b_p(\lambda) = b_p(442) \,.\, (\lambda/442)^{-sbp} \quad (23)$$

with randn, the normal distributed random number and $b_p(442)$, the particle scattering at the reference wavelength 442nm.

Only one phase function is used for the particle scattering component, which is that of Petzold as described in Mobley (1994) and reproduced in table 4.6.1.1-1 below. This phase function yields a backscattering factor b_b/b of 0.02, which about is the mean backscattering factor of the Helgoland time series measured with the BB-4 instrument.

θ	$\tilde{\beta}_{p1}(\theta)$	θ	$\tilde{\beta}_{p1}(\theta)$
1.00E-01	1.77E+03	5.00E+01	2.28E-02
1.26E-01	1.30E+03	5.50E+01	1.70E-02
1.58E-01	9.50E+02	6.00E+01	1.31E-02
2.00E-01	6.99E+02	6.50E+01	1.05E-02
2.51E-01	5.14E+02	7.00E+01	8.49E-03
3.16E-01	3.76E+02	7.50E+01	6.98E-03
3.98E-01	2.76E+02	8.00E+01	5.84E-03
5.01E-01	2.01E+02	8.50E+01	4.95E-03
6.31E-01	1.44E+02	9.00E+01	4.29E-03
7.94E-01	1.02E+02	9.50E+01	3.78E-03
1.00E+00	7.16E+01	1.00E+02	3.40E-03
1.26E+00	4.96E+01	1.05E+02	3.12E-03
1.58E+00	3.40E+01	1.10E+02	2.91E-03
2.00E+00	2.28E+01	1.15E+02	2.80E-03
2.51E+00	1.52E+01	1.20E+02	2.69E-03
3.16E+00	1.00E+01	1.25E+02	2.57E-03
3.98E+00	6.58E+00	1.30E+02	2.48E-03
5.01E+00	4.30E+00	1.35E+02	2.38E-03
6.31E+00	2.81E+00	1.40E+02	2.33E-03
7.94E+00	1.82E+00	1.45E+02	2.31E-03
1.00E+01	1.15E+00	1.50E+02	2.36E-03
1.50E+01	4.89E-01	1.55E+02	2.51E-03
2.00E+01	2.44E-01	1.60E+02	2.66E-03
2.50E+01	1.47E-01	1.65E+02	2.83E-03
3.00E+01	8.61E-02	1.70E+02	3.03E-03
3.50E+01	5.93E-02	1.75E+02	3.09E-03
4.00E+01	4.21E-02	1.80E+02	3.15E-03
4.50E+01	3.07E-02		

Table 4.6.2.1-1. Normalised volume scattering function for marine particles as derived by Mobley (1994) from Petzold's measurements.

4.6.2.2 Absorption of bleached particles and gelbstoff

The absorption of all constituents other than phytoplankton pigments is defined here as the sum of the absorption by gelbstoff (*i.e.* of any material which passes a filter with a pore size of about 0.2 µm) and the absorption by the bleached filter pad, *i.e.* of any material, which remains on a filter of type Whatman GF/F after bleaching. The absorption spectrum is described by an exponential decrease so that the absorption a at any wavelength of MERIS can be computed by

$$a(\lambda) = a(442).e^{-s.(442-\lambda)} \tag{24}$$

with $a(442)$ the absorption at the reference wavelength, *i.e.* 442 nm (MERIS band 2) and an absorption exponent s which is different for the dissolved and the particulate fraction. This exponent has been derived from measurements by fitting an exponential curve to a measured absorption spectrum. In case of the Helgoland data set, the exponent was determined for the most relevant wavelength range 400 – 550 nm. For the dissolved part it is 0.0138 ± 0.00284 and for the particulate part 0.0072 ± 0.00108

COASTlOOC values have been derived from the wavelength range 350-500, this gives a higher mean exponent of 0.0176 ± 0.002. When using this wavelength range we got a mean exponent of 0.0154 ± 0.0019 from the Helgoland series.

The mean exponent of particle absorption of the COASTlOOC data set is 0.0123 with a standard deviation of 0.00126, again derived from the wavelength range 350 – 500 nm.

Since the dissolved and particulate absorption fraction has to be combined to one, i.e. the absorption of all water constituents except phytoplankton pigments, a_y, we use the covariance between the dissolved and particulate absorption from the Helgoland data set, as expressed in the following relationships with randu, the random number from a uniform distribution between 0 and 1:

$$a_{yd}(442) = [\ 0.005 \ ...\ 1.5] \quad (25)$$
$$a_{yd}(442)=\exp(\mathbf{ln}\ (0.005)+randu*(\mathbf{ln}\ (1.5)- \mathbf{ln}\ (0.005))) \quad (26)$$
$$a_{yp}(442)= 2*rand*a_{yd}(442) \quad (27)$$

The spectral exponent was computed as:

$$s_{yd} = 0.014 + randn*0.003 \quad (28)$$
$$s_{yp} = 0.007 + randn*0.001 \quad (29)$$
$$a_{yd}(\lambda) = a_{yd}(442) * \exp(-s_{yd}*(\lambda - 442)) \quad (30)$$
$$a_{yp}(\lambda) = a_{yp}(442) * \exp(-s_{yp}*(\lambda - 442)) \quad (31)$$

4.6.2.3 Pigment Absorption

The pigment absorption component is determined from measurements of filter pad absorption. It is the absorption of the bleachable fraction of the material, which does not pass the filter, *i.e.* the difference between the absorption of the filter pad before and after bleaching.

The time series of Helgoland shows two different types of spectra with all transitions, a typical summer spectrum with a clear maximum around 440 nm and a winter spectrum without a clear maximum but with a nearly exponential decrease in the blue-green spectral range. Since it is assumed that the winter spectra are dominated by detritus which contain degradation products of chlorophyll only the summer spectrum have been used for the component model. In order to include the variance of these summer spectra, a set of 77 spectra haven been selected with a clear absorption peak at 442 nm. One of these spectra is selected randomly for the computation of the reflectances. The 77 spectra were selected after normalisation by $a_{pig}(442)$ according to the following criteria:

$$a_{pign}(442) / a_{pign}(412) > 0.98 \quad (32)$$
$$a_{pign}(442) / a_{pign}(448) > 1.0 \quad (33)$$

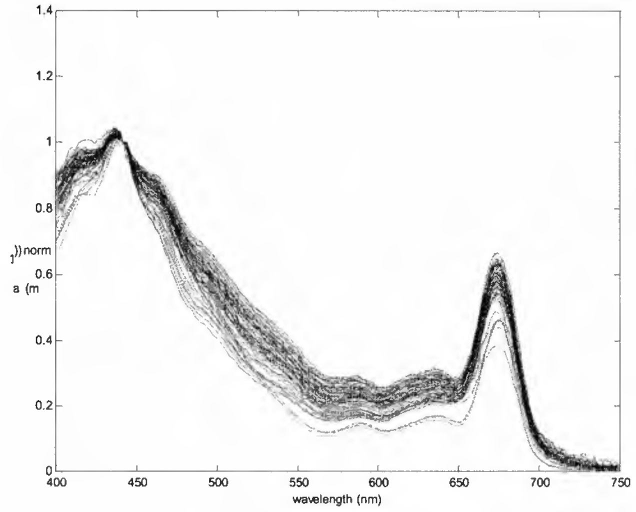

Figure 4.6: Normalized pigment absorption spectra selected from the data base of site Helgoland

4.6.2.4 Co-variations of scattering particles and phytoplankton

Particle scattering is not varied independently from the absorption of particles and phytoplankton in order to exclude unrealistic combinations of high particle absorption without any scattering. Thus, the minimum scattering of the range from which particle scattering is randomly sampled depends on the absorption by particles a_p and phytoplankton a_{pig}, which are sampled first, while the maximum of the particle scattering range is fixed.

The relationship between particle and phytoplankton absorption and minimum scattering is calculated using the following FORTRAN sequence:

```
b_p1=((conc_apig/0.05118)**(1.0/0.6266249))**0.766*550/442*0.416
b_p2 =(conc_apart/0.0216)**(1.0/1.0247)*1.002*0.5
log_b=ln ((b_p1+b_p2)*0.5)
if(log_b.lt.log_bpart_an) log_b=log_bpart_an
conc_bpart=exp(log_b+ran1(iseed)*(log_bpart_en-log_b))
```

b_p1 is the scattering of phytoplankton as a function of phytoplankton absorption conc_apig at 442 nm and b_p2 is the scattering of particulate matter as a function of the absorption of particles conc_apart at 442. The sum of both is reduced by a factor of 0.5 in order to extend the sampling range for particle scattering into the minimum direction.

4.6.3 RELATIONSHIPS BETWEEN CONCENTRATIONS AND OPTICAL PROPERTIES

The component model of water constituents as discussed here uses absorption or scattering at MERIS band 2 (442 nm) as the primary quantitative unit. However, the MERIS Level 2 products are not these optical units but an estimate of the corresponding concentrations of chlorophyll and total suspended matter dry weight (TSM). Thus, the particle scattering at 442 nm is converted into TSM concentration [g m^{-3}] and the pigment absorption at 442 nm into chlorophyll concentration [mg m^{-3}], while the absorption of bleached particles and gelbstoff is not converted. The conversion factor or backward conversion equation is published in order to enable users to compute the initial optical units and then apply their own conversion algorithms, which might be better adapted to their area under research.

4.6.3.1 Relationship between particle scattering and TSM dry weight

According to the COAST I OOC results,

$$b_p(555) = A_{bp}(555) * <TSM> \ (g\ m^{-3}) \qquad (34)$$

with A_{bp}= 0.5 $m^2\ g^{-1}$ and a factor of variation of 1.2.

The absorption of these particles after bleaching is

$$a_p(443)= A_{ap}*<TSM>^{Bap} \qquad (35)$$

with A_{ap}= 0.0216 and B_{ap}=1.0247 and a factor of variation of A_{ap} of 1.84

Since the single scattering albedo near the IR region is close to 1, the value of 0.93 for λ around 780 nm is used to modify the conversion factor of 0.5 for non absorbing particles. Because of the assumed spectral scattering exponent of 0.4, the conversion factor is estimated according to the following scheme:

$$b_p(442)=b_p(780)*(442/780)^{-0.4} \qquad (36)$$

the conversion factor for non absorbing particles is then

$$A_{bp}(442) = (442/780)^{-0.4} * 0.92*0.5 = 0.577 \qquad (37)$$

$$b_p(442) = A_{bp}(442) * <TSM> \ (g\ m^{-3}) \qquad (38)$$

and the reverse relationship

$$<TSM> \ (g\ m^{-3}) = 1.73 * b_p(442) \qquad (39)$$

4.6.3.2 Relationship between pigment absorption and chlorophyll a concentration

The relationship between chlorophyll *a* concentration and the difference of the absorption at 442 nm of the filterpad before and after bleaching was determined for the 77 selected spectra as:

$$\mathbf{ln}\ (chl)= 3.2662+0.77135*\mathbf{ln}\ (a_{pig}(442\ nm)) \qquad (40)$$

$$chl = 26.212* <a_{pig}(442)>^{0.77135} \qquad (41)$$

with a correlation coefficient of r = 0.69475

The inverse relationship is

$$a_{pig}(442) = 0.041457*<chl>^{0.62576} \qquad (42)$$

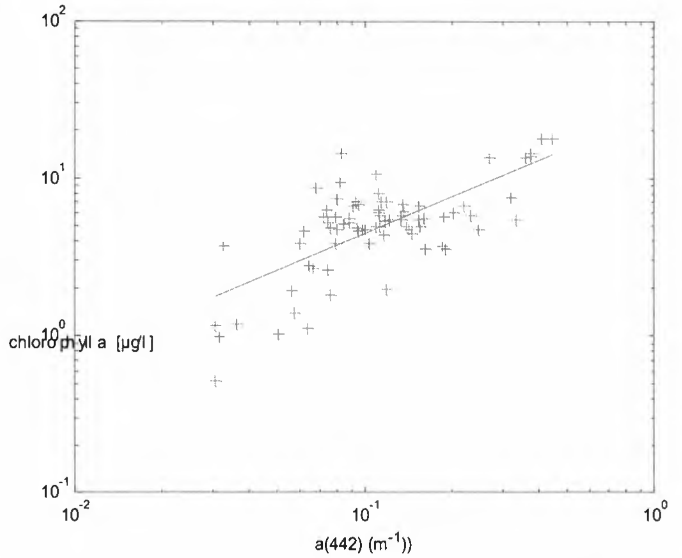

Figure 4.7: Relationship between absorption at 442 nm and chlorophyll a concentration

4.6.3.3 Conversion factors used in the bio-optical model

Concentration	*Optical property*	*Conversion factor*
TSM dry weight g m^{-3}	scattering of non absorbing particles at 442 nm $[m^{-1}]$	TSM (g m^{-3}) = 1.37 * $b_p(442)$
gelbstoff absorption at 442 nm m^{-1}	absorption of bleached particles and gelbstoff at 442 nm $[m^{-1}]$	$a_{yp}(442)$= 2*randu*$a_{yd}(442)$ $a_y(442)=a_{yd}(442)+a_{yp}(442)$
chlorophyll a mg m^{-3}	pigment absorption at 442 nm m^{-1}	chl = 26.212* $\langle a_{pig}(442)\rangle^{0.77135}$

Table 4.6.3.3-1. Conversion factors used in the bio-optical model.

4.7 AOP CALCULATIONS (INCLUDING BIDIRECTIONALITY)

4.7.1 RADIATIVE TRANSFER SIMULATIONS/CALCULATIONS

Using the ocean part of the reference model, one should be able to calculate the directional reflectance just below the sea surface, $\rho_u^{0^-}(\lambda,\theta_s,\theta',\Delta\phi)$ (or other AOPs or derived quantities), using geophysical parameters as inputs (*[chl]* only for Case 1 waters, and [Chl], *SPM* and $a_{y2}(443)$ for Case 2 waters).

A first approach consists in using the parameterisations presented in sections 4.2 to 4.6 to derive IOPs and introduce them into radiative transfer simulations with the relevant boundary conditions (sea state, barometric pressure etc.). The output of these simulations are radiances in all directions, which can be integrated in different manners to derive various plane or scalar irradiances, from which various quantities can be derived, such as

f'(λ,θ_s), which is defined as:

$$f'(\lambda,\theta_s) = \frac{E_u(\lambda,\theta_s)}{E_d(\lambda,\theta_s)} \frac{b_b(\lambda)+a(\lambda)}{b_b(\lambda)} \tag{43}$$

f(λ,θ_s), which is defined as:

$$f(\lambda,\theta_s) = \frac{E_u(\lambda,\theta_s)}{E_d(\lambda,\theta_s)} \frac{a(\lambda)}{b_b(\lambda)} \tag{44}$$

Q $(\lambda,\theta',\theta_s,\Delta\phi)$, which is defined as:

$$Q(\lambda,\theta_s,\theta',\Delta\phi) = \frac{E_u(\lambda,\theta_s)}{L_u(\lambda,\theta_s,\theta',\Delta\phi)} \tag{45}$$

and the directional reflectance just below the sea surface, which is

$$\rho_u^{0^-}(\lambda,\theta_s,\theta',\Delta\phi) = \pi . \frac{R(\lambda)}{Q(\lambda,\theta_s,\theta',\Delta\phi)} \tag{46}$$

where R(λ) is the irradiance reflectance just below sea surface [defined as the ratio of upward to downward irradiance, $E_u(\lambda)$ / $E_d(\lambda)$; Eq. (10)], and Q (λ, θ_S, θ', Δφ) is the bi-directionality factor. Eq. (46) is obtained when considering that :

$$\rho_u^{0^-}(\lambda,\theta_s,\theta',\Delta\phi) = \pi . \frac{L_u(\lambda,\theta_s,\theta',\Delta\phi)}{E_d(0^+)(\lambda,\theta_s)} \tag{47}$$

The water-leaving reflectance, $\rho_w^{0+}(\lambda,\theta_s,\theta_v,\Delta\phi)$, (*i.e.*, above the sea surface) is expressed as:

$$\rho_w^{0+}(\lambda,\theta_s,\theta_v,\Delta\phi) = \frac{1-\rho_F(W,\theta')}{n^2} . \rho_u^{0^-}(\lambda,\theta_s,\theta',\Delta\phi) \tag{48}$$

where ρ_F(W, θ') is interpolated by-linearly from table 4.7-1 below.

W (m.s^{-1}) θ' (deg) \	0	4	10	16
0	0.0211	0.0211	0.0213	0.0217
10	0.0211	0.0213	0.0218	0.0228
20	0.0218	0.0227	0.0255	0.0334
30	0.0265	0.0325	0.0613	0.0961
35	0.0350	0.0602	0.1234	0.1686
40	0.0588	0.1559	0.2367	0.2741
45	0.1529	0.3801	0.4065	0.4131
50	1.0000	0.6718	0.5988	0.5629
55	1.0000	0.8905	0.7715	0.7055
60	1.0000	0.9807	0.8967	0.8277

Table 4.7-1: Values of ρ_F(W, θ'), the mean Fresnel reflection coefficient for the water-air interface, as function of wind speed W and view angle θ', (Austin, 1974).

When the Raman scattering is ignored, the functions f(λ), f'(λ) and Q(λ,θ_s,θ_v, Δϕ) are obtained through monochromatic radiative transfer calculations using a_1(λ) and b_1(λ) or a_2(λ) and b_2(λ) as calculated using the parameterisation presented in sections 4.4 (pure sea water), 4.5 (Case 1 waters) and 4.6 (Case 2 waters), and a normalised volume scattering function. When the Raman scattering is accounted for, radiative transfer calculations must include the wavelength domain involved for the excitation of the Raman emission.

In case f'/Q (or f/Q) lookup tables are developed, they should have the following entries:

- ✓ The molecular to total scattering ratio $\frac{b_w}{b}$ as derived from parameterisations in section 4.
- ✓ The single scattering albedo $\frac{b}{a+b}$ as derived from parameterisations in section 4
- ✓ Sun zenith angle θ_s
- ✓ Viewing angle θ'
- ✓ Azimuth difference angle Δϕ

The atmospheric optical thickness τ(550) should be specified (it is not necessarily an entry to the lookup table).

4.7.2 SEMI-ANALYTICAL CALCULATIONS

When the reflectance R(λ) in Eq. (46) is replaced by :

$$R(\lambda) = f'(\lambda)\frac{b_b(\lambda)}{a(\lambda)+b_b(\lambda)} \tag{49}$$

or by

$$R(\lambda) = f(\lambda)\frac{b_b(\lambda)}{a(\lambda)} \quad \text{(only usable when } b_b \ll a) \tag{49'}$$

Then $\rho_w^{0+}(\lambda,\theta_s,\theta_v,\Delta\phi)$ can be expressed as :

$$\rho_w^{0+}(\lambda,\theta_s,\theta',\Delta\phi) = \pi \;\Re(\theta') \;\frac{f(\lambda,\theta_s)}{Q(\lambda,\theta_s,\theta',\Delta\phi)} \left[\frac{b_b(\lambda)}{a(\lambda)}\right] \quad (50)$$

which is also obtained by combining the following basic equations (see also the table of symbols in section 2.5):

$$R = \frac{E_u}{E_d} = f\,\frac{b_b}{a} \quad ; \quad Q = \frac{E_u}{L_u} \quad ; \quad L_w = L_u\,\frac{1-\rho_F}{n^2} \quad ; \quad E_d(0^-) = E_d(0^+)\,\frac{1-\bar{\rho}}{1-\bar{r}R}$$

The semi-analytical Eq. (50) can be used along with the parameterisations developed in section 4.2 to 4.6.1. In that case, $a(\lambda)$ and $b_b(\lambda)$ can be broken into individual contributions by the different water constituents, following the "analytical approach" (but see introduction to section 4.5.1).

$$a(\lambda) = \sum_{n=1}^{N} a_n(\lambda) \quad (51)$$

$$b_b(\lambda) = \sum_{n=1}^{N} \tilde{b}_{bn}(\lambda) b_n(\lambda) \quad (52)$$

where the subscript n indicates a given optically significant seawater constituent, $b_n(\lambda)$ is the *scattering coefficient* of the nth substance and $\tilde{b}_{bn}(\lambda)$ is the *ratio of backscattering to scattering* (or *backscattering efficiency*) of the nth substance.

In Eq. (50) above, the "gothic" $\Re$ factor (Morel and Gentili, 1996) is interpolated from table 4.7-2 below.

W (m.s^{-1}) θ' (deg) \	0	4	8	16
0	0.528883	0.528867	0.528824	0.528581
1	0.528899	0.528856	0.528797	0.528597
2	0.528894	0.528883	0.528775	0.528613
3	0.528878	0.52884	0.528829	0.528613
4	0.528867	0.528883	0.528845	0.528592
5	0.528872	0.528905	0.528824	0.528597
6	0.528878	0.528851	0.528829	0.528559
7	0.528856	0.528856	0.528824	0.528402
8	0.528851	0.528867	0.528862	0.528359
9	0.528856	0.528878	0.52877	0.528278
10	0.528856	0.528883	0.528764	0.528089
11	0.528899	0.528905	0.528673	0.527738
12	0.528889	0.528802	0.528608	0.527625

W ($m.s^{-1}$) θ' (deg) \	0	4	8	16
13	0.528883	0.528775	0.528532	0.527392
14	0.528851	0.5287	0.528489	0.52689
15	0.528813	0.528608	0.528316	0.526447
16	0.528732	0.528554	0.528089	0.525945
17	0.528727	0.528446	0.528008	0.525048
18	0.528646	0.528381	0.527846	0.52387
19	0.528613	0.5283	0.5275	0.522865
20	0.528548	0.528084	0.527279	0.52198
21	0.528467	0.5279	0.526998	0.520192
22	0.528365	0.527679	0.526144	0.518177
23	0.52824	0.527371	0.525448	0.515962
24	0.528014	0.526976	0.524616	0.51318
25	0.527851	0.526831	0.523416	0.510576
26	0.527614	0.526053	0.522061	0.507005
27	0.52736	0.525593	0.52051	0.503111
28	0.526982	0.524902	0.51842	0.498773
29	0.526474	0.523508	0.515708	0.493392
30	0.52602	0.521947	0.511937	0.487402
31	0.525307	0.520035	0.50794	0.48133
32	0.524545	0.517836	0.503089	0.474475
33	0.5236	0.514968	0.497228	0.46648
34	0.522309	0.510771	0.490238	0.45802
35	0.520899	0.505082	0.482119	0.448756
36	0.51909	0.498659	0.472968	0.438514
37	0.516891	0.490292	0.461931	0.428472
38	0.513801	0.47965	0.44975	0.417047
39	0.510274	0.46742	0.436121	0.404482
40	0.505412	0.451889	0.421482	0.391841
41	0.499173	0.434063	0.405481	0.378471
42	0.48872	0.413638	0.387114	0.363265
43	0.474221	0.390988	0.368575	0.348366
44	0.449583	0.365242	0.346011	0.333381
45	0.412601	0.336671	0.324193	0.317797
46	0.359554	0.306188	0.302239	0.302866
47	0.287908	0.275208	0.280156	0.287767
48	0.209752	0.243574	0.256517	0.270011
49	0.136037	0.21375	0.234029	0.254097
50	0.0755841	0.184504	0.21093	0.237464
51	0.0361985	0.154728	0.189511	0.221885
52	0.0140559	0.128167	0.168395	0.20649
53	0.00447281	0.103831	0.146798	0.19118
54	0.0011182	0.0826552	0.127189	0.175709
55	0.000226882	0.0627274	0.108666	0.161335
56	0	0.0460786	0.0914604	0.145221
57	0	0.0326278	0.0748656	0.130527
58	0	0.0220994	0.0596105	0.116007
59	0	0.0141207	0.0463325	0.101784

W ($m.s^{-1}$) θ' (deg) \	0	4	8	16
60	0	0.00872415	0.035345	0.0883597
61	0	0.00485635	0.0259402	0.0748602
62	0	0.00252271	0.0180317	0.0623547
63	0	0.00122624	0.012257	0.0503408
64	0	0.000502381	0.00773019	0.0400446
65	0	0.000199872	0.00458625	0.0306453
66	0	0	0.00265776	0.0225315
67	0	0	0.00127486	0.0157467
68	0	0	0.000648234	0.010604
69	0	0	0.000318715	0.00674163
70	0	0	0.000113441	0.00397043
71	0	0	0	0.00202573
72	0	0	0	0.00100476
73	0	0	0	0.000426754
74	0	0	0	0.000162058
75	0	0	0	0
76	0	0	0	0
77	0	0	0	0
78	0	0	0	0
79	0	0	0	0
80	0	0	0	0
81	0	0	0	0
82	0	0	0	0
83	0	0	0	0
84	0	0	0	0
85	0	0	0	0
86	0	0	0	0
87	0	0	0	0
88	0	0	0	0
89	0	0	0	0
90	0	0	0	0

Table 4.7-2: Values of $\Re$ as function of wind speed W and view angle θ'

5. Sea surface state

5.1 Specular Reflection

The effect of the air-sea interface shape on Fresnel reflection and refraction will be accounted for by applying statistics of Cox and Munk (1954), assuming an isotropic distribution of waves and a variable wind speed.

If a code like FUB's MOMO is used to calculate TOA radiances (reflectances), then the glint reflectance at the TOA level has to be calculated independently (see below), and subtracted from the total signal calculated by the code at the TOA (for any combination of θ_S, θ_V, and $\Delta\phi$). In its actual state, this code does not provide information on the history of photons and cannot therefore separate the contributions from the sea surface from the total TOA signal. When generating the LUTs with the coefficients of the quadratic equation linking [ρ_{path} / ρ_r] to τ_a) for atmospheric correction of MERIS data, this subtraction must be performed on the reflectances for the pure Rayleigh atmospheres (ρ_r) as well as for the realistic atmospheres (molecules + aerosols, ρ_{path}), before the corresponding reflectances are ratioed and related to the aerosol optical thickness.

As far as a standard version of the MOMO code is used, the following surface model is considered for calculation of the glint reflectance. Within the surface model, the facet slopes are assumed to be normally distributed, independently of the wind direction. The probability density of surface slopes for the direction (θ_S, θ_V, $\Delta\phi$) is given by (Cox and Munk, 1954)

$$p(\theta_s,\theta_v,\Delta\phi) = \frac{1}{\pi\,\sigma^2}\exp\left(\frac{-\tan^2(\beta)}{\sigma^2}\right)$$

where β is the angle between the local normal and the normal to the facet :

$$\cos(\beta) = (\cos(\theta_v) + \cos(\theta_s)) / (2\cos(\omega))$$

$$\text{with } \cos(2\omega) = \cos(\theta_v)\cos(\theta_s) - \sin(\theta_v)\sin(\theta_s)\cos(\Delta\phi)$$

and σ is the root mean square of slopes, and is a function of wind speed, W, through (Cox and Munk, 1954) :

$$\sigma^2 = 0.003 + 5.12\ 10^{-3}\ W$$

Shadowing effects are not accounted for. The reflectance ρ_G is then

$$\rho_G = \pi\,\rho_F\ p(\theta_s, \theta_v, \Delta\phi) / (4\cos(\theta_v)\cos(\theta_s)\cos^4(\beta))$$

where ρ_F is the Fresnel reflectance at the air-sea interface. Finally, the value of ρ_G at the TOA level is :

$$\rho_G \, T(\theta_v) \, T(\theta_s)$$

where $T(\theta)$ is the direct transmittance of the atmosphere for angle θ, and is equal to $e^{-\tau/\cos(\theta v)}$, with τ the total optical thickness (Rayleigh + aerosols + absorbing gases, when applicable).

5.2 White Caps

White caps are not accounted for.

6. - Atmosphere

Atmosphere properties shall be provided at least for the following MERIS bands (see wavelengths in section 3 above):

- 1, 2, 3, 4, 5, 6, 7, 8, 9, 12, 13, for all ocean-related processing;
- 1, 2, 3, 4, 5, 6, 7, 8, 9, 10, 11, 12, 13, 14, 15 for all land-related processing;
- 10, 11 for all cloud-related processing;
- 10, 12, 13, 14, 15 for all water vapour-related processing;

6.1 - Constituents

The atmosphere shall be considered to be composed of:

1. air (molecular scattering, O_2 absorption);
2. ozone (absorption);
3. water vapour (absorption);
4. aerosols (scattering and absorption);
5. clouds (scattering and absorption).

Other atmosphere constituents: gases, rain... are neglected.

Absorption by gases (O_2, ozone, water vapour) may be treated separately from the rest of atmosphere constituents, so that radiative transfer simulations consider only the absorption of aerosols and scattering by aerosol and molecules.

6.2 - Polarisation

The radiation transfer through the atmosphere should be treated with polarisation.

6.3 - Sampling

It shall be possible to parameterise:

- the zenith and azimuth angle sampling of the radiative transfer model
- the vertical layering of the atmosphere, with a resolution equal to or better than 1km from 0 to 50 km altitude. Within each layer it shall be possible to specify either:
    - the type and optical thickness (or extinction coefficient) of a homogenous aerosol

    or
    - the type and optical thickness (or extinction coefficient) of a homogeneous cloud

  A total of 20 layers (some may be thicker than 1 km) are enough for an accurate calculation of the TOA total reflectance.

6.4 - Surface properties

The surface below the atmosphere shall be modelled by either:

- a water body with properties as described in sections 4 and 5 above;

or

- a land surface with properties as described in section 8 below;

The surface will be considered infinite and homogeneous.

6.5 - Air pressure at ground

The air pressure at surface at 0m elevation shall be 1013.25 hPa.

6.6 - RAYLEIGH SCATTERING

The vertical profile of molecular scattering shall be taken from Elterman (1968), scaled so that the total optical thickness has the values in table 6.6-1 below. The sea level pressure shall be 1013.25 hPa.

The total optical thickness of Rayleigh scattering τ_r will be taken from table 6.6-1 below.

λ	412.5	442.5	490.0	510.0	560.0	620.0	665.0	708.75	778.75	865.0
τ_r	0.314085	0.235229	0.154853	0.131495	0.089808	0.059387	0.044703	0.034542	0.023609	0.015456

Table 6.6-1: Optical thickness of Rayleigh scattering
(computed from the approximate formula of Travis and Hansen
$\tau_r = P/P0.[8.524e\text{-}3.\lambda^{-4} + 9.63e\text{-}5.\lambda^{-6} + 1.1e\text{-}7.\lambda^{-8}]$ with λ in micrometer)

The Rayleigh scattering phase function should be computed as :

$$\tilde{\beta}_r(\psi,\lambda) = \frac{3}{4\pi * 4\,(1+2\gamma)} \left[(1+3\gamma)+(1-\gamma)\cos^2(\psi)\right]$$

where

$$\gamma = \frac{\delta}{2-\delta}$$

and δ is the depolarisation factor = 0.0279.

In principle, δ is wavelength-dependent. That dependency should be accounted for in a later version of this document.

6.7 - OXYGEN

When simulations include gaseous absorption, the vertical profile of O_2 shall be taken from Elterman (1968), for a standard atmospheric pressure of 1013.25 hPa. The O_2 absorption spectrum shall be taken from Rothman *et al*, 1983.

6.8 - OZONE

When simulations include gaseous absorption, the vertical ozone profile shall be taken from Elterman(1968). The standard total ozone column content shall be 0.350 atm.cm. The ozone absorption spectrum shall be taken from Rothman *et al*, 1983.

6.9 - WATER VAPOUR

When simulations include gaseous absorption, the vertical water vapour profile shall be taken from Elterman(1968). The standard total water vapour column content shall be 1.42 $g.cm^{-2}$. The water vapour absorption spectrum shall be taken from Rothman *et al*, 1983.

6.10 - AEROSOLS

6.10.1 - AEROSOL MODELS AND PROPERTIES

Two sets of aerosol models shall be taken from:

1. ATBD volume 7: atmosphere corrections above case 1 waters, section 3.1.1.5.2
2. ATBD volume 15: atmosphere corrections above land, section 2.3.3

Atmosphere corrections above water and above land follow slightly different philosophies.

Above water, *basic constituents* are mixed homogeneously to build up *models*, as explained below; vertical profiles of models build up *assemblages*, as explained on §6.10.3 and described in §12.
Above land, *models* are homogeneous in terms of composition as well as vertically.

Aerosol models shall be defined each as a homogeneous mixture of basic constituents. Each basic constituent shall be a population of spherical particles characterised by:

1. its complex refraction index at all wavelengths (see section 10 below);
2. its particle size distribution function: log-normal, Junge power-law distribution or modified Gamma distribution (see below);
3. the parameters of the particle size distribution function (see below).

The 6 basic constituents are the following:

a) sea salt solution in water (oceanic)
b) water soluble particles
c) dust-like particles
d) desert dust aerosols
e) soot-like particles
f) sulphuric acid solution in water

An additional constituent, used in several models, is built by combination of two of the above:

g) rural aerosol mixture (70% of water soluble particles *(b)*, and 30% of dust-like particles *(c)*)

The models are the following:

1) Maritime model (Shettle and Fenn, 1979)
2) Urban model (Shettle and Fenn, 1979)
3) Continental model (WCRP, 1986)
4) Stratospheric model (WCRP, 1986)
5) Desert dust model (Schütz, 1980)
6) POLDER models (reference TBD). POLDER models are made of a single component of spherical droplets for the whole size spectrum, with a power-law size distribution. Therefore they do not appear in table 6.10.1-1 below.

Tables 6.10.1-1 below show the proportions of constituents in each model.

Aerosol model	Components	Volume %	Particle %
Maritime	Rural aerosol mixtures‡		99
(Shettle and Fenn, 1979)	oceanic (Sea-salt solution in water)		1
Urban	Rural aerosol mixtures‡		80
(Shettle and Fenn, 1979)	Soot		20
Continental	Water soluble	29	93.876
(WCRP, 1986)	Dust-like	70	2.27 10^{-6}
	Soot	1	0.06123
Dust	Desert dusts	100	100
(Schütz, 1980)			
H_2SO_4	75% solution of	100	100
(WCRP, 1986)	sulphuric acid in water		

‡ 70% of water soluble particles, and 30% of dust-like particles.

Table 6.10.1-1: Aerosol components and their respective contributions (as percent of the volume, or as percent of the number of particles) in the composition of the aerosol models. The principle of «external mixing» is applied when calculating the optical properties of the aerosol models.

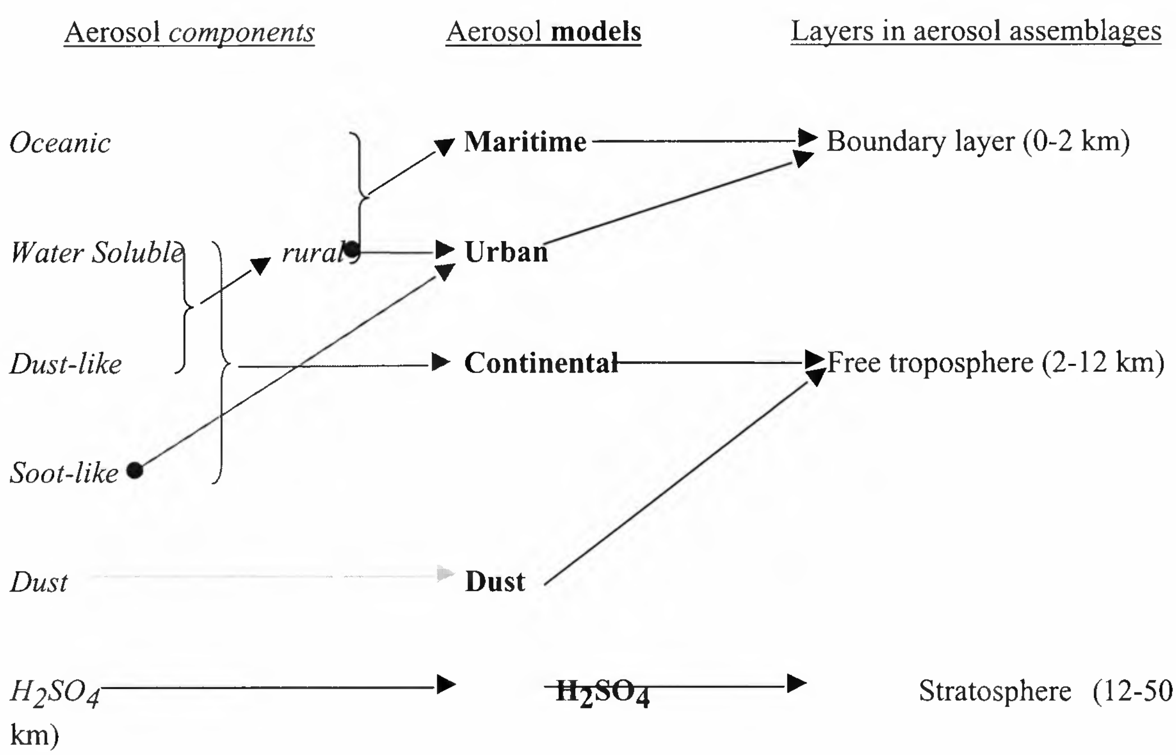

Figure 6.1: principle of aerosol assemblages

Aerosol model or aerosol component		Parameters of the lognormal size distribution r_0	$\sigma/\ln(10)$	$\exp(\sigma)$	
Rural	RH 70%	0.02846	0.35	2.238721	
(water soluble + dust-like)	RH 80%	0.03274			
(Shettle and Fenn, 1979)	RH 85%	0.03679			
	RH 90%	0.03884			
	RH 95%	0.04238			
	RH 99%	0.05215			
Oceanic	RH 70%	0.2041	0.40	2.511886	
(sea-salt solution in water)	RH 80%	0.3180			
(Shettle and Fenn, 1979)	RH 85%	0.3777			
	RH 90%	0.3803			
	RH 95%	0.4606			
	RH 99%	0.7505			
Urban	RH 70%	0.02911	0.35	2.238721	
(Shettle and Fenn, 1979)	RH 80%	0.03514			
	RH 85%	0.03961			
	RH 90%	0.04187			
	RH 95%	0.04904			
	RH 99%	0.05996			
Continental (WCRP, 1986)					
Water soluble		0.005	0.475671	2.99	
Dust-like		0.500	0.475671	2.99	
Soot		0.0118	0.301030	2.00	
Desert Dust (Schütz, 1980)		0.500	0.342423	2.20	
		Parameters of the gamma modified size distribution			
		A	α	γ	b
75% H_2SO_4 (WCRP, 1986)		324	1	1	18
POLDER models		$n(r) \approx r^{(\alpha-3)}$	α		
models 1, 5, 9			0.0		
models 2, 6, 10			0.5		
models 3, 7, 11			1.0		
models 4, 8, 12			1.5		

Table 6.10.1-2: Parameters defining the size distribution of the various aerosol models (separately for each component of the continental model)

The tables in section 10 show the refractive indices of the aerosol models.

6.10.2 - AEROSOL PHASE FUNCTION & SINGLE SCATTERING ALBEDO

Aerosol phase function, extinction and scattering coefficients, single scattering albedo, asymmetry factor shall be computed according to Mie theory, based on the parameters identified in section 6.10.1 above.

The table in section 11 (divided into 3 parts) summarises the results of Mie computations. For each aerosol model, and for each wavelength, there are 2 lines : the first one for the scattering (b) and attenuation (c) coefficients (thus 2 successive values for each wavelength), the second one for the single scattering albedo (ω) and the asymmetry factor (g).

The plots in section 13 show the scattering phase function at 550nm, of the aerosol models. A full set of discretised phase functions can be retrieved as a binary file from the following ftp server: `ftp.acri.fr`, login: `meris`: password: `envisat`, file: `pub/phase_functions.tar.Z` (archive created with the Unix `tar` utility and compressed by the Unix `compress` utility).

6.10.3 - AEROSOL VERTICAL PROFILES

Aerosol assemblages shall be specified by:

1. a boundary layer aerosol: model, optical thickness at 560nm, between 0 and 2 km altitude
2. a tropospheric layer aerosol: model, optical thickness at 560nm, between 2 and 12 km altitude
3. a stratospheric layer aerosol: model, optical thickness at 560nm, above 12 km altitude

The 33 assemblages used for atmosphere corrections above water are described in section 12 below.

The POLDER models used for atmosphere corrections above land shall be distributed following:

$$\delta(z) = \delta(0).e^{-z/H}$$

where $\delta(z)$ is the optical thickness at altitude z, H the scale height; H = 2 km for all POLDER models.

6.11 - REFERENCE ATMOSPHERE

For the purposes of validation and of look-up table computation (*i.e.* those which do not require variations of the atmosphere properties), a reference atmosphere has been defined with the following parameters:

Rayleigh scattering as defined in 6.6 above, with a sea level pressure of 1013.25 hPa
boundary layer aerosol: maritime model with relative humidity = 90%, τ_{a560}: 0.2
tropospheric, stratospheric aerosols: none
total ozone: none
total water vapour: none
wind speed: 3 $m.s^{-1}$

7. - Clouds

7.1 - Water clouds

Cloud types shall be taken from ATBD volume 1, Cloud albedo and optical thickness, section 3.1.2.1. Each cloud type is specified a population of water droplets with a modified gamma-function distribution, characterised by its effective radius (μm).

The cloud scattering phase function, extinction and scattering coefficients, shall be computed according to Mie theory, based on the cloud parameters identified above.

Clouds shall be specified by a type and an extinction coefficient (m^{-1}) in each atmosphere layer.

7.2 - Cirrus clouds

It shall be possible to specify layer(s) of cirrus cloud, whose optical properties: scattering phase function, extinction and scattering coefficients, shall be taken from Brogniez *et al.* (1995).

8. - Land Surface

When not represented by specific tables (*e.g.* DDV reflectance and coupling terms), land surfaces shall be modelled as a Lambertian reflecting surface characterised by its albedo (dimensionless) at all MERIS channel wavelengths.

The following table 8-1 provides, as example, spectra for different types of surface.

Wavelength	412.5	442.5	490	510	560	620	665	681.25	708.75	753.75	778.75	865	885	900
Surface type														
clear water	0.0145	0.0138	0.0134	0.0119	0.0100	0.0042	0.0034	0.0033	0.0026	0.0022	0.0022	0.0021	0.0019	0.0000
water	0.0135	0.0135	0.0152	0.0157	0.0157	0.0057	0.0042	0.0043	0.0027	0.0019	0.0019	0.0018	0.0019	0.0000
turbid water	0.0212	0.0238	0.0304	0.0331	0.0360	0.0160	0.0108	0.0097	0.0058	0.0022	0.0022	0.0021	0.0019	0.0000
brown soil	0.0181	0.0602	0.0991	0.1341	0.1928	0.2576	0.2904	0.3001	0.3159	0.3452	0.3473	0.3542	0.3688	0.3708
podzol	0.0614	0.0739	0.0884	0.0955	0.1100	0.1324	0.1601	0.1726	0.1958	0.2400	0.2440	0.2567	0.3206	0.3321
conif	0.0149	0.0156	0.0264	0.0512	0.0682	0.0375	0.0250	0.0247	0.1047	0.3763	0.3823	0.3921	0.6144	0.6195
grass	0.0388	0.0408	0.0435	0.0715	0.1089	0.0662	0.0468	0.0461	0.1345	0.4544	0.4626	0.4749	0.4997	0.5060
oat	0.0380	0.0370	0.0450	0.0480	0.0760	0.0590	0.0580	0.0720	0.0870	0.2300	0.2360	0.2440	0.2480	0.2430
snow fine	0.9894	0.9916	0.9922	0.9910	0.9898	0.9837	0.9776	0.9764	0.9690	0.9570	0.9552	0.9551	0.9534	0.9337
snow medium	0.9806	0.9845	0.9852	0.9832	0.9809	0.9707	0.9590	0.9560	0.9475	0.9277	0.9249	0.9249	0.9152	0.8806
snow coarse	0.9714	0.9767	0.9773	0.9752	0.9712	0.9565	0.9391	0.9359	0.9227	0.8955	0.8913	0.8913	0.8762	0.8284
ice	0.8455	0.8409	0.8380	0.8350	0.827	0.8040	0.7787	0.7691	0.7523	0.7174	0.7140	0.7037	0.6511	0.6398

Table 8-1 : Surface reflectances in MERIS simulator

9. - Sun irradiance

Sun irradiance when needed, shall be taken from Thuilier *et al.* (1998a, 1998b). It shall be corrected for the day of year according to the following approximate formulae:

$$M = 0.9856.(J - 4).\frac{\pi}{180}$$

$$E(J) = E_0 . \frac{1}{(1 - 0.01673.\cos M)^2}$$

where J is the day of year.

10. - Tables of refractive indices

The following table 10-1 provides the complex refractive index of all aerosol models at all MERIS channel wavelengths. nr: real part, ni: imaginary part.

Wavelength	412.5		442.5		490		510	
	nr	ni	nr	ni	nr	ni	nr	ni
Rural, RH = 70%	1.502	-.504E-02	1.502	-.504E-02	1.501	-.504E-02	1.501	-.504E-02
Rural, RH = 80%	1.446	-.331E-02	1.445	-.331E-02	1.444	-.331E-02	1.444	-.331E-02
Rural, RH = 85%	1.423	-.261E-02	1.422	-.261E-02	1.421	-.261E-02	1.421	-.261E-02
Rural, RH = 90%	1.403	-.198E-02	1.402	-.198E-02	1.401	-.198E-02	1.400	-.198E-02
Rural, RH = 95%	1.388	-.153E-02	1.387	-.153E-02	1.385	-.153E-02	1.385	-.153E-02
Rural, RH = 99%	1.365	-.819E-03	1.364	-.819E-03	1.362	-.819E-03	1.361	-.819E-03
Oceanic, RH = 70%	1.417	-.147E-07	1.416	-.128E-07	1.415	-.975E-08	1.414	-.622E-08
Oceanic, RH = 80%	1.359	-.516E-08	1.358	-.444E-08	1.356	-.331E-08	1.355	-.249E-08
Oceanic, RH = 85%	1.350	-.362E-08	1.348	-.309E-08	1.346	-.227E-08	1.346	-.188E-08
Oceanic, RH = 90%	1.350	-.375E-08	1.349	-.319E-08	1.347	-.235E-08	1.348	-.193E-08
Oceanic, RH = 95%	1.347	-.287E-08	1.345	-.242E-08	1.342	-.175E-08	1.341	-.158E-08
Oceanic, RH = 99%	1.340	-.200E-08	1.339	-.165E-08	1.337	-.116E-08	1.336	-.124E-08
Urban, RH = 70%	1.488	-.610E-01	1.487	-.606E-01	1.486	-.600E-01	1.486	-.600E-01
Urban, RH = 80%	1.424	-.347E-01	1.423	-.345E-01	1.421	-.341E-01	1.420	-.341E-01
Urban, RH = 85%	1.403	-.265E-01	1.403	-.263E-01	1.401	-.260E-01	1.400	-.260E-01
Urban, RH = 90%	1.389	-.205E-01	1.389	-.204E-01	1.388	-.202E-01	1.386	-.202E-01
Urban, RH = 95%	1.370	-.128E-01	1.369	-.127E-01	1.367	-.125E-01	1.368	-.125E-01
Urban, RH = 99%	1.350	-.470E-02	1.349	-.466E-02	1.347	-.461E-02	1.346	-.461E-02
Water soluble (WCRP86)	1.530	-.500E-02	1.530	-.500E-02	1.530	-.500E-02	1.530	-.500E-02
Dust-like (WCRP86)†	1.530	-.800E-02	1.530	-.800E-02	1.530	-.800E-02	1.530	-.800E-02
Soot (WCRP86) †	1.750	-.459E+00	1.750	-.455E+00	1.750	-.450E+00	1.750	-.450E+00
Dust, (Schütz, 1980)	1.530	-.550E-02	1.530	-.550E-02	1.530	-.550E-02	1.530	-.550E-02
75 % H_2SO_4 solution	1.439	-.100E-07	1.436	-.100E-07	1.432	-.100E-07	1.431	-.100E-07

Table 10-1: Refractive index of aerosol components/models

Wavelength	560		620		665		681.25	
	nr	ni	nr	ni	nr	ni	nr	ni
Rural, RH = 70%	1.501	-.563E-02	1.501	-.563E-02	1.501	-.594E-02	1.501	-.610E-02
Rural, RH = 80%	1.443	-.370E-02	1.443	-.370E-02	1.443	-.390E-02	1.443	-.401E-02
Rural, RH = 85%	1.420	-.291E-02	1.420	-.291E-02	1.419	-.307E-02	1.419	-.315E-02
Rural, RH = 90%	1.399	-.222E-02	1.399	-.222E-02	1.398	-.234E-02	1.398	-.240E-02
Rural, RH = 95%	1.384	-.171E-02	1.383	-.171E-02	1.382	-.180E-02	1.382	-.185E-02
Rural, RH = 99%	1.360	-.916E-03	1.359	-.916E-03	1.359	-.965E-03	1.359	-.990E-03
Oceanic, RH = 70%	1.412	-.720E-08	1.409	-.154E-07	1.408	-.417E-07	1.408	-.541E-07
Oceanic, RH = 80%	1.354	-.452E-08	1.352	-.137E-07	1.351	-.281E-07	1.351	-.344E-07
Oceanic, RH = 85%	1.344	-.406E-08	1.343	-.133E-07	1.342	-.258E-07	1.342	-.311E-07
Oceanic, RH = 90%	1.345	-.406E-08	1.344	-.131E-07	1.343	-.258E-07	1.343	-.313E-07
Oceanic, RH = 95%	1.340	-.382E-08	1.339	-.130E-07	1.338	-.246E-07	1.338	-.295E-07
Oceanic, RH = 99%	1.335	-.357E-08	1.334	-.127E-07	1.333	-.233E-07	1.333	-.277E-07
Urban, RH = 70%	1.486	-.589E-01	1.485	-.580E-01	1.485	-.580E-01	1.485	-.580E-01
Urban, RH = 80%	1.420	-.335E-01	1.419	-.330E-01	1.419	-.330E-01	1.419	-.331E-01
Urban, RH = 85%	1.399	-.256E-01	1.399	-.252E-01	1.398	-.252E-01	1.398	-.252E-01
Urban, RH = 90%	1.384	-.198E-01	1.384	-.195E-01	1.383	-.195E-01	1.383	-.196E-01
Urban, RH = 95%	1.365	-.124E-01	1.364	-.121E-01	1.363	-.122E-01	1.363	-.122E-01
Urban, RH = 99%	1.345	-.453E-02	1.344	-.446E-02	1.343	-.446E-02	1.343	-.446E-02
Water soluble (WCRP86)	1.530	-.600E-02	1.530	-.600E-02	1.530	-.652E-02	1.530	-.679E-02
Dust-like (WCRP86)†	1.530	-.800E-02	1.530	-.800E-02	1.530	-.800E-02	1.530	-.800E-02
Soot (WCRP86) †	1.750	-.439E+00	1.750	-.432E+00	1.750	-.430E+00	1.750	-.430E+00
Dust, (Schütz, 1980)	1.530	-.550E-02	1.530	-.550E-02	1.530	-.550E-02	1.530	-.550E-02
75 % H_2SO_4 solution	1.430	-.106E-07	1.429	-.140E-07	1.428	-.174E-07	1.428	-.188E-07

Table 10-1(cont): Refractive index of aerosol components/models

Wavelength	708.75		753.75		760		778.75	
	nr	ni	nr	ni	nr	ni	nr	ni
Rural, RH = 70%	1.500	-.649E-02	1.498	-.730E-02	1.497	-.743E-02	1.496	-.775E-02
Rural, RH = 80%	1.442	-.426E-02	1.440	-.480E-02	1.440	-.488E-02	1.439	-.509E-02
Rural, RH = 85%	1.419	-.335E-02	1.417	-.377E-02	1.417	-.384E-02	1.416	-.401E-02
Rural, RH = 90%	1.398	-.255E-02	1.396	-.287E-02	1.396	-.292E-02	1.395	-.305E-02
Rural, RH = 95%	1.382	-.197E-02	1.381	-.221E-02	1.380	-.225E-02	1.380	-.235E-02
Rural, RH = 99%	1.359	-.105E-02	1.358	-.119E-02	1.358	-.121E-02	1.357	-.126E-02
Oceanic, RH = 70%	1.407	-.200E-06	1.406	-.622E-06	1.406	-.681E-06	1.405	-.857E-06
Oceanic, RH = 80%	1.351	-.943E-07	1.350	-.265E-06	1.350	-.289E-06	1.349	-.360E-06
Oceanic, RH = 85%	1.342	-.772E-07	1.341	-.207E-06	1.341	-.225E-06	1.341	-.280E-06
Oceanic, RH = 90%	1.343	-.786E-07	1.342	-.212E-06	1.342	-.231E-06	1.341	-.287E-06
Oceanic, RH = 95%	1.338	-.690E-07	1.337	-.180E-06	1.337	-.195E-06	1.336	-.241E-06
Oceanic, RH = 99%	1.333	-.594E-07	1.332	-.147E-06	1.332	-.160E-06	1.331	-.196E-06
Urban, RH = 70%	1.484	-.583E-01	1.483	-.587E-01	1.483	-.588E-01	1.482	-.590E-01
Urban, RH = 80%	1.419	-.332E-01	1.417	-.335E-01	1.417	-.335E-01	1.416	-.336E-01
Urban, RH = 85%	1.398	-.253E-01	1.397	-.255E-01	1.396	-.256E-01	1.396	-.256E-01
Urban, RH = 90%	1.383	-.196E-01	1.382	-.198E-01	1.381	-.198E-01	1.381	-.199E-01
Urban, RH = 95%	1.363	-.122E-01	1.362	-.123E-01	1.362	-.123E-01	1.361	-.124E-01
Urban, RH = 99%	1.343	-.448E-02	1.342	-.452E-02	1.342	-.453E-02	1.342	-.454E-02
Water soluble (WCRP86)†	1.529	-.744E-02	1.526	-.880E-02	1.526	-.899E-02	1.525	-.955E-02
Dust-like (WCRP86)†	1.529	-.800E-02	1.526	-.800E-02	1.526	-.800E-02	1.525	-.800E-02
Soot (WCRP86)†	1.750	-.430E+00	1.750	-.430E+00	1.750	-.430E+00	1.750	-.430E+00
Dust, (Schütz, 1980)	1.530	-.550E-02	1.530	-.550E-02	1.530	-.550E-02	1.530	-.550E-02
75 % H_2SO_4 solution	1.428	-.340E-07	1.427	-.772E-07	1.427	-.832E-07	1.426	-.101E-06

Table 10-1 (cont): Refractive index of aerosol components/models

Wavelength	865		885		900	
	nr	ni	nr	ni	nr	ni
Rural, RH = 70%	1.492	-.929E-02	1.492	-.959E-02	1.492	-.982E-02
Rural, RH = 80%	1.436	-.611E-02	1.436	-.630E-02	1.436	-.645E-02
Rural, RH = 85%	1.413	-.481E-02	1.413	-.496E-02	1.413	-.508E-02
Rural, RH = 90%	1.393	-.366E-02	1.393	-.378E-02	1.393	-.387E-02
Rural, RH = 95%	1.378	-.281E-02	1.378	-.290E-02	1.378	-.297E-02
Rural, RH = 99%	1.356	-.151E-02	1.356	-.156E-02	1.355	-.160E-02
Oceanic, RH = 70%	1.402	-.404E-05	1.401	-.162E-04	1.401	-.210E-04
Oceanic, RH = 80%	1.348	-.138E-05	1.347	-.493E-05	1.347	-.636E-05
Oceanic, RH = 85%	1.339	-.973E-06	1.339	-.326E-05	1.339	-.418E-05
Oceanic, RH = 90%	1.340	-.985E-06	1.340	-.327E-05	1.339	-.418E-05
Oceanic, RH = 95%	1.335	-.740E-06	1.335	-.223E-05	1.334	-.283E-05
Oceanic, RH = 99%	1.330	-.498E-06	1.330	-.121E-05	1.329	-.150E-05
Urban, RH = 70%	1.479	-.600E-01	1.479	-.604E-01	1.479	-.605E-01
Urban, RH = 80%	1.414	-.341E-01	1.414	-.344E-01	1.414	-.344E-01
Urban, RH = 85%	1.394	-.260E-01	1.393	-.262E-01	1.393	-.263E-01
Urban, RH = 90%	1.379	-.201E-01	1.379	-.203E-01	1.379	-.203E-01
Urban, RH = 95%	1.360	-.125E-01	1.360	-.126E-01	1.360	-.126E-01
Urban, RH = 99%	1.341	-.462E-02	1.341	-.464E-02	1.340	-.466E-02
Water soluble (WCRP86)	1.520	-.121E-01	1.520	-.127E-01	1.520	-.130E-01
Dust-like (WCRP86)†	1.520	-.800E-02	1.520	-.800E-02	1.520	-.800E-02
Soot (WCRP86) †	1.750	-.430E+00	1.750	-.431E+00	1.750	-.432E+00
Dust, (Schütz, 1980)	1.530	-.550E-02	1.530	-.550E-02	1.530	-.550E-02
75 % H_2SO_4 solution	1.425	-.212E-06	1.424	-.377E-06	1.424	-.443E-06

Table 10-1 (cont): Refractive index of aerosol components/models

‡ S&F79 stands for Shettle and Fenn (1979).

† WCRP86 stands for WCRP (1986).

model no	nr	ni
1	1.33	0
2	*Idem*	*Idem*
3	*Idem*	*Idem*
4	*Idem*	*Idem*
5	1.44	0
6	*Idem*	*Idem*
7	*Idem*	*Idem*
8	*Idem*	*Idem*
9	1.55	-0.008
10	1.55	-0.0065
11	1.55	-0.005
12	1.55	-0.0023

Table 10-2 : Refractive index of land aerosol models

Note: the refractive indices in table 10-2 are independent of wavelength.

11. – Tables of aerosols optical properties (ATBD 2.7)

For each aerosol model, and for each wavelength, there are 2 lines : the first one for the scattering (b) and attenuation (c) coefficients (thus 2 successive values for each wavelength), the second one for the single scattering albedo (ω) and the asymmetry factor (g).

λ	412.5		442.5		490		510		560	
H2SO4	.148329	.14833D+00	.139728	.13973D+00	.126184	.12618D+00	.120614	.12061D+00	.107559	.10756D+00
H2SO4	1.000000	.73911D+00	1.000000	.73855D+00	1.000000	.73505D+00	1.000000	.73249D+00	1.000000	.72401D+00
conti	.000683	.75657D-03	.000632	.70070D-03	.000563	.62566D-03	.000537	.59688D-03	.000474	.53112D-03
conti	.902636	.64101D+00	.901856	.64038D+00	.900226	.63945D+00	.899168	.63861D+00	.891938	.63692D+00
des50	4.850898	.61657D+01	4.939096	.62082D+01	5.065333	.62711D+01	5.116927	.62981D+01	5.240319	.63644D+01
des50	.786751	.80923D+00	.795575	.80246D+00	.807732	.79299D+00	.812458	.78919D+00	.823385	.78033D+00
mar70	.030204	.30650D-01	.029395	.29805D-01	.028263	.28625D-01	.027819	.28164D-01	.026822	.27163D-01
mar70	.985458	.72349D+00	.986277	.72250D+00	.987366	.72147D+00	.987775	.72142D+00	.987446	.72057D+00
mar80	.057857	.58295D-01	.056887	.57289D-01	.055569	.55926D-01	.055006	.55345D-01	.053836	.54173D-01
mar80	.992492	.77352D+00	.992985	.77283D+00	.993629	.77216D+00	.993863	.77304D+00	.993767	.77253D+00
mar85	.079569	.80059D-01	.078356	.78805D-01	.076715	.77115D-01	.076006	.76387D-01	.074549	.74928D-01
mar85	.993892	.78640D+00	.994294	.78577D+00	.994818	.78469D+00	.995009	.78504D+00	.994933	.78447D+00
mar90	.083267	.83701D-01	.081929	.82328D-01	.079985	.80339D-01	.079195	.79533D-01	.077586	.77924D-01
mar90	.994824	.78935D+00	.995160	.78774D+00	.995590	.78711D+00	.995753	.78648D+00	.995661	.78514D+00
mar95	.114715	.11515D+00	.113103	.11350D+00	.110920	.11128D+00	.110126	.11047D+00	.108099	.10844D+00
mar95	.996227	.80157D+00	.996476	.80079D+00	.996804	.79938D+00	.996926	.79838D+00	.996870	.79753D+00
mar99	.265249	.26569D+00	.263162	.26356D+00	.260031	.26039D+00	.258592	.25893D+00	.255927	.25627D+00
mar99	.998360	.82527D+00	.998476	.82397D+00	.998625	.82281D+00	.998680	.82326D+00	.998661	.82128D+00
urb70	.010416	.14453D-01	.009725	.13491D-01	.008772	.12176D-01	.008397	.11674D-01	.007564	.10515D-01
urb70	.720650	.71094D+00	.720892	.70423D+00	.720470	.69427D+00	.719327	.69007D+00	.719420	.67963D+00
urb80	.017550	.21936D-01	.016437	.20513D-01	.014856	.18521D-01	.014213	.17734D-01	.012853	.16013D-01
urb80	.800071	.74399D+00	.801320	.73859D+00	.802124	.73085D+00	.801451	.72775D+00	.802615	.71878D+00
urb85	.024571	.29516D-01	.023168	.27764D-01	.021070	.25201D-01	.020211	.24179D-01	.018333	.21891D-01
urb85	.832462	.75824D+00	.834441	.75308D+00	.836095	.74641D+00	.835894	.74375D+00	.837461	.73623D+00
urb90	.028832	.33512D-01	.027208	.31552D-01	.024837	.28736D-01	.023776	.27516D-01	.021529	.24870D-01
urb90	.860340	.76506D+00	.862324	.76034D+00	.864306	.75381D+00	.864095	.75191D+00	.865669	.74546D+00
urb95	.044996	.49900D-01	.042636	.47170D-01	.039165	.43216D-01	.037920	.41815D-01	.034508	.38000D-01
urb95	.901731	.77777D+00	.903877	.77461D+00	.906263	.77002D+00	.906867	.76708D+00	.908106	.76265D+00
urb99	.109992	.11529D+00	.105894	.11079D+00	.099538	.10391D+00	.096809	.10100D+00	.090518	.94257D-01
urb99	.954029	.79220D+00	.955808	.79089D+00	.957931	.78901D+00	.958493	.78829D+00	.960330	.78529D+00

Table 11-1: Optical properties of aerosol models

λ	620		665		681.25		708.75[3]		753.75	
H2SO4	.093177	.93177D-01	.083373	.83373D-01	.080217	.80217D-01	*.075642*	*.75642D-01*	.067148	.67148D-01
H2SO4	1.000000	.71177D+00	1.000000	.70161D+00	1.000000	.69769D+00	*1.000000*	*.69173D+00*	1.000000	.67946D+00
conti	.000410	.46227D-03	.000369	.41838D-03	.000355	.40401D-03	*.000334*	*.38263D-03*	.000295	.34365D-03
conti	.887941	.63232D+00	.881477	.62844D+00	.878570	.62681D+00	*.873113*	*.62460D+00*	.859658	.62055D+00
des50	5.379658	.64431D+01	5.478536	.65012D+01	5.512597	.65216D+01	*5.562956*	*.65526D+01*	5.659404	.66119D+01
des50	.834953	.77074D+00	.842699	.76422D+00	.845289	.76204D+00	*.848970*	*.75887D+00*	.855940	.75298D+00
mar70	.025765	.26065D-01	.025074	.25363D-01	.024821	.25108D-01	*.024474*	*.24762D-01*	.023799	.24098D-01
mar70	.988500	.72116D+00	.988616	.72101D+00	.988562	.72149D+00	*.988354*	*.72154D+00*	.987578	.72319D+00
mar80	.052733	.53031D-01	.051928	.52215D-01	.051723	.52010D-01	*.051367*	*.51655D-01*	.050617	.50918D-01
mar80	.994382	.77165D+00	.994489	.77220D+00	.994490	.77125D+00	*.994416*	*.77125D+00*	.994098	.77190D+00
mar85	.073127	.73463D-01	.072108	.72432D-01	.071856	.72180D-01	*.071389*	*.71715D-01*	.070522	.70863D-01
mar85	.995428	.78318D+00	.995519	.78312D+00	.995520	.78210D+00	*.995457*	*.78220D+00*	.995196	.78193D+00
mar90	.075906	.76205D-01	.074685	.74975D-01	.074340	.74629D-01	*.073877*	*.74168D-01*	.072794	.73098D-01
mar90	.996071	.78369D+00	.996138	.78413D+00	.996134	.78344D+00	*.996078*	*.78245D+00*	.995837	.78293D+00
mar95	.106171	.10647D+00	.104899	.10519D+00	.104517	.10481D+00	*.103878*	*.10417D+00*	.102806	.10311D+00
mar95	.997175	.79567D+00	.997229	.79444D+00	.997227	.79403D+00	*.997185*	*.79380D+00*	.997020	.79309D+00
mar99	.253413	.25372D+00	.251371	.25167D+00	.251086	.25138D+00	*.250386*	*.25069D+00*	.248840	.24916D+00
mar99	.998798	.81815D+00	.998822	.81805D+00	.998824	.81637D+00	*.998806*	*.81523D+00*	.998731	.81425D+00
urb70	.006663	.92878D-02	.006067	.85043D-02	.005869	.82479D-02	*.005585*	*.78833D-02*	.005036	.71879D-02
urb70	.717350	.66807D+00	.713362	.65961D+00	.711527	.65668D+00	*.708479*	*.65236D+00*	.700551	.64459D+00
urb80	.011367	.14174D-01	.010389	.12993D-01	.010064	.12606D-01	*.009598*	*.12053D-01*	.008683	.10981D-01
urb80	.802019	.70881D+00	.799570	.70132D+00	.798355	.69872D+00	*.796322*	*.69486D+00*	.790774	.68808D+00
urb85	.016369	.19527D-01	.014983	.17914D-01	.014536	.17398D-01	*.013894*	*.16660D-01*	.012669	.15258D-01
urb85	.838259	.72687D+00	.836383	.72053D+00	.835487	.71816D+00	*.834012*	*.71462D+00*	.830285	.70810D+00
urb90	.019251	.22205D-01	.017637	.20378D-01	.017116	.19794D-01	*.016370*	*.18957D-01*	.014943	.17363D-01
urb90	.866947	.73666D+00	.865478	.73072D+00	.864712	.72847D+00	*.863522*	*.72512D+00*	.860637	.71893D+00
urb95	.031043	.34127D-01	.028635	.31493D-01	.027856	.30647D-01	*.026733*	*.29428D-01*	.024560	.27080D-01
urb95	.909647	.75588D+00	.909257	.75100D+00	.908948	.74908D+00	*.908426*	*.74621D+00*	.906943	.74097D+00
urb99	.083358	.86663D-01	.078219	.81282D-01	.076536	.79526D-01	*.074081*	*.76970D-01*	.069214	.71923D-01
urb99	.961867	.78136D+00	.962319	.77848D+00	.962398	.77724D+00	*.962460*	*.77536D+00*	.962332	.77216D+00

Table 11-1 (cont): Optical properties of aerosol models

[3] The values in *Italic type* are subject to change in a future revision of this document.

λ	760		778.75[4]		865		890		900	
H2SO4	.066022	.66022D-01	*.063550*	*.63550D-01*	.050916	.50916D-01	.047788	.47789D-01	.046675	.46675D-01
H2SO4	.999999	.67759D+00	*1.000000*	*.67369D+00*	.999999	.64892D+00	.999997	.64193D+00	.999997	.63902D+00
conti	.000291	.33881D-03	*.000280*	*.32802D-03*	.000225	.27228D-03	.000213	.25996D-03	.000209	.25530D-03
conti	.857921	.61979D+00	*.853615*	*.61842D+00*	.826760	.60843D+00	.820058	.60532D+00	.817381	.60415D+00
des50	5.672920	.66200D+01	*5.702191*	*.66388D+01*	5.866978	.67438D+01	5.909829	.67712D+01	5.926989	.67828D+01
des50	.856938	.75219D+00	*.858914*	*.75047D+00*	.869978	.74120D+00	.872792	.73890D+00	.873822	.73800D+00
mar70	.023697	.23997D-01	*.023520*	*.23823D-01*	.022468	.22783D-01	.022219	.22539D-01	.022113	.22434D-01
mar70	.987500	.72339D+00	*.987288*	*.72379D+00*	.986172	.72648D+00	.985816	.72707D+00	.985662	.72748D+00
mar80	.050522	.50824D-01	*.050304*	*.50609D-01*	.049185	.49505D-01	.048913	.49238D-01	.048822	.49148D-01
mar80	.994067	.77197D+00	*.993978*	*.77242D+00*	.993548	.77417D+00	.993406	.77502D+00	.993353	.77502D+00
mar85	.070405	.70746D-01	*.070101*	*.70447D-01*	.068762	.69125D-01	.068455	.68824D-01	.068346	.68718D-01
mar85	.995171	.78194D+00	*.995101*	*.78235D+00*	.994747	.78343D+00	.994633	.78347D+00	.994590	.78345D+00
mar90	.072670	.72976D-01	*.072381*	*.72690D-01*	.070823	.71149D-01	.070498	.70830D-01	.070389	.70724D-01
mar90	.995813	.78280D+00	*.995748*	*.78289D+00*	.995418	.78369D+00	.995305	.78335D+00	.995265	.78353D+00
mar95	.102614	.10292D+00	*.102366*	*.10268D+00*	.100757	.10109D+00	.100379	.10072D+00	.100151	.10049D+00
mar95	.997006	.79303D+00	*.996963*	*.79227D+00*	.996736	.79184D+00	.996652	.79161D+00	.996619	.79269D+00
mar99	.248665	.24898D+00	*.248109*	*.24843D+00*	.246070	.24642D+00	.245582	.24594D+00	.245419	.24578D+00
mar99	.998724	.81400D+00	*.998703*	*.81411D+00*	.998596	.81246D+00	.998539	.81208D+00	.998517	.81221D+00
urb70	.004965	.70978D-02	*.004804*	*.68950D-02*	.003992	.58645D-02	.003805	.56277D-02	.003733	.55367D-02
urb70	.699532	.64339D+00	*.696767*	*.64113D+00*	.680769	.62703D+00	.676164	.62297D+00	.674303	.62136D+00
urb80	.008567	.10844D-01	*.008325*	*.10557D-01*	.006963	.89599D-02	.006651	.85949D-02	.006531	.84546D-02
urb80	.790077	.68699D+00	*.788515*	*.68467D+00*	.777071	.67219D+00	.773787	.66850D+00	.772451	.66703D+00
urb85	.012466	.15029D-01	*.012129*	*.14643D-01*	.010257	.12507D-01	.009782	.11972D-01	.009614	.11781D-01
urb85	.829429	.70752D+00	*.828296*	*.70537D+00*	.820083	.69361D+00	.817115	.69060D+00	.816075	.68924D+00
urb90	.014705	.17100D-01	*.014313*	*.16661D-01*	.012128	.14226D-01	.011616	.13659D-01	.011418	.13441D-01
urb90	.859943	.71842D+00	*.859063*	*.71637D+00*	.852546	.70517D+00	.850411	.70190D+00	.849539	.70059D+00
urb95	.024272	.26769D-01	*.023670*	*.26117D-01*	.020272	.22457D-01	.019470	.21599D-01	.019160	.21269D-01
urb95	.906747	.74014D+00	*.906295*	*.73835D+00*	.902670	.72870D+00	.901403	.72581D+00	.900883	.72466D+00
urb99	.068563	.71247D-01	*.067190*	*.69824D-01*	.059382	.61749D-01	.057447	.59753D-01	.056502	.58781D-01
urb99	.962318	.77160D+00	*.962271*	*.77041D+00*	.961677	.76366D+00	.961418	.76160D+00	.961223	.76132D+00

Table 11-1 (cont): Optical properties of aerosol models

[4] The values in *Italic type* are subject to change in a future revision of this document.

12. - Tables describing the aerosol assemblages (ATBD 2.7)

Table 12-1 below describes the aerosol assemblages used when defining and testing the MERIS atmospheric corrections over Case 1 waters. For the 33 assemblages but the first one, the stratosphere contains the H_2SO_4 aerosol, with $\tau_a(550) = 0.005$. For assemblage #0, the stratosphere is aerosol-free.

Assemblage #	Boundary layer (0-2 km)	Free troposphere (2-12 km)
0	Maritime aerosol model (S&F79) RH = 99% $\tau_a(550)$ in {0.03, 0.1, 0.3, 0.5, 2}	Aerosol-free
1	Maritime aerosol model (S&F79) RH = 70% $\tau_a(550)$ in {0.03, 0.1, 0.3, 0.5, 2}	Continental aerosol (WCRP, 1986) $\tau_a(550) = 0.025$
2	Maritime aerosol model (S&F79) RH = 80% $\tau_a(550)$ in {0.03, 0.1, 0.3, 0.5, 2}	Continental aerosol (WCRP, 1986) $\tau_a(550) = 0.025$
3	Maritime aerosol model (S&F79) RH = 95% $\tau_a(550)$ in {0.03, 0.1, 0.3, 0.5, 2}	Continental aerosol (WCRP, 1986) $\tau_a(550) = 0.025$
4	Maritime aerosol model (S&F79) RH = 99% $\tau_a(550)$ in {0.03, 0.1, 0.3, 0.5, 2}	Continental aerosol (WCRP, 1986) $\tau_a(550) = 0.025$
5	Urban aerosol model (S&F79) RH = 70% $\tau_a(550)$ in {0.03, 0.1, 0.3, 0.5, 2}	Continental aerosol (WCRP, 1986) $\tau_a(550) = 0.025$
6	Urban aerosol model (S&F79) RH = 80% $\tau_a(550)$ in {0.03, 0.1, 0.3, 0.5, 2}	Continental aerosol (WCRP, 1986) $\tau_a(550) = 0.025$
7	Urban aerosol model (S&F79) RH = 95% $\tau_a(550)$ in {0.03, 0.1, 0.3, 0.5, 2}	Continental aerosol (WCRP, 1986) $\tau_a(550) = 0.025$
8	Urban aerosol model (S&F79) RH = 99% $\tau_a(550)$ in {0.03, 0.1, 0.3, 0.5, 2}	Continental aerosol (WCRP, 1986) $\tau_a(550) = 0.025$

Table 12-1: Aerosol assemblages used in atmosphere corrections above ocean

9	Maritime aerosol model (S&F79) RH = 70% $\tau_{tropo}(550)^{\bullet}$ in {0.05, 0.2, 0.5, 0.8, 2.}	Continental aerosol (WCRP, 1986) $\tau_a(550)$ = 25% of τ_{tropo}
10	Maritime aerosol model (S&F79) RH = 70% $\tau_{tropo}(550)$ in {0.05, 0.2, 0.5, 0.8, 2.}	Continental aerosol (WCRP, 1986) $\tau_a(550)$ = 50% of τ_{tropo}
11	Maritime aerosol model (S&F79) RH = 70% $\tau_{tropo}(550)$ in {0.05, 0.2, 0.5, 0.8, 2.}	Continental aerosol (WCRP, 1986) $\tau_a(550)$ = 75% of τ_{tropo}
12	Maritime aerosol model (S&F79) RH = 80% $\tau_{tropo}(550)$ in {0.05, 0.2, 0.5, 0.8, 2.}	Continental aerosol (WCRP, 1986) $\tau_a(550)$ = 25% of τ_{tropo}
13	Maritime aerosol model (S&F79) RH = 80% $\tau_{tropo}(550)$ in {0.05, 0.2, 0.5, 0.8, 2.}	Continental aerosol (WCRP, 1986) $\tau_a(550)$ = 50% of τ_{tropo}
14	Maritime aerosol model (S&F79) RH = 80% $\tau_{tropo}(550)$ in {0.05, 0.2, 0.5, 0.8, 2.}	Continental aerosol (WCRP, 1986) $\tau_a(550)$ = 75% of τ_{tropo}
15	Maritime aerosol model (S&F79) RH = 95% $\tau_{tropo}(550)$ in {0.05, 0.2, 0.5, 0.8, 2.}	Continental aerosol (WCRP, 1986) $\tau_a(550)$ = 25% of τ_{tropo}
16	Maritime aerosol model (S&F79) RH = 95% $\tau_{tropo}(550)$ in {0.05, 0.2, 0.5, 0.8, 2.}	Continental aerosol (WCRP, 1986) $\tau_a(550)$ = 50% of τ_{tropo}
17	Maritime aerosol model (S&F79) RH = 95% $\tau_{tropo}(550)$ in {0.05, 0.2, 0.5, 0.8, 2.}	Continental aerosol (WCRP, 1986) $\tau_a(550)$ = 75% of τ_{tropo}
18	Maritime aerosol model (S&F79) RH = 99% $\tau_{tropo}(550)$ in {0.05, 0.2, 0.5, 0.8, 2.}	Continental aerosol (WCRP, 1986) $\tau_a(550)$ = 25% of τ_{tropo}
19	Maritime aerosol model (S&F79) RH = 99% $\tau_{tropo}(550)$ in {0.05, 0.2, 0.5, 0.8, 2.}	Continental aerosol (WCRP, 1986) $\tau_a(550)$ = 50% of τ_{tropo}
20	Maritime aerosol model (S&F79) RH = 99% $\tau_{tropo}(550)$ in {0.05, 0.2, 0.5, 0.8, 2.}	Continental aerosol (WCRP, 1986) $\tau_a(550)$ = 75% of τ_{tropo}

Table 12-1(cont): Aerosol assemblages used in atmosphere corrections above ocean

21	Maritime aerosol model (S&F79) RH = 70% $\tau_{tropo}(550)$ in {0.05, 0.2, 0.5, 0.8, 2.}	Desert dust (Schütz, 1980) $\tau_a(550)$ = 25% of τ_{tropo}
22	Maritime aerosol model (S&F79) RH = 70% $\tau_{tropo}(550)$ in {0.05, 0.2, 0.5, 0.8, 2.}	Desert dust (Schütz, 1980) $\tau_a(550)$ = 50% of τ_{tropo}
23	Maritime aerosol model (S&F79) RH = 70% $\tau_{tropo}(550)$ in {0.05, 0.2, 0.5, 0.8, 2.}	Desert dust (Schütz, 1980) $\tau_a(550)$ = 75% of τ_{tropo}
24	Maritime aerosol model (S&F79) RH = 80% $\tau_{tropo}(550)$ in {0.05, 0.2, 0.5, 0.8, 2.}	Desert dust (Schütz, 1980) $\tau_a(550)$ = 25% of τ_{tropo}
25	Maritime aerosol model (S&F79) RH = 80% $\tau_{tropo}(550)$ in {0.05, 0.2, 0.5, 0.8, 2.}	Desert dust (Schütz, 1980) $\tau_a(550)$ = 50% of τ_{tropo}
26	Maritime aerosol model (S&F79) RH = 80% $\tau_{tropo}(550)$ in {0.05, 0.2, 0.5, 0.8, 2.}	Desert dust (Schütz, 1980) $\tau_a(550)$ = 75% of τ_{tropo}
27	Maritime aerosol model (S&F79) RH = 95% $\tau_{tropo}(550)$ in {0.05, 0.2, 0.5, 0.8, 2.}	Desert dust (Schütz, 1980) $\tau_a(550)$ = 25% of τ_{tropo}
28	Maritime aerosol model (S&F79) RH = 95% $\tau_{tropo}(550)$ in {0.05, 0.2, 0.5, 0.8, 2.}	Desert dust (Schütz, 1980) $\tau_a(550)$ = 50% of τ_{tropo}
29	Maritime aerosol model (S&F79) RH = 95% $\tau_{tropo}(550)$ in {0.05, 0.2, 0.5, 0.8, 2.}	Desert dust (Schütz, 1980) $\tau_a(550)$ = 75% of τ_{tropo}
30	Maritime aerosol model (S&F79) RH = 99% $\tau_{tropo}(550)$ in {0.05, 0.2, 0.5, 0.8, 2.}	Desert dust (Schütz, 1980) $\tau_a(550)$ = 25% of τ_{tropo}
31	Maritime aerosol model (S&F79) RH = 99% $\tau_{tropo}(550)$ in {0.05, 0.2, 0.5, 0.8, 2.}	Desert dust (Schütz, 1980) $\tau_a(550)$ = 50% of τ_{tropo}
32	Maritime aerosol model (S&F79) RH = 99% $\tau_{tropo}(550)$ in {0.05, 0.2, 0.5, 0.8, 2.}	Desert dust (Schütz, 1980) $\tau_a(550)$ = 75% of τ_{tropo}

• : NOTE : τ_{tropo} stands now for the whole troposphere (*i.e.*, 0-12 km), while τ_a was only for the boundary layer in cases 1 to 8.

Table 12-1 (cont): Aerosol assemblages used in atmosphere corrections above ocean

13. - Aerosol phase functions

The figures below show the aerosol scattering phase function at the wavelength 550nm, for the aerosol models. Figure 13-1 shows the aerosol models from ATBD 2.7, figure 13-2 the models from ATBD 2.15.

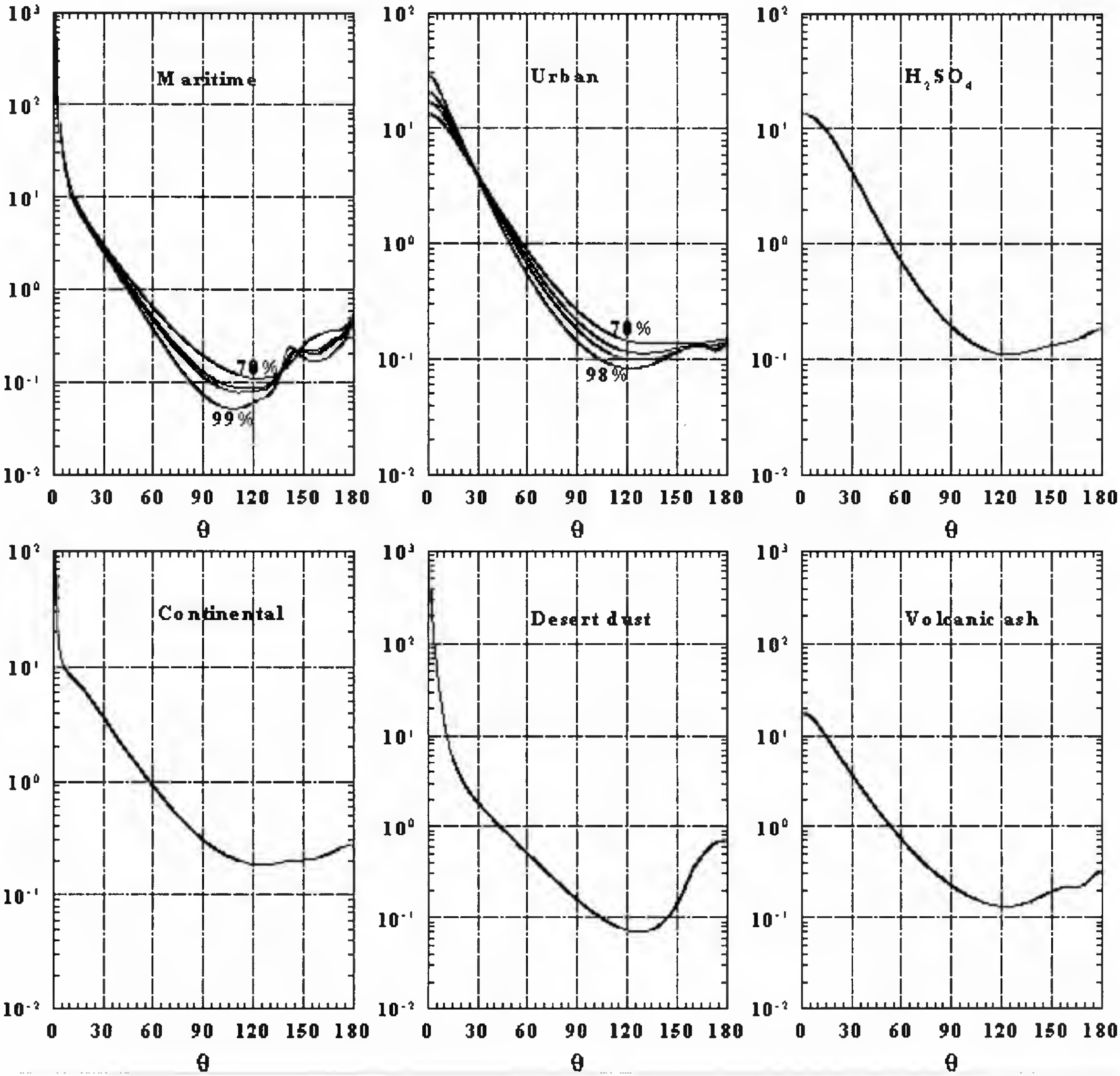

Figure 13-1: Scattering phase functions for the aerosol models of ATBD 2.7

Figure 13-2: Scattering phase functions for the aerosol models of ATBD 2.15

14. - Spectral dependency of aerosol optical thickness

14.1 – Aerosol Assemblages (Atm. Cor. above water)

For the 33 aerosol assemblages listed in table 12-1 above, the spectral dependency of optical thickness is tabulated at the first 13 bands and at 5 optical thicknesses in table 14-1 below. The line labelled $\tau_a(560)$ or $\tau_{tropo}(560)$ refers to the optical thickness of the boundary layer + tropospheric aerosol at 560nm (see table 12-1). The values in *Italic type* are subject to change in a future revision of this document.

Spectral dependency of optical thickness for assemblage 0					
$\tau_a(560)$	0.03	0.1	0.3	0.5	2.0
412	0.031100001	0.103400002	0.310299882	0.516999986	2.06829992
443	0.0307	0.102499901	0.307799965	0.512899897	2.051899806
490	0.030400001	0.101399998	0.303999894	0.506700002	2.027200022
510	0.030300001	0.100799904	0.302399884	0.50400001	2.015899937
560	0.029899999	0.0998	0.299199905	0.498699886	1.99510003
620	0.0296	0.098700005	0.296200007	0.493799886	1.975200006
665	0.029400001	0.097900005	0.293799997	0.489799884	1.95919986
681	0.029400001	0.097799995	0.293599979	0.4892999	1.956999858
708.75	*0.029300001*	*0.097599998*	*0.292800007*	*0.487899914*	*1.951500054*
753	0.028999999	0.096899998	0.290999878	0.484899999	1.939700053
761	0.028999999	0.096899998	0.290699988	0.484600019	1.938399953
778.75	*0.028999999*	*0.0968*	*0.290199875*	*0.483500018*	*1.934099879*
865	0.0288	0.096	0.2878	0.4794999	1.9184
Spectral dependency of optical thickness for assemblage 1					
$\tau_a(560)$	0.03	0.1	0.3	0.5	2.0
412	0.075099999	0.153500006	0.377499891	0.601599877	2.282000106
443	0.071300001	0.147499991	0.365299902	0.583299882	2.217200059
490	0.065899999	0.139299903	0.348400002	0.557799867	2.127100003
510	0.0638	0.135900004	0.341699994	0.547499985	2.091499975
560	0.059000002	0.128499896	0.327099987	0.525600028	2.014900038
620	0.054200003	0.120800003	0.311299989	0.501899992	1.930899942
665	0.050900003	0.115700002	0.301099903	0.486400024	1.876899872
681	0.049700002	0.114000006	0.297500019	0.481099909	1.857499918
708.75	*0.0483*	*0.111599899*	*0.292599987*	*0.47369998*	*1.831199946*
753	0.045200001	0.106799896	0.282999883	0.459099978	1.780400008
761	0.045000005	0.106399901	0.281799985	0.457099987	1.772799944
778.75	*0.0441*	*0.104999902*	*0.279199973*	*0.453199986*	*1.759300027*
865	0.0398	0.0981	0.2646999	0.4311999	1.6803

Table 14-1: Spectral dependency of aerosol optical thickness

Spectral dependency of optical thickness for assemblage 2					
$\tau_a(560)$	0.03	0.1	0.3	0.5	2.0
412	0.073600001	0.148699898	0.362999872	0.577199991	2.184099819
443	0.070100001	0.143999991	0.354600015	0.565099998	2.144999883
490	0.065499996	0.137499998	0.343100002	0.548699901	2.090799928
510	0.063399997	0.134599901	0.338200001	0.541700023	2.0678
560	0.059099996	0.128700008	0.32759998	0.526400012	2.017799944
620	0.054900002	0.123099907	0.318099986	0.512999883	1.975299817
665	0.051799999	0.118799995	0.310200005	0.501899894	1.93819988
681	0.050899999	0.117900002	0.309099974	0.500299864	1.934399963
708.75	*0.049600002*	*0.115699908*	*0.305099899*	*0.494599887*	*1.914999888*
753	0.046799998	0.112399904	0.299599983	0.486799876	1.890799887
761	0.046599997	0.112099898	0.298799893	0.485799981	1.887299975
778.75	*0.0458*	*0.110600005*	*0.295999986*	*0.481300005*	*1.871799994*
865	0.0421	0.1053999	0.2867	0.4677	1.8264
Spectral dependency of optical thickness for assemblage 3					
$\tau_a(560)$	0.03	0.1	0.3	0.5	2.0
412	0.073299994	0.147300004	0.358999987	0.570500023	2.157600053
443	0.069799996	0.142800003	0.351399875	0.560099893	2.124399954
490	0.065199997	0.136899991	0.341300015	0.545799917	2.079500044
510	0.063299995	0.134499898	0.337500011	0.540400028	2.063000117
560	0.059099996	0.128999996	0.328299902	0.527499976	2.022100073
620	0.054999999	0.123399899	0.3191	0.514699874	1.982300067
665	0.051899999	0.1196999	0.312900001	0.506199999	1.956100122
681	0.050999999	0.118500007	0.311100012	0.503799917	1.948300167
708.75	*0.049899999*	*0.116900005*	*0.308299893*	*0.499599928*	*1.935500094*
753	0.047299996	0.113499908	0.30299999	0.492499919	1.913800047
761	0.046899997	0.1130999	0.302399915	0.491400032	1.909999958
778.75	*0.046199996*	*0.112299899*	*0.300999908*	*0.489700023*	*1.904900073*
865	0.0428	0.1077	0.2935	0.4793999	1.8725
Spectral dependency of optical thickness for assemblage 4					
$\tau_a(560)$	0.03	0.1	0.3	0.5	2.0
412	0.0726	0.144899903	0.351799989	0.558499846	2.109800179
443	0.069300004	0.1410999	0.346399994	0.551499895	2.090500142
490	0.065000002	0.135999905	0.338599863	0.541299891	2.061800052
510	0.063199998	0.13369989	0.335299994	0.536899944	2.048800079
560	0.059200003	0.129099994	0.328499984	0.527999861	2.024400035
620	0.055200003	0.124299995	0.321799895	0.519399997	2.000799952
665	0.052400004	0.120899893	0.316799969	0.512799932	1.982200098
681	0.051600005	0.119999894	0.31579999	0.511500016	1.979200099
708.75	*0.050400004*	*0.118699903*	*0.313899882*	*0.509000023*	*1.972599987*
753	0.047800001	0.115699899	0.309799907	0.503699992	1.958499986
761	0.047600005	0.115499996	0.309299992	0.503199852	1.957000112
778.75	*0.046900001*	*0.114699903*	*0.308099959*	*0.501399856*	*1.952000115*
865	0.0437	0.1108999	0.3027	0.4943999	1.9333

Table 14-1: Spectral dependency of aerosol optical thickness (cont.)

Spectral dependency of optical thickness for assemblage 5					
$\tau_a(560)$	0.03	0.1	0.3	0.5	2.0
412	0.081800002	0.176100004	0.445499963	0.714799992	2.734400171
443	0.076300006	0.16419991	0.415599983	0.666899961	2.552200237
490	0.068700002	0.148100012	0.374799918	0.601800015	2.303200016
510	0.0656	0.141699997	0.359200003	0.576699971	2.207999935
560	0.058699999	0.127199908	0.323100005	0.518999865	1.988400082
620	0.051500002	0.112099998	0.285100001	0.458299909	1.756000116
665	0.0468	0.102200006	0.260599995	0.419099914	1.607600002
681	0.045300002	0.098999998	0.252700007	0.406300023	1.559000109
708.75	*0.043200001*	*0.094600001*	*0.241399997*	*0.388299926*	*1.489900013*
753	0.038800001	0.085799999	0.219599893	0.353700007	1.358000072
761	0.038499999	0.084800002	0.217	0.349200008	1.341000007
778.75	*0.037099999*	*0.082099997*	*0.210600007*	*0.338999997*	*1.302600058*
865	0.0312	0.0695	0.1788	0.2879999	1.1076
Spectral dependency of optical thickness for assemblage 6					
$\tau_a(560)$	0.03	0.1	0.3	0.5	2.0
412	0.0817	0.17580001	0.444200015	0.71269988	2.726299822
443	0.076200001	0.164199904	0.41519993	0.66630002	2.549199855
490	0.068700002	0.148000006	0.374599914	0.601299992	2.301500104
510	0.065500002	0.141500007	0.35849993	0.575499905	2.20339977
560	0.058700003	0.127199907	0.3232	0.519200021	1.989299896
620	0.051700002	0.11230001	0.285800014	0.459199907	1.760299991
665	0.046900002	0.102500003	0.261500004	0.420599907	1.613399873
681	0.045400001	0.099300003	0.253600005	0.407900008	1.56509993
708.75	*0.0433*	*0.094800011*	*0.242400016*	*0.389899917*	*1.496299949*
753	0.038900002	0.086000006	0.220399895	0.354799879	1.362799946
761	0.038600002	0.085000003	0.2177	0.350499986	1.34579998
778.75	*0.037200003*	*0.082599999*	*0.211699904*	*0.340999978*	*1.309999858*
865	0.0314	0.0698	0.1794	0.2890999	1.1116
Spectral dependency of optical thickness for assemblage 7					
$\tau_a(560)$	0.03	0.1	0.3	0.5	2.0
412	0.080200001	0.170499994	0.428599909	0.686599991	2.622100129
443	0.075199994	0.160500014	0.404500006	0.648400016	2.477899958
490	0.0682	0.146399904	0.369800016	0.593299926	2.269499898
510	0.065399998	0.141000002	0.357199917	0.573599864	2.195300071
560	0.0588	0.127599894	0.324000019	0.520499984	1.994399982
620	0.052	0.113799996	0.290400007	0.46689997	1.790399919
665	0.047499998	0.104500002	0.267199912	0.430199997	1.651699975
681	0.045999999	0.101400007	0.259900005	0.41839989	1.606999892
708.75	*0.043999997*	*0.097100002*	*0.249300007*	*0.401600006*	*1.542899965*
753	0.039799998	0.088900002	0.228899904	0.368899981	1.419100001
761	0.039399998	0.087899997	0.226300016	0.3646999	1.402899985
778.75	*0.038099998*	*0.085399998*	*0.2203999*	*0.355499895*	*1.368499915*
865	0.0324	0.073	0.1891999	0.3052999	1.1763

Table 14-1: Spectral dependency of aerosol optical thickness (cont.)

Spectral dependency of optical thickness for assemblage 8					
$\tau_a(560)$	0.03	0.1	0.3	0.5	2.0
412	0.077699997	0.162200004	0.403600005	0.644800019	2.45509998
443	0.07329999	0.154599903	0.386500009	0.618499867	2.357899874
490	0.067299996	0.143400004	0.360900014	0.578499961	2.20979996
510	0.064699998	0.138600011	0.349999986	0.561599899	2.147300027
560	0.058899995	0.127900006	0.325300012	0.522699906	2.002599978
620	0.052799998	0.1163	0.297699994	0.479199906	1.839900057
665	0.048599998	0.107999901	0.278199999	0.448399982	1.724599864
681	0.0471	0.105399899	0.271899895	0.438399913	1.687000048
708.75	*0.045199999*	*0.101700001*	*0.262699998*	*0.423999907*	*1.632400007*
753	0.041299997	0.093999999	0.244599894	0.395300016	1.524400054
761	0.040999999	0.093099999	0.242399895	0.391399895	1.510099944
778.75	*0.039799999*	*0.090899999*	*0.2371*	*0.383399989*	*1.479599913*
865	0.0342	0.0796	0.2087	0.3380999	1.3076
Spectral dependency of optical thickness for assemblage 9					
$\tau_{tropo}(560)$	0.05	0.2	0.5	0.8	2.0
412	0.067199993	0.244299912	0.600700046	0.957199872	2.382999751
443	0.064599995	0.23410001	0.575900012	0.917999917	2.284899907
490	0.060599999	0.22030001	0.542100041	0.863799963	2.150800019
510	0.059099994	0.214900008	0.529000002	0.842700016	2.098499953
560	0.055199995	0.202800014	0.499099912	0.795999956	1.982599963
620	0.051299996	0.189700013	0.467900024	0.745699951	1.85849994
665	0.048999995	0.181299906	0.447700025	0.713899888	1.779199879
681	0.048099997	0.178399918	0.440699993	0.702799983	1.751799966
708.75	*0.046899997*	*0.174500015*	*0.430799994*	*0.687399913*	*1.71309997*
753	0.044699998	0.166700009	0.412299921	0.657899928	1.640099871
761	0.044399997	0.165700004	0.409899883	0.653899984	1.630299972
778.75	*0.043900002*	*0.163699902*	*0.404800005*	*0.645900017*	*1.610800052*
865	0.0406	0.1521999	0.3771	0.6021999	1.5017
Spectral dependency of optical thickness for assemblage 10					
$\tau_{tropo}(560)$	0.05	0.2	0.5	0.8	2.0
412	0.069499998	0.257899922	0.634699995	1.011500017	2.518900051
443	0.0658	0.2443	0.601099911	0.957799933	2.385000119
490	0.060800001	0.225499912	0.55519999	0.884599943	2.203100059
510	0.058600001	0.218299909	0.537499897	0.856699969	2.133100045
560	0.054099999	0.201700017	0.497399898	0.792999921	1.974899996
620	0.049499999	0.18440001	0.454999995	0.725399977	1.807500078
665	0.046199997	0.173500006	0.428000003	0.682500026	1.700600118
681	0.045200002	0.169799904	0.41909989	0.668099887	1.664600008
708.75	*0.043699999*	*0.164399911*	*0.405799885*	*0.647199909*	*1.612499949*
753	0.0409	0.154200003	0.381099917	0.608299922	1.516199934
761	0.0405	0.153200012	0.378199914	0.603299972	1.503400065
778.75	*0.039599998*	*0.150399996*	*0.371500005*	*0.592499898*	*1.477100077*
865	0.0357	0.1354999	0.3355999	0.5356999	1.336

Table 14-1: Spectral dependency of aerosol optical thickness (cont.)

Spectral dependency of optical thickness for assemblage 11					
$\tau_{tropo}(560)$	0.05	0.2	0.5	0.8	2.0
412	0.074199998	0.27149998	0.668699931	1.065899915	2.654800083
443	0.0696	0.254200009	0.625899926	0.997799899	2.485100171
490	0.063	0.230699996	0.568099989	0.905699939	2.255599991
510	0.060499998	0.221499988	0.545999898	0.870299855	2.167500137
560	0.054799998	0.201100011	0.49529991	0.789799973	1.967000127
620	0.048899998	0.179499893	0.442299997	0.705100024	1.756300046
665	0.0452	0.165600005	0.408299901	0.651199885	1.621799969
681	0.0438	0.160999994	0.397099911	0.633099923	1.577500096
708.75	*0.042099999*	*0.154400006*	*0.380599887*	*0.606899931*	*1.512100056*
753	0.038400001	0.142000009	0.35009991	0.558500014	1.391700047
761	0.037999998	0.14049999	0.346399991	0.55239988	1.376500074
778.75	*0.037200001*	*0.136999994*	*0.338099913*	*0.539099894*	*1.343600049*
865	0.0322	0.1189	0.2943	0.4693999	1.17
Spectral dependency of optical thickness for assemblage 12					
$\tau_{tropo}(560)$	0.05	0.2	0.5	0.8	2.0
412	0.065500001	0.237099885	0.582400035	0.927999861	2.309799984
443	0.063199998	0.228699992	0.562399934	0.896399869	2.230799943
490	0.0599	0.217700005	0.535399911	0.852799855	2.123599977
510	0.058500001	0.213199995	0.524499993	0.835499953	2.080700017
560	0.055199999	0.202999995	0.499699885	0.796899904	1.984800049
620	0.052200003	0.193099991	0.476199873	0.759099859	1.891999884
665	0.050100002	0.185900004	0.4591999	0.732299879	1.825300008
681	0.049499999	0.18419999	0.455099887	0.725799923	1.809400054
708.75	*0.0485*	*0.180800004*	*0.446699984*	*0.712399855*	*1.776000077*
753	0.046700001	0.175099896	0.433099986	0.691	1.723000053
761	0.046500003	0.174299986	0.431399999	0.688199842	1.716099903
778.75	*0.046100003*	*0.172199902*	*0.425999986*	*0.679600013*	*1.695099975*
865	0.0433	0.1632	0.4045999	0.6459	1.6113
Spectral dependency of optical thickness for assemblage 13					
$\tau_{tropo}(560)$	0.05	0.2	0.5	0.8	2.0
412	0.068199997	0.253099999	0.622600016	0.992099986	2.470000037
443	0.064999996	0.2407999	0.591999895	0.943299984	2.348699946
490	0.060299997	0.223699887	0.550599981	0.877399938	2.184899948
510	0.058400001	0.216999991	0.534500012	0.851899936	2.121200058
560	0.054099999	0.201900003	0.497900014	0.793499993	1.976400031
620	0.049899995	0.186700004	0.460599906	0.73429975	1.829699967
665	0.046999995	0.1765999	0.435600006	0.694899949	1.731199891
681	0.0462	0.173699898	0.428699921	0.683399972	1.70309988
708.75	*0.044799998*	*0.168500009*	*0.416299895*	*0.663799874*	*1.654499947*
753	0.042199999	0.159799902	0.395099925	0.630399955	1.571400001
761	0.041899998	0.158899993	0.392599898	0.626099968	1.560799841
778.75	*0.041099999*	*0.156000008*	*0.385699898*	*0.615000008*	*1.533499846*
865	0.0375	0.1428	0.3538999	0.5651	1.409

Table 14-1: Spectral dependency of aerosol optical thickness (cont.)

Spectral dependency of optical thickness for assemblage 14					
$\tau_{tropo}(560)$	0.05	0.2	0.5	0.8	2.0
412	0.073599997	0.269100006	0.662599944	1.056200012	2.630399911
443	0.068999999	0.25249993	0.62149987	0.990599915	2.466899941
490	0.062799995	0.22980001	0.565999965	0.901999892	2.246499972
510	0.060400001	0.221000006	0.544499851	0.867899923	2.161699864
560	0.054799999	0.201200006	0.495499874	0.790200011	1.967799968
620	0.049299997	0.180599905	0.444999884	0.709599887	1.767400004
665	0.045699998	0.167099903	0.412199888	0.657299888	1.637299888
681	0.044299999	0.163099907	0.401899878	0.640799902	1.596699811
708.75	*0.042599998*	*0.15639991*	*0.385899894*	*0.615299893*	*1.533000002*
753	0.039099998	0.144899905	0.356999976	0.56959994	1.419399883
761	0.038699997	0.143299907	0.353599999	0.563899853	1.405199945
778.75	*0.0379*	*0.139899903*	*0.345199995*	*0.550299908*	*1.371699988*
865	0.0331	0.1226	0.3036	0.484	1.2065
Spectral dependency of optical thickness for assemblage 15					
$\tau_{tropo}(560)$	0.05	0.2	0.5	0.8	2.0
412	0.064900002	0.234999991	0.577500018	0.919999915	2.289799931
443	0.062899995	0.227299892	0.558500007	0.890099985	2.215300094
490	0.059700001	0.216800013	0.533199941	0.849499881	2.115000064
510	0.058399997	0.212699903	0.523599945	0.834100032	2.0769998
560	0.055299999	0.2034	0.500499904	0.798099854	1.988000004
620	0.052299997	0.193499901	0.477499911	0.761199975	1.896999939
665	0.050599999	0.187099914	0.462399993	0.737799842	1.838600024
681	0.049800001	0.185299899	0.457699913	0.730000009	1.819799938
708.75	*0.048799995*	*0.182199991*	*0.450500027*	*0.718699848*	*1.791299992*
753	0.047199998	0.176799989	0.43720002	0.697899946	1.740099911
761	0.046999996	0.175999998	0.435599894	0.694999995	1.733100016
778.75	*0.046799999*	*0.174700004*	*0.432000026*	*0.689599875*	*1.719900001*
865	0.0441	0.1665999	0.4132	0.6599	1.646
Spectral dependency of optical thickness for assemblage 16					
$\tau_{tropo}(560)$	0.05	0.2	0.5	0.8	2.0
412	0.067900003	0.251699914	0.619300019	0.986700009	2.456799815
443	0.064699998	0.239599913	0.589599911	0.939100035	2.338599866
490	0.060199996	0.223099921	0.549300019	0.875100064	2.179199804
510	0.058299998	0.216900014	0.5338	0.851000058	2.118799884
560	0.054199999	0.20220001	0.498299962	0.794399941	1.978399893
620	0.050099999	0.186999908	0.461399989	0.735700049	1.833199947
665	0.0471	0.17749991	0.437799975	0.69840008	1.740099885
681	0.046200001	0.1742999	0.430399905	0.686300044	1.710100011
708.75	*0.0451*	*0.169699919*	*0.418699874*	*0.668000009*	*1.664599989*
753	0.042499999	0.160900009	0.3977999	0.634999868	1.582800012
761	0.042299998	0.159900003	0.395499925	0.630699908	1.572099991
778.75	*0.041399998*	*0.157700017*	*0.389799987*	*0.62170004*	*1.549899949*
865	0.0381	0.1450999	0.3596999	0.5742	1.4321

Table 14-1: Spectral dependency of aerosol optical thickness (cont.)

Spectral dependency of optical thickness for assemblage 17					
$\tau_{tropo}(560)$	0.05	0.2	0.5	0.8	2.0
412	0.073399996	0.268400018	0.660899852	1.053600017	2.623699919
443	0.068999999	0.251899888	0.620199894	0.988599957	2.461900179
490	0.062700002	0.22959989	0.565299936	0.900900053	2.243599981
510	0.060199996	0.220799999	0.544200012	0.867599901	2.160399967
560	0.054799999	0.201299991	0.495899888	0.790500004	1.968899962
620	0.049399998	0.180699905	0.445499974	0.710300042	1.76910002
665	0.0458	0.167500002	0.413199982	0.659200021	1.641600114
681	0.044399997	0.163299903	0.402699896	0.64230004	1.600200147
708.75	*0.042799998*	*0.156999903*	*0.387199911*	*0.617299957*	*1.538000073*
753	0.039299996	0.145299893	0.358399996	0.571900031	1.425100075
761	0.038800001	0.143799897	0.355100007	0.566099924	1.410800039
778.75	*0.038100001*	*0.140699893*	*0.347199893*	*0.553599885*	*1.380100083*
865	0.0333	0.1237	0.3064	0.4886	1.2182
Spectral dependency of optical thickness for assemblage 18					
$\tau_{tropo}(560)$	0.05	0.2	0.5	0.8	2.0
412	0.063899998	0.231499891	0.56859988	0.905699913	2.25389995
443	0.062199997	0.224599896	0.552199909	0.879899959	2.189899776
490	0.059299998	0.215399889	0.529799881	0.844099898	2.101699913
510	0.058299999	0.211699887	0.520799856	0.829900029	2.06640004
560	0.0554	0.203499984	0.500999938	0.798799884	1.989799968
620	0.052799999	0.194899992	0.480999983	0.766800006	1.911099921
665	0.051099999	0.189199881	0.467299882	0.745599976	1.858299927
681	0.050299998	0.187499884	0.463599884	0.73940006	1.842999996
708.75	*0.049499997*	*0.185099889*	*0.457399998*	*0.729799953*	*1.819199918*
753	0.048000001	0.180099897	0.445699996	0.711300011	1.773699955
761	0.047800002	0.179599988	0.444400019	0.709200048	1.768300093
778.75	*0.047699997*	*0.178099892*	*0.440900008*	*0.703700058*	*1.755199946*
865	0.0454	0.1712	0.4246	0.678	1.6914
Spectral dependency of optical thickness for assemblage 19					
$\tau_{tropo}(560)$	0.05	0.2	0.5	0.8	2.0
412	0.067300001	0.249299892	0.613199993	0.977099875	2.432900062
443	0.064200001	0.237899889	0.585299914	0.932399907	2.321500092
490	0.06	0.222199997	0.546999971	0.871699964	2.170399988
510	0.058	0.216100006	0.532100006	0.84809999	2.111700079
560	0.054200003	0.202299993	0.498699889	0.794999901	1.979700006
620	0.050299999	0.187899998	0.463800031	0.73949993	1.842499971
665	0.047500001	0.178699901	0.441100013	0.70369997	1.753300049
681	0.046700002	0.175799901	0.434299983	0.692399938	1.725500088
708.75	*0.045400003*	*0.171499886*	*0.423499919*	*0.67549987*	*1.683300045*
753	0.043000003	0.163099893	0.403399978	0.643999869	1.605200045
761	0.042800004	0.162299896	0.401299892	0.640099975	1.595500101
778.75	*0.042000001*	*0.160099884*	*0.395599973*	*0.631199897*	*1.5736001*
865	0.0389	0.1482999	0.3673	0.5863999	1.4625

Table 14-1: Spectral dependency of aerosol optical thickness (cont.)

Spectral dependency of optical thickness for assemblage 20					
$\tau_{tropo}(560)$	0.05	0.2	0.5	0.8	2.0
412	0.073200006	0.267299989	0.657999899	1.048799935	2.611700064
443	0.068800006	0.250999891	0.617999957	0.985099933	2.453300037
490	0.062500003	0.228999998	0.56400002	0.899099982	2.239099992
510	0.060200001	0.220499992	0.543199901	0.866100018	2.156899961
560	0.054800004	0.201299981	0.495999909	0.790799959	1.969400114
620	0.049400003	0.181199885	0.446600014	0.712199999	1.773800079
665	0.046000001	0.168099889	0.414800023	0.661800002	1.64820009
681	0.044600001	0.164099899	0.404800019	0.6454	1.6079001
708.75	*0.043000005*	*0.157899896*	*0.389399903*	*0.621099872*	*1.54740006*
753	0.039700002	0.146499902	0.36129993	0.576300007	1.436300135
761	0.039200001	0.145099893	0.357899996	0.570800028	1.422600085
778.75	*0.038500003*	*0.141799999*	*0.350100038*	*0.558399959*	*1.391800101*
865	0.0338	0.1253	0.3101999	0.4948	1.2332
Spectral dependency of optical thickness for assemblage 21					
$\tau_{tropo}(560)$	0.05	0.2	0.5	0.8	2.0
412	0.061799997	0.223299892	0.548099859	0.872799868	2.172399932
443	0.0604	0.218699992	0.537100014	0.855399937	2.128900138
490	0.0586	0.212099995	0.521499872	0.830999944	2.068799895
510	0.057699997	0.209499896	0.515599999	0.821499997	2.04530002
560	0.055599998	0.203799994	0.50249987	0.801000135	1.995000003
620	0.053499999	0.197699977	0.48829988	0.77869992	1.940300022
665	0.0524	0.194099893	0.479499875	0.764500079	1.906000032
681	0.0519	0.192599882	0.476099912	0.75959996	1.893600054
708.75	*0.051300002*	*0.190899986*	*0.471800004*	*0.753000077*	*1.877100091*
753	0.0501	0.187099888	0.463299913	0.739700072	1.844699981
761	0.050000003	0.186499887	0.462299925	0.737700017	1.839700005
778.75	*0.049499996*	*0.185899996*	*0.459999989*	*0.734300045*	*1.831599933*
865	0.0478	0.1801999	0.4471	0.7143999	1.7823
Spectral dependency of optical thickness for assemblage 22					
$\tau_{tropo}(560)$	0.05	0.2	0.5	0.8	2.0
412	0.059100002	0.215700003	0.529299916	0.843099919	2.09770016
443	0.057999997	0.212899988	0.523100048	0.83319992	2.07320001
490	0.056600003	0.209099908	0.514400028	0.819199867	2.039499887
510	0.056000002	0.207499896	0.51090002	0.813900066	2.026500016
560	0.054699998	0.204299987	0.503600017	0.802799973	1.999699826
620	0.053500003	0.200800004	0.495999909	0.791000004	1.971299855
665	0.052599999	0.198899985	0.491600044	0.783899872	1.954399936
681	0.052199999	0.197999899	0.489699928	0.781299844	1.947999943
708.75	*0.051900002*	*0.197199994*	*0.48779993*	*0.778199946*	*1.940099885*
753	0.051100001	0.194999903	0.483500008	0.771700051	1.924799974
761	0.050900001	0.194999993	0.482799916	0.770899983	1.922399972
778.75	*0.050599998*	*0.194599984*	*0.481899997*	*0.769099841*	*1.91889992*
865	0.0497	0.1916999	0.4757999	0.7598999	1.8968

Table 14-1: Spectral dependency of aerosol optical thickness (cont.)

Spectral dependency of optical thickness for assemblage 23					
$\tau_{tropo}(560)$	0.05	0.2	0.5	0.8	2.0
412	0.058200001	0.208299921	0.510699901	0.813099891	2.022999952
443	0.057600003	0.20739992	0.50909991	0.810599961	2.01730005
490	0.056999999	0.206100015	0.506900008	0.807499856	2.010000038
510	0.056499999	0.205499902	0.506200029	0.806299883	2.007499995
560	0.055800003	0.204900006	0.50469999	0.804599983	2.004200039
620	0.055100001	0.204099905	0.503699995	0.803300019	2.002100024
665	0.054800002	0.203799898	0.503699874	0.803399922	2.002600028
681	0.054600001	0.203400015	0.503299876	0.803099882	2.002700126
708.75	*0.054500003*	*0.203600005*	*0.503599978*	*0.80350001*	*2.003700034*
753	0.054000003	0.203	0.503499966	0.803699913	2.004899996
761	0.054000003	0.2032999	0.503599978	0.803800001	2.004899996
778.75	*0.053800001*	*0.203200002*	*0.503699995*	*0.804299992*	*2.006200177*
865	0.0536	0.2032999	0.5044999	0.8057999	2.0112
Spectral dependency of optical thickness for assemblage 24					
$\tau_{tropo}(560)$	0.05	0.2	0.5	0.8	2.0
412	0.0601	0.216099898	0.529799879	0.843599943	2.099200042
443	0.059	0.213300005	0.523599919	0.833800038	2.074800189
490	0.057899995	0.209499895	0.514800035	0.819999873	2.04160005
510	0.057100001	0.207800009	0.51109986	0.814299985	2.027500022
560	0.055599998	0.203999989	0.503099914	0.801899963	1.997200013
620	0.054399999	0.2010999	0.496599926	0.792099966	1.973799935
665	0.053499999	0.1987	0.490999908	0.782899945	1.952100144
681	0.0533	0.198399999	0.490499936	0.782599912	1.951200054
708.75	*0.052899997*	*0.197200003*	*0.487700011*	*0.777999951*	*1.94000012*
753	0.052099996	0.195500002	0.484100037	0.77280009	1.927600153
761	0.052099996	0.195099897	0.483799896	0.772000021	1.925499993
778.75	*0.051699999*	*0.194399883*	*0.481200028*	*0.768000043*	*1.9159*
865	0.0505	0.1912	0.4745999	0.7581	1.8919
Spectral dependency of optical thickness for assemblage 25					
$\tau_{tropo}(560)$	0.05	0.2	0.5	0.8	2.0
412	0.057799999	0.210899993	0.517199857	0.823699989	2.048799971
443	0.057200001	0.209399891	0.513999986	0.818699845	2.036900075
490	0.056100002	0.20729989	0.509799909	0.811999944	2.021300145
510	0.0558	0.206200013	0.507899872	0.809099938	2.014600068
560	0.0547	0.204500002	0.504099912	0.80330002	2.001199932
620	0.053899997	0.203099913	0.501599904	0.799899914	1.993499984
665	0.053399996	0.201999895	0.499199972	0.796299869	1.98500004
681	0.053199997	0.201899904	0.499299983	0.796600016	1.986500063
708.75	*0.052999998*	*0.201300006*	*0.498299899*	*0.794799947*	*1.982100022*
753	0.0524	0.200599902	0.497500021	0.793799841	1.980000038
761	0.052299997	0.200699894	0.497199919	0.79370001	1.979799985
778.75	*0.052099998*	*0.20020001*	*0.496099993*	*0.79159988*	*1.975299918*
865	0.0515	0.199	0.4941	0.7892999	1.9698

Table 14-1: Spectral dependency of aerosol optical thickness (cont.)

Spectral dependency of optical thickness for assemblage 26					
$\tau_{tropo}(560)$	0.05	0.2	0.5	0.8	2.0
412	0.057599999	0.205899892	0.504599917	0.803399942	1.998600024
443	0.057000003	0.205699903	0.5047	0.803399983	1.999100072
490	0.056800002	0.205199998	0.504800022	0.803799937	2.000900103
510	0.056400001	0.204999898	0.5047	0.803899886	2.001700017
560	0.055799998	0.204999997	0.50489992	0.805000034	2.005000192
620	0.055500004	0.205199899	0.506399923	0.807799878	2.013200166
665	0.055300003	0.205299901	0.507599897	0.809499927	2.018100087
681	0.055100002	0.205499902	0.508099907	0.810799925	2.021900065
708.75	*0.055000002*	*0.205599902*	*0.508899924*	*0.811900016*	*2.024600122*
753	0.054700001	0.205899892	0.510399865	0.814799916	2.032600035
761	0.054700001	0.206099894	0.510800012	0.815300007	2.033600132
778.75	*0.0545*	*0.206100005*	*0.510800012*	*0.815499914*	*2.034300117*
865	0.0545	0.207	0.5137999	0.8203999	2.0477
Spectral dependency of optical thickness for assemblage 27					
$\tau_{tropo}(560)$	0.05	0.2	0.5	0.8	2.0
412	0.059499999	0.213999998	0.524899996	0.835600067	2.079200091
443	0.058699996	0.211899919	0.519699865	0.827499959	2.059300008
490	0.0577	0.208600008	0.512599966	0.816699994	2.032999953
510	0.056999996	0.207299918	0.510199984	0.812900057	2.023799898
560	0.055700002	0.204400013	0.503899887	0.803100031	2.000400108
620	0.0545	0.201499901	0.497900012	0.794199988	1.978799994
665	0.054000002	0.199899998	0.494199893	0.788399903	1.96539999
681	0.053599998	0.199499898	0.493099985	0.78679995	1.961599887
708.75	*0.053199999*	*0.198599998*	*0.491499975*	*0.784299913*	*1.955300079*
753	0.052600001	0.197200013	0.488200018	0.779700051	1.944699945
761	0.052600001	0.196799986	0.487999853	0.778800068	1.94249996
778.75	*0.052400002*	*0.196899993*	*0.487199992*	*0.777999948*	*1.940700053*
865	0.0513	0.1945999	0.4832	0.7721	1.9266
Spectral dependency of optical thickness for assemblage 28					
$\tau_{tropo}(560)$	0.05	0.2	0.5	0.8	2.0
412	0.057500002	0.209499909	0.513900017	0.81830001	2.035600035
443	0.056900001	0.208199904	0.511600037	0.814499985	2.026799887
490	0.056	0.206699887	0.508499903	0.809699941	2.015600028
510	0.0557	0.206100015	0.507200008	0.808199955	2.01220012
560	0.054799998	0.204800009	0.504499919	0.804199868	2.003199945
620	0.054100003	0.20340001	0.502399934	0.801299936	1.997000013
665	0.053500002	0.202899916	0.50140003	0.79979995	1.993899938
681	0.053200002	0.202499889	0.50099992	0.799499951	1.993499863
708.75	*0.053300002*	*0.202499889*	*0.500699875*	*0.798999985*	*1.992199994*
753	0.052700001	0.201700003	0.50020001	0.7983999	1.991399964
761	0.052700001	0.201700003	0.50010001	0.798299868	1.991099913
778.75	*0.052400001*	*0.201900017*	*0.50020001*	*0.798300012*	*1.991700015*
865	0.0521	0.2013	0.4998999	0.7983999	1.9929

Table 14-1: Spectral dependency of aerosol optical thickness (cont.)

Spectral dependency of optical thickness for assemblage 29					
$\tau_{tropo}(560)$	0.05	0.2	0.5	0.8	2.0
412	0.057400001	0.205199898	0.502900006	0.800799988	1.991899891
443	0.057000005	0.205099887	0.503399909	0.801399953	1.994099927
490	0.056699998	0.204999886	0.504100026	0.802699963	1.997999936
510	0.0562	0.204799902	0.504399995	0.803599848	2.00039994
560	0.055799998	0.205099997	0.505299917	0.805299983	2.006099824
620	0.0556	0.205299896	0.506900008	0.808499968	2.014899888
665	0.055400002	0.205699904	0.50859987	0.81140009	2.022399769
681	0.055199998	0.205699904	0.508899907	0.812300025	2.025399903
708.75	*0.055199998*	*0.206199897*	*0.510199899*	*0.813899939*	*2.029599782*
753	0.054900005	0.206299898	0.511799872	0.817099882	2.038299923
761	0.054800002	0.206599905	0.512299992	0.817499859	2.039200046
778.75	*0.0547*	*0.206899989*	*0.512799896*	*0.818799968*	*2.042700016*
865	0.0547	0.2081	0.5166	0.8249999	2.0594
Spectral dependency of optical thickness for assemblage 30					
$\tau_{tropo}(560)$	0.05	0.2	0.5	0.8	2.0
412	0.058499997	0.210500004	0.515999982	0.821300061	2.043299987
443	0.058000001	0.209199908	0.513399924	0.817299981	2.033900035
490	0.057300004	0.207199908	0.509199959	0.811299873	2.019699998
510	0.056899995	0.206299892	0.507399941	0.808699878	2.01320001
560	0.055799996	0.204500003	0.504400009	0.803799918	2.002199878
620	0.054999999	0.202900013	0.501399904	0.799799941	1.992900084
665	0.054499997	0.201999901	0.499099896	0.796199931	1.985100114
681	0.054100001	0.201699888	0.499000016	0.796199931	1.984799917
708.75	*0.0539*	*0.201499895*	*0.498400032*	*0.795399988*	*1.983199954*
753	0.053399998	0.200499907	0.496700012	0.793100024	1.978299929
761	0.053399998	0.200399911	0.49680001	0.792999984	1.977700007
778.75	*0.053300003*	*0.200299891*	*0.496100023*	*0.792099907*	*1.975999906*
865	0.0526	0.1992	0.4946	0.7902001	1.972
Spectral dependency of optical thickness for assemblage 31					
$\tau_{tropo}(560)$	0.05	0.2	0.5	0.8	2.0
412	0.056899998	0.207099995	0.507799975	0.808699894	2.011700037
443	0.056400001	0.206499898	0.507300041	0.807799869	2.009700146
490	0.055799994	0.205799996	0.506200056	0.806299967	2.006800009
510	0.0554	0.205299998	0.505500056	0.805299979	2.005100052
560	0.054799999	0.2049	0.504899937	0.804799912	2.004499962
620	0.054299995	0.204300001	0.504799935	0.805099907	2.006300011
665	0.053900001	0.204099892	0.504700018	0.805099996	2.007100186
681	0.053700001	0.203999903	0.504899937	0.805599966	2.008899992
708.75	*0.053599998*	*0.204299891*	*0.505500056*	*0.806499894*	*2.010900105*
753	0.053199997	0.203899903	0.505800039	0.807399911	2.0138
761	0.053199997	0.204099892	0.505900042	0.807699955	2.01449996
778.75	*0.052999997*	*0.204299891*	*0.505999954*	*0.807799869*	*2.015399985*
865	0.0529	0.2045	0.5074999	0.8105999	2.0233

Table 14-1: Spectral dependency of aerosol optical thickness (cont.)

Spectral dependency of optical thickness for assemblage 32					
$\tau_{tropo}(560)$	0.05	0.2	0.5	0.8	2.0
412	0.0572	0.204099993	0.499999974	0.796000022	1.979900106
443	0.0568	0.204199886	0.501199881	0.797900012	1.985500053
490	0.056500001	0.204399996	0.50279996	0.800900012	1.99350006
510	0.056200003	0.204499901	0.503400007	0.802100007	1.996900022
560	0.055799996	0.205099996	0.505399971	0.805599999	2.006599999
620	0.0556	0.205799907	0.507999983	0.810400004	2.019599911
665	0.0556	0.206299897	0.51019989	0.814000022	2.029000076
681	0.055399997	0.206499907	0.51099988	0.81540002	2.033099982
708.75	*0.055399997*	*0.2070999*	*0.512399891*	*0.817700025*	*2.039000136*
753	0.055300001	0.207499897	0.514699861	0.821500005	2.049499981
761	0.0552	0.207900006	0.515099965	0.8222	2.051000146
778.75	*0.055100002*	*0.207999899*	*0.515699893*	*0.823599998*	*2.054399984*
865	0.0552	0.2097	0.5203999	0.8311999	2.0744

Table 14-1: Spectral dependency of aerosol optical thickness (cont.)

14.2 – AEROSOL MODELS (ATM. COR. ABOVE LAND)

For the 12 aerosol models used in atmosphere corrections above land, spectral dependency is modelled by an Angström law:

$$\frac{\tau_a(\lambda 1)}{\tau_a(\lambda 2)} = \left(\frac{\lambda 1}{\lambda 2}\right)^{-ang}$$

where the Angström exponent ang is given as function of model index in table 14-2 below.

Model index	Angström exponent
1	0.
2	0.5
3	1.
4	1.5
5	0.
6	0.5
7	1.
8	1.5
9	0.
10	0.5
11	1.
12	1.5

Table 14-2: Angström exponent of aerosol models

15. - Aerosol forward scattering probability

For the 33 aerosol assemblages listed in table 12 above, the forward scattering probability (determined by the phase function of its components) is tabulated at the first 9 bands in table 15-1 below. The values in *Italic type* are subject to change in a future revision of this document.

Assem. number	Wavelength								
	412	442	490	510	560	620	665	681	708.75
0	0.95220435	0.95163769	0.9510839	0.95121557	0.95037538	0.94893587	0.94888401	0.94812208	*0.94763219*
1	0.91486955	0.91477072	0.91462493	0.91463816	0.91431713	0.91423959	0.91406727	0.91414958	*0.91408324*
2	0.92483139	0.92624503	0.92650348	0.92695171	0.92631418	0.9269433	0.92665964	0.92697424	*0.92641336*
3	0.93273771	0.93305683	0.93329775	0.93319803	0.93352538	0.93323815	0.9331249	0.93305022	*0.93313313*
4	0.93743938	0.93776524	0.9383387	0.93878329	0.93898249	0.93848908	0.93896866	0.9384768	*0.93831503*
5	0.9224956	0.92078632	0.91805184	0.91680104	0.91358191	0.90955627	0.90654105	0.90541255	*0.90381426*
6	0.9308458	0.92968893	0.92785454	0.92704833	0.92457747	0.92139393	0.91898376	0.91805524	*0.91674417*
7	0.93694854	0.93668658	0.93615931	0.93561369	0.93486518	0.93313426	0.93190819	0.93132675	*0.9305256*
8	0.93722183	0.93770158	0.93825942	0.93843758	0.93847942	0.93801206	0.93767536	0.93741876	*0.93708998*
9	0.91316563	0.91309375	0.91300696	0.91302228	0.91279823	0.91279638	0.91265017	0.91273087	*0.9126907*
10	0.90659547	0.90665561	0.90677148	0.90675777	0.90671062	0.90644091	0.90615302	0.9061231	*0.90601349*
11	0.90068358	0.90073097	0.90079528	0.90066892	0.90055078	0.89972132	0.89906639	0.89878583	*0.89847481*
12	0.92248535	0.92387438	0.92423993	0.92468703	0.92420679	0.92497259	0.92475492	0.9250744	*0.92459512*
13	0.91229123	0.91339928	0.91400957	0.91434842	0.91436565	0.91491312	0.91476297	0.91500813	*0.91467625*
14	0.90330935	0.90390927	0.90429145	0.90439373	0.90439475	0.90414244	0.90367609	0.90362775	*0.90323383*
15	0.92989808	0.93030351	0.93066376	0.93058467	0.93106687	0.9309963	0.93095946	0.930924	*0.93105203*
16	0.91684842	0.91739482	0.91814506	0.91821593	0.91898394	0.9190864	0.91918325	0.91918021	*0.91938812*
17	0.90542269	0.90578693	0.90630329	0.90626627	0.906712	0.90630239	0.90603656	0.90585428	*0.90582401*
18	0.93427777	0.93470085	0.93541509	0.93587333	0.93625516	0.93603975	0.93660408	0.93615609	*0.93607819*
19	0.91942817	0.92007536	0.92116904	0.92161602	0.92247367	0.92262775	0.92323041	0.92300272	*0.92311907*
20	0.90659195	0.90700877	0.90771931	0.90792769	0.90845597	0.90818202	0.90823263	0.90797347	*0.90792745*
21	0.92596793	0.92526329	0.92425066	0.92394692	0.92279786	0.92199624	0.92124665	0.92116255	*0.92080271*
22	0.93178713	0.93067014	0.92904925	0.92844915	0.92672151	0.92507249	0.92378324	0.92345268	*0.92282951*
23	0.93803823	0.93639994	0.93400687	0.93305725	0.93062013	0.92804581	0.92619658	0.92563015	*0.92472774*
24	0.93661988	0.93713015	0.93606287	0.9360041	0.93414068	0.93353248	0.93237257	0.93237615	*0.93145794*
25	0.93919599	0.93882656	0.93705332	0.93657404	0.93425965	0.93264955	0.93103993	0.93076193	*0.92973834*
26	0.94190544	0.9405961	0.93806779	0.93715185	0.93437815	0.93178517	0.9297502	0.92919868	*0.92809254*
27	0.94489872	0.94411439	0.94279021	0.94208264	0.94094771	0.9393	0.93813407	0.93776917	*0.93733317*
28	0.94485098	0.94357121	0.94158393	0.94065505	0.9387902	0.9364602	0.93483466	0.93430632	*0.93359786*
29	0.94480145	0.94300956	0.94035405	0.93920267	0.93663782	0.93367279	0.93162173	0.9309414	*0.92999244*
30	0.94996476	0.94901365	0.94781142	0.94756556	0.94610584	0.94408733	0.94334638	0.94255823	*0.94185996*
31	0.94828081	0.94687492	0.94495136	0.94432139	0.94222599	0.93964076	0.93828619	0.93748921	*0.9366045*
32	0.94654489	0.94467551	0.94204044	0.94104242	0.93834943	0.93526125	0.93333662	0.93252838	*0.93149108*

Table 15-1: Aerosol scattering probability

Note: this parameter is not applicable to the 12 aerosol models used in atmosphere corrections above land.